Institut für Nutzpflanzenwissenschaften und Ressourcenschutz

Identification of host genes with a role in sex determination of the plant parasitic cyst nematode, *Heterodera schachtii*

Dissertation

zur

Erlangung des Grades

Doktor der Agrarwissenschaften (Dr. agr.)

der
Landwirtschaftlichen Fakultät
der
Rheinischen Friedrich-Wilhelms-Universität Bonn

von

Muhammad Shahzad Anjam

aus

Hafizabad, Pakistan

Bonn 2017

Referent: Prof. Dr. Florian M.W. Grundler
Externer Korreferent: Prof. Dr. Tina Kyndt

Tag der mündlichen Prüfung: 13-06-2017

Angefertigt mit Genehmigung der Landwirtschaftlichen Fakultät der Universität Bonn

Table of Contents

Abstract

Cyst nematodes are biotrophic parasites that infect plant roots and cause physiological and structural modifications leading to the formation of syncytial nurse cells. They are sexually dimorphic but the sexual phenotype appears only after feeding has started. Because the sex ratio varies with environmental conditions and the genotype of the host plant, it is generally assumed that both factors play a decisive role in sex determination of cyst nematodes. Under favorable conditions, more females develop, whereas mainly male nematodes develop under adverse conditions. Since the presence of females determines reproduction and thereby soil infestation levels, the sex ratio is very important in agricultural practices: resistant crop cultivars, which suppress female formation, are often used to control cyst nematodes. However, the molecular mechanisms underlying this phenomenon have remained mostly unknown. In this study, a comparative transcriptomic analysis of male- and female-associated syncytia (MAS and FAS, respectively) of cyst nematode *Heterodera schachtii* was performed at early stages of infection to identify the host factors influencing sexual development. Therefore, a method was developed to predict the sex of developing nematodes on the basis of an empirically developed growth curve. In this way, syncytia associated to future males or females could be sampled at an early developmental stage, when typical sex-related traits of the juveniles were not yet visible. The transcriptome of the nurse cells was analyzed from samples taken by laser capture microdissection from root tissue of host plant *Arabidopsis thaliana*. A novel protocol was developed in order to improve the quality of the sampled RNA. The data revealed that gene categories belonging to cell wall biosynthesis, modification and metabolism were particularly up-regulated in FAS, whereas the transcriptome of MAS showed an enrichment of gene categories related to defense and nutrient deficiency. These results were further complemented by ultrastructural analyses and gene regulation studies via promoter::reporter lines. All the data point out that changes in the cell wall, suppression of host defense and availability of nutrients are important factors promoting the development of female nematodes. The data led to the assumption that knocking out genes that are differentially up-regulated might influence sexual differentiation of the nematodes. Therefore, knockout mutants for ten candidate genes (*CWLP1, BGLU28, BHLH101, DIN2, MLP like protein 423, SHVL3, IRX12, LAC11, LNG1, LTPG6*) were used to study their importance via nematode infection assays. Three mutants (*ltpg6, lng1* and *irx12*) of genes, which are differentially up-regulated in FAS, showed a significant decrease in the number of females as compared to the control. On the other hand, the number of males

increased significantly in two of them (*lng1 and irx12*). In conclusion, our study supports the role of the host plant on the sex determination of cyst nematodes. Manipulation of the identified host factors may provide new options for breeding resistant crop plants in future.

Zusammenfassung

Zystennematoden sind biotrophe Parasiten. Sie befallen die Wurzeln ihrer Wirtspflanzen und bewirken dort physiologische und strukturelle Veränderungen, die zur Bildung von syncytialen Nährzellen führen. Zystennematoden sind getrennt geschlechtlich, die sexuelle Differenzierung der jungen Larven findet aber erst nach Beginn der Nahrungsaufnahme statt. Da das Geschlechterverhältnis in Abhängigkeit von Umweltbedingungen und dem Genotyp der Wirtspflanze stark variiert, wird angenommen, dass die Geschlechtsdeterminaton bei Zystennematoden von diesen Faktoren wesentlich bestimmt wird. Unter günstigen Bedingungen entwickeln sich mehr Weibchen, während sich unter ungünstigen hauptsächlich Männchen bilden. Da die Entwicklung von Weibchen die Reproduktion und damit den Verseuchungsgrad des Bodens mit Nematoden maßgeblich bestimmt, ist das Geschlechterverhältnis entspechend wichtig in der landwirtschaftlichen Praxis: Resistente Sorten, die die Bildung von Weibchen unterdrücken, werden oft zur Bekämpfung von Zystennematoden eingesetzt. Die molekularen Mechanismen, die diesem Phänomen zugrunde liegen, sind bisher weitgehend unbekannt. In der vorliegenden Arbeit wurde eine vergleichende Transkriptomanalyse von Männchen- und Weibchen-assoziierten Syncytien (MAS bzw. WAS) von Zystennematoden *Heterodera schachtii* in einem frühen Infektionsstadium durchgeführt, um Faktoren der Wirtspflanze zu identifizieren, welche die Geschlechtsentwicklung der Nematoden beeinflussen. Hierzu wurde eine Methode entwickelt, die es erlaubte, das Geschlecht von sich entwickelnden Nematoden mit Hilfe einer empirisch ermittelten Wachstumskurve vorherzusagen. Auf diese Weise konnten Proben aus sehr jungen Syncytien zu einem Zeitpunkt gewonnen, werden zu dem das Geschlecht der Larven noch nicht anhand der typischen Geschlechtsmerkmale erkennbar war. Das Transkriptom der Nährzellen wurde von Proben analysiert, die mit Hilfe einer Laser-Capture-Mikrodissektionsvorrichtung aus dem Wurzelgewebe der Wirtspflanze *Arabidopsis thaliana* entnommen worden waren. Es wurde ein neuartiges Protokoll entwickelt, mit dem die Qualität der zu analysierenden RNA wesentlich verbessert werden konnte. Die Untersuchungen ergaben, dass Gene aus den Kategorien Zellwandbiosynthese, -modifizierung und -metabolismus in WAS aufreguliert waren, während das Transkriptom von MAS durch die Anreicherung von Genkategorien in den Bereichen Abwehr und Nährstoffmangel gekennzeichnet waren. Diese Ergebnisse wurden durch ultrastrukturelle Untersuchungen und Genregulationsanalysen mit Promoter::Reporter Linien ergänzt. Die Untersuchungen machten deutlich, dass Zellwandumbildung, Unterdrückung von Abwehr

und Verfügbarkeit von Nährstoffen wichtige Faktoren sind, welche besonders zur Entwicklung von Weibchen beitragen. Dies führte zur Schlussfolgerung, dass das Ausschalten von Genen, die spezifisch aufreguliert sind, die geschlechtliche Differenzierung der Nematoden beeinflussen könnte. Daher wurden Knockout-Mutanten für zehn Kandidatengene (*CWLP1, BGLU28, BHLH101, DIN2, MLP like protein 423, SHVL3, IRX12, LAC11, LNG1, LTPG6*) in Infektionsversuchen hinsichtlich der Bedeutung der Gene für die Geschlechtsentwicklung der Nematoden untersucht. Die Resultate ergaben, dass drei Mutanten von Genen (*ltpg6, lng1* and *irx12*), die besonders in WAS aufreguliert sind, zu einer signifikanten Reduktion von Weibchen im Vergleich zur Kontrolle führten. Andererseits nahm die Anzahl von Männchen bei zwei dieser Mutanten (*lng1* and *irx12*) siginfikant zu. Die Untersuchungen unterstreichen die Rolle der Wirtspflanze bei der Geschlechtsdetermination von Zystennematoden. Die Manipulation der identifizierten Wirtsfaktoren könnte neue Optionen für die Züchtung resistenter Nutzpflanzen eröffnen.

List of Figures

List of Tables

Acronyms and abbreviations

A	Autosomal chromosomes
BGLU	Beta-Glucosidase
C	Cortex
cDNA	Complementary DNA
CKX	Cytokinin Oxidase/Dehydrogenase
C_T	Cycle Threshold
Cv	Cultivar
CW	Cell wall
CWLP	Cell Wall-Plasma Membrane Linker Protein
ddH_2O	Double distilled water
DEPC	Diethylpyrocarbonate
DPI	Days Post Infection
e.g.,	exempli gratia (For example)
EAA	Ethanol Acetic Acid
EDTA	Ethylenediaminetetraacetic acid
ER	Endoplasmic reticulum
ESD	Environmental Sex Determination
FAS	Female Associated Syncytia
FP	Feeding plug
FT	Feeding tube
GC	Giant Cells
GO	Gene Ontology
GUS	Beta-glucuronidase
H. schachtii	*Heterodera schachtii*
HAI	Hour After Infection
IRX	Irregular Xylem
ISC	Initial Syncytial Cell
J2	Juvenile stage 2
$K_3(Fe(CN)_6)$	Potassium Ferricyanide
$K_4(Fe(CN)_6)$	Potassium Ferrocyanide
kDa	Kilo Dalton

Acronyms and abbreviations

L2	Larval stage 2
LCM	Laser Capture Microdissection
LNG	Logifolia
LTPG	Glycosylphosphatidylinositol-Anchored Lipid Protein Transfer 6
MAS	Male Associated Syncytia
$MgCl_2$	Magnesium Chloride
mRNA	Messenger RNA
Mx	Meta xylem
Na_3PO_4	Tri-Sodium Phosphate
NaOCl	Sodium Hypochlorite
Ne	Necrosis
ng/µL	Nanogram/Microliter
nsLTPs	Non-Specific Lipid Transfer Proteins
Nu	Nucleus
OCT	Optimum Cutting Temperature
Pd	Peridermis like tissue
PDF	Plant Defensin Family
PEN	Polyethylene Napthalate
PET	Polyethylene Teraphthalate
PFA	Paraformaldehyde
pg/µL	Picogram/Microliter
PGIP	Polygalacturonase-Inhibiting Protein
PGs	Polygalacturonases
PPNs	Plant-Parasitic Nematodes
qRT-PCR	Quantitative Reverse Transcription Polymerase Chain Reaction
RIN	RNA Integrity Number (Based on scale 10)
RKN	Root Knot Nematode
RMA	Robust Multi-array Average
RNA-seq	RNA Sequencing
RT-PCR	Reverse Transcription Polymerase Chain Reaction
S	Syncytium
SAR	Systemic Acquired Resistance

Acronyms and abbreviations

SE	Standard error
St	Stylet
T-DNA	Transfer DNA
UTR	Untranslated Region
V	Vacuole
v/v	Volume/Volume
Vs	Versus
w/v	Weight/Volume
WRKY	Wrky DNA-Binding Protein
X	Xylem
X,Y,Z	For sex chromosomes
µ	Micron
µM	Micro Molar

1. Introduction and review of literature

Nematodes, also known as roundworms, are multicellular organisms with unsegmented, worm-like, symmetrical body morphology. They are invertebrates and classified into a large phylum "Nematoda". Nematodes are impressively huge in number comprising more than 25,000 species. The species in this phylum are extremely versatile in all aspects, including morphology, feeding habits, reproduction, and habitat. Although the majority of nematodes are microscopic (<1 mm in length), the longest nematode (the females of *Placentonema gigantissima*) ever recorded was 8 meters in length (Gibbons, 2005). Nematodes are adaptive to nearly all environmental conditions on the planet. Some of the species have been isolated from extreme environmental conditions like the hot springs of New Zealand, lacunae of arctic ice and sulfur-rich marine sediments (reviewed by De Ley, 2006). Because of nematode-borne infections in humans, animals, and plants, nematodes have a high socioeconomic impact all over the world. According to an estimate, more than 1 billion people worldwide are being affected with diseases caused by nematodes. Gastrointestinal diseases are among major infections caused by nematodes, which adversely affect the health and performance of livestock, small ruminants, and pet animals. Even marine life is not safe from parasitic nematodes. Lastly, agriculture losses due to nematode infections exceed $80 billion annually (Nicol et al., 2011). Nevertheless, because of their high feeding diversity and specialized parasitism, some of the nematode species are used as a biological control for insect pests.

1.1. Anatomical features of nematode

Nematodes are one of the simplest multicellular organisms with no circulatory system, consisting of a single long tube, called an elementary canal. The elementary canal has two openings; one is at the anterior side used as the mouth, whereas the other opening is at the posterior end, called anus (Figure 1) to excrete undigested food (Fae, 2010). The mouth opens into a cavity, called stoma or buccal cavity, which is followed by a pharynx (esophagus), small intestine and rectum (Gibbons, 2005).

Depending on the feeding habits, nematodes show a great variation in the shape of their mouths. The bacterial feeding nematodes have a tube-like structure at the mouth for bacterial ingestion (Figure 2A), whereas fungal feeders have a needle-like structure to penetrate the fungal cell and uptake cellular contents (Figure 2B). Particularly, in all plant-parasitic nematodes, the mouth contains a hollow spear-like needle, called stylet (Figure 2C), which is

used by nematodes to puncture the host cell to extract food. The stylet is also used to secrete proteins and enzymes into host tissues to facilitate parasitism. In contrast to plant-parasitic species, certain predatory species of nematodes have large stoma to engulf prey (Figure 2D). The stoma is usually equipped with teeth which are immovable in the case of *Mononchus* and movable in *Ironus* (reviewed by Munn & Munn, 2005; Sommer & Ogawa, 2013).

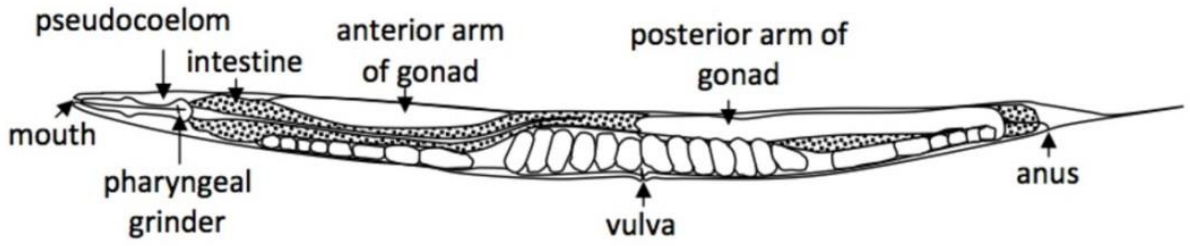

Figure 1: General anatomical features of a nematode (http://theconversation.com/animals-in-research-c-elegans-roundworm-14163)

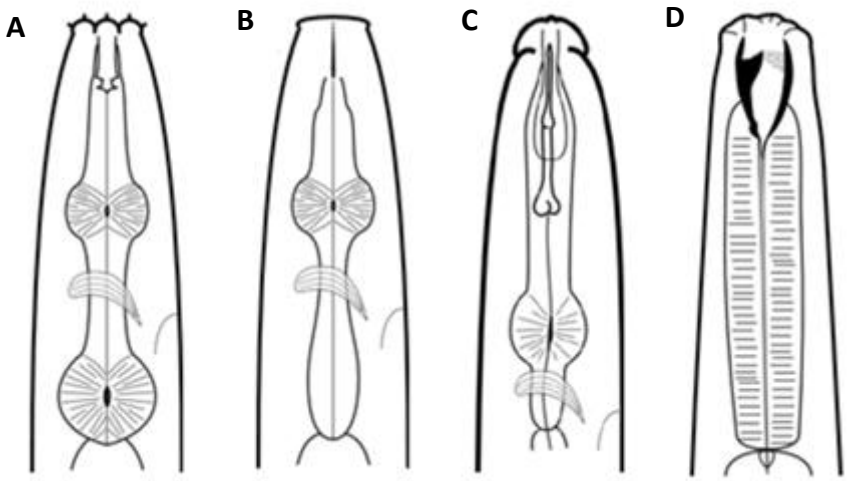

Figure 2: Schematic diagrams indicating mouth variations among different groups of nematodes. (A) bacterial feeder (B) fungal feeder (C) plant-parasitic (D) predator (http://articles.extension.org/pages/24726/soil-nematodes-in-organic-farming-systems).

The oral cavity of nematodes opens into a muscular pharynx (also referred as esophagus), which is in most cases used for food ingestion through pharyngeal pumping. The pharynx is located between the buccal cavity and the intestine. The pharynx has ventral glands, triradiate lumen and visceral nervous system with receptors and neurons connected with nerve ring. In parasitic nematodes, the oesophageal glands are specialized to produce proteins or effectors, which are released in host tissues to establish parasitism. The pharynx connects to intestine through one or more, one-way valves (pharyngeo-intestinal valve), which force the food into

the intestine (Munn & Munn, 2005; Decraemer & Hunt, 2006). However in certain species of nematodes such as fungal feeders, *Hexatylus viviparous*, the pharyngeal pumping and pre-rectal valve are not present. In these nematodes, ingestion is presumably facilitated by the turgor pressure of host fungus and by the movement of rectal muscles (Munn & Munn, 2005). The mouth opening, stoma, pharyngeal and cervical regions are collectively referred as stomodeum, which makes part of the digestive system. The other two parts of the digestive system include mesenteron and proctodeum (Gibbons, 2005).

Mesenteron (intestine) is composed of a tube made up of a single layer of epithelial cells with or without clear lumen lined with microvilli. The intestine mainly functions for nutrient absorption, storage and secretions of proteins and enzymes. Nevertheless, in certain genera of plant-parasitic nematodes such as *Heterodera* and *Meloidogyne*, the intestine does not contain microvilli on luminal surface and serves as a storage organ (reviewed by Rafiq, 2000). The last region of the digestive system is proctodeum lined with cuticle, consists of rectum and anus. The posterior end of the intestine may differentiate into a pre-rectum, which is separated from the intestine by an intestino-rectal valve or a sphincter. The rectum is lined with cuticle, and in females, it ends at the small opening called anus. The reproductive opening of the female is a vulva, which is separated from the anus. However, in the case of a male, the anal opening also functions for the reproductive system; therefore, in the male, it is referred as a cloaca. However, in some species, rectum and anus are poorly developed or probably non-functional. Nevertheless, there are glands, which open into the rectum, called rectal glands. The number of rectal glands; however, varies in species. In *Meloidogyne*, six large rectal glands produce gelatinous matrix where eggs are deposited. In the male, rectal glands consist of three to five pair of cells forming a loop of ducts that runs interiorly between spicules and open via a dorsal wall of the cloaca (Munn & Munn, 2005; Decraemer & Hunt, 2006).

The nervous system of nematodes is extremely basic and in contrast to high behavioral diversity, nervous system seems conservative in both free-living and parasitic nematodes. The organizational setup of the nervous system is quite simple. It has two rings of neurons, one around the pharynx called cirumpharyngeal, which is the main part of the nervous system. The second neuronal ring is located in the posterior region of nematode body. Longitudinal nerves connect these two rings thus covering both extremities of the nematode body. Phasmids (post-anal organs) are found in certain parasitic species of nematodes. These

organs are connected with neurons and are involved in ‘chemo-sensing’ (Elmer et al., 1961). The reason for high plasticity in nematodes seems to be due to signaling molecules rather than variants of the nervous system. More than 30% neurons of *Ascaris suum* (pig gastrointestinal parasitic nematode) have been reported showing rigorous similarities in shape, size and position to neurons of *Caenorhabditis elegans* (Angstadt et al., 1989; Nanda & Stretton, 2010). The neurons are relatively unbranched with single gap junction that is sufficient for functional coupling between neurons. In nematodes, neuronal intercellular signaling is accomplished by small molecule transmitters (like acetylcholine, serotonin, and glycine) and large neuropeptides (insulin-like peptides (INSs), neuropeptide-like proteins (NLPs) and Phe-Met-Arg-Phe-amide-like peptides (FLPs), which in general work together at synaptic junctions. There are 250 neuropeptides that have been known in *C. elegans* and our knowledge of complements with parasitic nematodes is growing with new reports (Mousley et al., 2013).

1.2. Habitat and diversity

Nematodes are adaptive to extremely diverse ecological conditions. They have been isolated from the hot and dry weather of deserts to icy conditions of arctic poles. Nevertheless, all the nematodes are aquatic in a way that they need a thin layer of liquid around their body for their survival and activity. So far, more than 25,000 species of nematodes have been documented, which shows their abundance on earth. Still many species of nematodes are believed yet to be described (De Ley, 2006; Perry & Moens, 2011). In consistency with adaptation to diverse habitats, nematodes show a large variety of anatomical, behavioral and feeding characteristics. Due to their diverse habitat, morphology and feeding style, nematodes had been under contentious debate regarding their classification. In literature, two classification schemes are found under the phylum Nematoda: The classical (Chitwood, 1958) is based on anatomical features of worms, whereas the recent classification is based on the sequence variation in a small subunit of ribosomal DNA (De Ley & Blaxter, 2002). This second type of classification has helped to place nematodes according to their evolutionary hierarchy. Regardless of taxonomical classification, major groups of nematodes are free-living or parasites of plants, animals, and insects.

1.3. Free-living nematodes

Free-living nematodes constitute the largest part of the phylum, covering approximately 50% of the described species (Pokharel, 2011). They are found abundantly in soil and in marine and freshwater. Generally, free-living nematodes feed on bacteria, algae or other nematodes as well as on other small animals. In spite of the high diversity in feeding mode, they all show a basic similar life cycle (Figure 3). The worm undergoes one moulting stage inside the egg and hatches as an active larva (L2; larva is also referred as a juvenile), which undergoes three additional moults to become an adult (Lee, 2005).

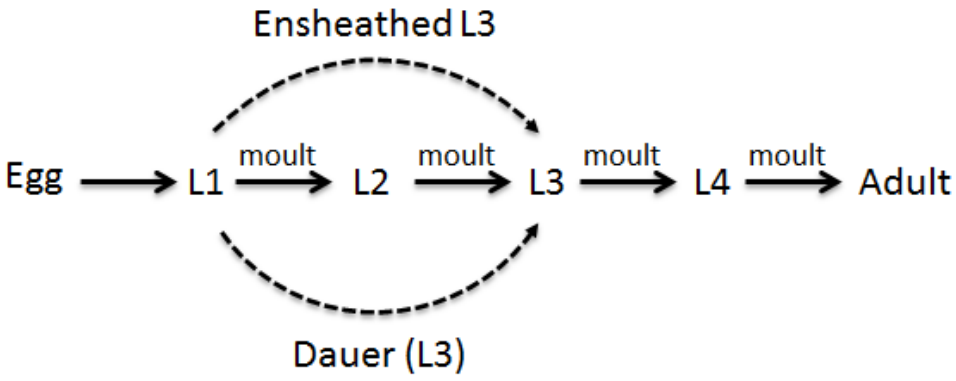

Figure 3: Basic life cycle of free-living nematodes. Some species during adverse feeding conditions undergo developmental arrest. Some of them are modified to L3 resistant dauer stage whereas some others convert to an obligatory ensheathed L3.

C. elegans is a free-living, bacterial-feeder, soil-borne nematode, which under optimal conditions completes its life cycle in three days. Its whole lifespan lasts for approximately two weeks. Due to its simple morphology and short life cycle, *C. elegans* has been intensively used as a model organism for basic research for four decades now. It has two sexes, hermaphrodite and male; however, the hermaphrodite is structurally a female. The hermaphrodites are either self-fertilized or fertilized by males but they cannot fertilize each other (Lee, 2005).

1.4. Parasitic nematodes

Parasitic nematodes infect nearly all species of animals and plants on earth. Some of the nematode species infect both humans and animals and thus can be transmitted from animals to humans (Robinson & Dalton, 2009). However, plant-parasitic and the majority of insect-parasitic nematodes are very specialized to their respective hosts. Animal- and plant-parasitic nematodes account for 15% and 10%, respectively, of the total number of described species

(Pokharel, 2011). Parasitic nematodes carry huge socioeconomic consequences as they have significant effects on the health and productivity of humans as well as animals and cause severe yield losses in important agricultural crops.

1.4.1. Human- and animal-parasitic nematodes

The human health issues caused by nematodes include diseases related to the respiratory and intestinal systems, anemia and blindness. Nematodes may infect the gastrointestinal system (*Ascaris lumbricoides*, *Trichuris trichuria*, *Ancylostoma duodenale*, *Necator americanus*, *Strongyloides stercoralis*, *Enterobius vermicularis*, *Trichinella spirosis*, *Toxocara canis*, *Toxocara cati*) and blood stream or tissues (*Wuchereia bancrofti*, *Loa loa*, *Onchocerca volvulus*, *Ancylostoma braziliense*). According to one estimate, around 1 billion people are affected by roundworms, 800 million by whipworms and 700 million by hookworms. Nematode species causing gastrointestinal diseases particularly in children are listed in Table 1.

Table 1: Gastrointestinal nematodes of medical importance (Albonico et al., 1999; Blackburn & Barry, 2011; Jasmer et al., 2003).

Nematode	Common Name	Infection	Health Issues
Ascaris lumbricoides	Roundworm	Ascariasis	• In children poor weight gain, malnutrition and learning problems
Trichuris trichiura	Whipworm	Trichuriasis	• In children poor intellectual and physical development • Blood loss may occur
Ancylostoma duodenale, Necator americanus	Hookworms	Ancylostomiasis	• Iron deficiency • Weight loss • Rash at entry site
Strongyloides stercoralis	Threadworm	Strongyloidiasis	• Acute and chronic infection • Fatal in hyper infection
Enterobius vermicularis	Pinworm	Enterobiasis	• Itching in and around anus • Restless nights • Loss of appetite
Trichinella spirosis	Trichinella	Trichiniasis	• Muscle pain • Weakness • Swelling around the eyes

Hookworms cause iron deficiency (anemia) in children and pregnant women, particularly in the developing world, and cause more than 60,000 deaths per year. Humans, as well as animals, can be infected with the roundworm and whipworm by ingesting their eggs through contaminated food. Once fertilized eggs of roundworm are swallowed, they reach to the small intestine where juveniles are hatched. Juveniles enter to intestinal mucosa and then through main blood stream end up in the lungs. They develop about 10-14 days within lungs, enter to

alveolar walls, pass through the bronchial tree and via throat swallowed up to the stomach. In the small intestine, they further grow to become adult ready to fertilize and produce new eggs. The whipworms primarily reside in the cecum and ascending colon. In contrast to the roundworms and the whipworms, the hookworms hatch outside the host body and the larvae become infectious after moulting over a period of the next 5-10 days; then on contact, the hookworms enter the human body and move to the lungs, where they are swallowed and ultimately migrate to the small intestine. The lifespan of an adult hookworm can range from 1–5 years depending upon the species (reviewed by Blackburn & Barry, 2011; Jasmer et al., 2003). The other very common infection that occurs via nematodes is the pinworm infection. The infection is caused by *Enterobius vermicularis*, and is extremely common in children of age 5-10, regardless of their socioeconomic status (Burkhart & Burkhart, 2005; Maykel & Steele, 2011). The symptoms include an itching rectum. The infection is incredibly disturbing, particularly at night when the female worms come out of the anus to lay their eggs. The infection is quite prevalent across the world without any distinction of culture, race or economic situation. Its prevalence among Indian, English and Thai children is 61%, 50% and 39%, respectively (Burkhart & Burkhart, 2005; Chan, 1997).

In addition, infections transmitted by zoonotic nematodes present an additional challenge to human health. The term zoonotic is used for animal-transmitted diseases. These nematode infections are primarily found in the areas where human and animals are in close contact. Similarly, family pets are also a source of zoonotic nematodes. Nematodes are among the major parasites of animal husbandry. In the Unites States, gastrointestinal diseases caused by nematodes are ranked among the top three diseases of livestock, with a significant economic impact of more than $2 billion annually (Robert & Louis, 2010). At least 41 species of helminths have been isolated from the bovine gastrointestinal tract. They infect a wide range of animals, including wild animals, ruminants, poultry, fish and insects. More than one billion US dollars are spent on antihelmintics to manage gastrointestinal diseases in livestock and pets (Witty, 1999).

In comparison to animal-parasitic, the insect-parasitic nematodes are very specialized and do not infect humans (Cranshaw & Zimmerman, 2013). Therefore, certain species of insect-parasitic nematodes are used as a biological control of insects in crops, particularly to manage soil-dwelling insects. In regard to biological control of insects, certain nematode species (*Steinernema carpocapsae, S. feltiae, S. riobrave*, *Heterorhabditis bacteriophora, H.*

marelatus, and *H. megidis*) are also commercially available (Barbercheck, 2005; Jasmer et al., 2003). Fifteen families of five orders of the phylum nematode are obligate parasites of insects. However, nematodes of the order Mermithida are parasitic to insects and arthropods including 25 species that have been reported as infective to mosquitoes. Therefore, these nematodes are considered as potential biological agents in limiting the mosquito population (Platzer, 1981; Poinar, 1985).

1.4.2. Plant-parasitic nematodes

More than 4,100 species of plant-parasitic nematodes have been reported so far (Decraemer & Hunt, 2006), which cause losses of $80-100 billion in crop damage every year (reviewed by Bird & Bird, 2001; Nicol et al., 2011). Plant-parasitic nematodes exhibit wide diversity in terms of interacting with their host. The plant parts serving as feeding targets for various nematode species include roots, stems, leaves, flowers and seeds. However, the majority of researchers in this field have focused on root-infecting nematodes due to their economic importance in agricultural crops. At some stage of their life cycle, plant-parasitic nematodes have a hollow stylet and a spear-shaped mouth for penetration and feeding. The presence of a stylet is not only a characteristic of plant-parasitic nematodes. A stylet also appears in some entomopathogenic and predatory nematodes (reviewed by Bird & Bird, 2001). Migratory ectoparasites move in soil and feed on roots as they encounter them, whereas migratory endoparasites penetrate and migrate inside the host and cause severe damage. Nevertheless, most of the economic damage is caused by a small group of sedentary endoparasites including root-knot and cyst nematodes (Reviewed by Jones et al., 2013). In the next paragraphs, I have described in detail the life cycle and mode of infection of root-knot and cyst nematodes. However, cyst nematodes are addressed in relatively more details because the present work focuses on the cyst nematode *Heterodera schachtii*.

1.4.3. Root-knot nematodes

Nematodes of the genus *Meloidogyne* are referred as root-knot nematodes. The genus comprises 90 species, including economically important species of *M. incognita, M. javanica, M. arenaria*. They parasitize a wide range of plants worldwide including vegetables, fruits, and ornamental trees. In most cases, they produce characteristic "giant cells" on the roots of the host plant. The development of feeding sites varies in size and morphology across different species of root-knot nematodes. The nematode completes its initial juvenile stage (J1) inside the egg and hatches as an active worm (J2) looking for the host root. Root

exudates including CO_2 likely act as attractants for juveniles. Chemosensory organs such as sensilla and amphids likely help juveniles to sense these exudates to find the root location. Upon finding a suitable root, the nematode penetrates inside the root away from the elongation zone and then moves intercellularly towards the root tip. The nematodes use cell wall degrading enzymes, stylet and head force to make space for movement in between the cells. From the meristem region, the nematode enters the vascular cylinder and selects several cells where it releases secretions to establish a feeding site. After entering the root, the nematode moves towards root tip likely to avoid endodermis (casperian strip and suberin), which may act as a barrier to nematode movement. During migration, the subventral glands of the nematode are more active producing secretions containing a cocktail of cell wall degradation enzymes such as cellulases, endoxylanases, pectatelyases and polygalacturonases that assist nematode movement (reviewed by Escobar et al., 2015; Wieczorek et al., 2014). However, after the establishment of the feeding site, dorsal glands of nematodes become more active. After initiation of the feeding sites, the nematode becomes sedentary. Infected cells undergo profound metabolic and morphological changes to serve their function as feeding sites and are called as giant cells. The cortex cells surrounding giant cells divide actively and become hypertrophied thus giving a gall-like appearance to the infected tissue (Figure 4). Inside the giant cells repeated cycles of endoreduplication occur and the large central vacuole divides into many smaller vacuoles. The cytoplasm becomes dense with abundant cellular organelles like mitochondria, endoplasmic reticulum, golgi bodies and ribosomes.

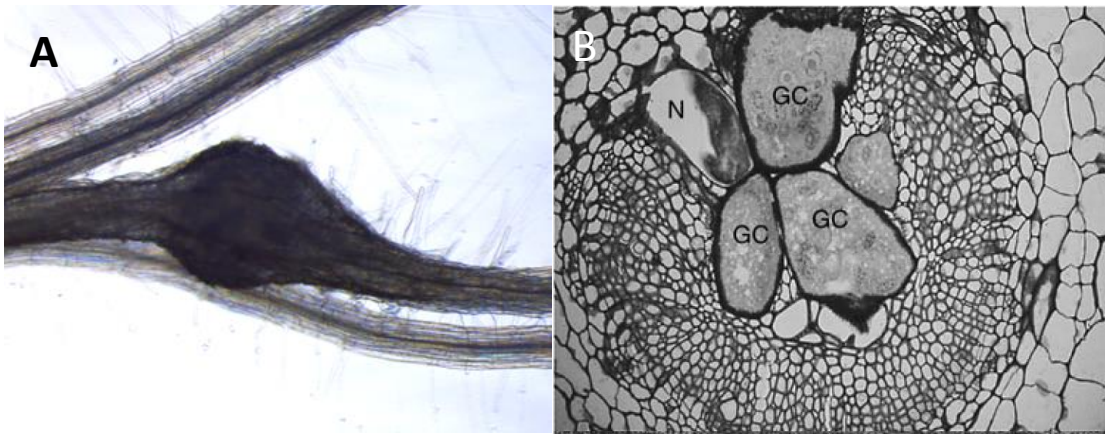

Figure 4: Feeding structure induced in roots of a host plant by a root-knot nematode (*Meloidogyne* spp). (A) Gall induced in the roots of *Arabidopsis thaliana* (photo taken by Julia Holbein). (B) Multinucleate giant cells (GC) surrounding sedentary nematode (N) inside the vascular cylinder (Bird & Digennaro, 2013).

These feeding sites become a sink for nutrients, and the nematode feeds from it for the rest of its life cycle. After continuous feeding, the nematode moults further two times (J3 and J4 stages) to become an adult. The adult female adopts pear shaped morphology. The J2 generally develops to a female and reproduce parthenogenetically. However, some males also develop and their percentage increases considerably under adverse conditions (reviewed by Bird & Bird, 2001; reviewed by Escobar et al., 2015).

1.4.4. Cyst nematodes

The nematode species of genera *Heterodera* and *Globodera* are collectively called cyst nematodes. These are cyst-forming sedentary endoparasites, which form specialized feeding structures inside the roots of the host plant. In beet cyst nematode *Heterodera schachtii*, the adult female contains hundreds of eggs, and dies after fertilization, becoming a brown cyst. This cyst protects the eggs inside and can withstand unfavorable conditions. The cyst may survive in the soil for several years before hatching. The cyst does not contain water, so it can survive in freezing conditions. The embryo inside the egg moults to a J2 stage similar to root-knot nematodes and stays inside the eggs in this dormant stage. The egg contains three layers: a lipid layer, a chitin layer, and a vitelline layer (inside to outside). The lipid layer is semi-permeable to water, ions, and gasses, the middle layer supports the juvenile movement, and the outermost layer plays a role in fertilization. Root exudates generally stimulate the hatching, which varies with the host range of the cyst nematodes. For example, the cysts of nematodes with a relatively broad host range such as *H. schachtii* and *H. avenae* can hatch in water. In comparison, *H. glycines* cysts partially depend on root exudates for hatching and cysts of *G. rostochiensis* and *G. pallida* are entirely dependent on root exudates for hatching. The hatching factors in these nematodes have been extensively studied leading to isolation of a few compounds from host plants that may stimulate hatching. For example, glycinoeclepin A (a terpenoid) for *H. glycines* have been proven a hatching inducers (reviewed by Bohlmann, 2015; reviewed by Sobczak & Golinowski, 2011). After hatching worms move in search for a suitable root, but the factors that influence the nematode attraction towards the host root are not well understood. For movement and host finding, nematode juveniles rely only on the reserve food and further feeding is only possible after establishing a feeding site inside the root. Therefore, in the absence of a suitable host they gradually consume their reserved food and slowly die (reviewed by Sobczak & Golinowski, 2011).

Upon finding a host root, the juveniles pierce the cell with their stylet and push their head to enter the root. In contrast to root-knot nematodes, cyst nematodes migrate intracellularly. Similar to other plant-parasitic nematodes, beet cyst nematodes release cell wall degrading enzymes that aid in migration. During migration, the behavior of the juvenile is quite aggressive, which is reflected in the strong stylet movement and thrusting of nematode head against host cell wall. The juveniles migrate until they reach the vascular cylinder. Upon reaching the vascular cylinder, stylet movement of juveniles becomes gentle and probes individual cells one by one for their suitability to be selected as an initial syncytial cell (ISC). If the protoplast ruptures, the nematode retracts their stylet and move to the next cell. In this way juveniles finally select an ISC and become sedentary. After the selection of ISC, the stylet remains inserted inside for approximately 7 hours (preparatory phase), with no pumping of metacarpal bulb observed indicating that there is no feeding or injection of secretions at this stage. After preparation phase, nematodes withdraw their stylet and insert it again inside ISC, which is accompanied by movement of the metacarpal bulb leading to a cocktail of secretions into the infected host cell (Wyss, 1992).

An important structure, which is developed to aid nematode's supply of nutrients, is a feeding tube. The feeding tube is like a sieve, which allows only molecules of certain sizes to be ingested. It was observed that fluorochrome-labelled dextran molecules of mass up to 20 kDa were ingested by *Heterodera schachtii* but of 40 kDa were rejected (Böckenhoff & Grundler, 1994). Moreover proteins of 22 kDa and 28 kDa also did not pass the feeding tube; however, in case of *Globodera rostochiensis*, green fluorescent protein (GFP) of 32 kDa was taken up by the nematode (Urwin et al., 1997; Urwin et al., 1998; Goverse et al., 1998). It is suggested that along with size, the shape and charge of the molecules could also be important factors in ingestion of biomolecules through the feeding tube (Eves-van den Akker et al., 2014).

Nevertheless, the secretions injected into the host (so-called effectors) are postulated to modulate the host defense response and to customize feeding structure. The ISC expands by incorporation of neighboring cells through the partial dissolution of cell wall leading to the formation of a syncytium (Golinowski et al., 1996; Wyss and Grundler, 1992). The role of several host and nematode cell wall modifying enzymes and proteins in syncytium formation has been described in detail (Smant et al., 1998; Wang et al., 1999; De Meutter et al., 2001; De Boer et al., 2002; Vanholme et al., 2007). Transcriptomic, metabolomics and ultrastructural analysis have revealed a wealth of data providing detailed insights into

massive changes that accompany syncytium formation (Wieczorek et al., 2006; Siddique et al., 2009; Szakasits et al., 2009; Hofmann et al., 2010). Inside the syncytium endoreduplication occurs, large vacuole is replaced by numerous small vacuoles and the cytosol is filled by cellular organelles like mitochondria, ribosomes, endoplasmic reticulum, Golgi apparatus and plastids (Sobczak & Golinowski, 2011; reviewed by Bohlmann, 2015) (Figure 5).

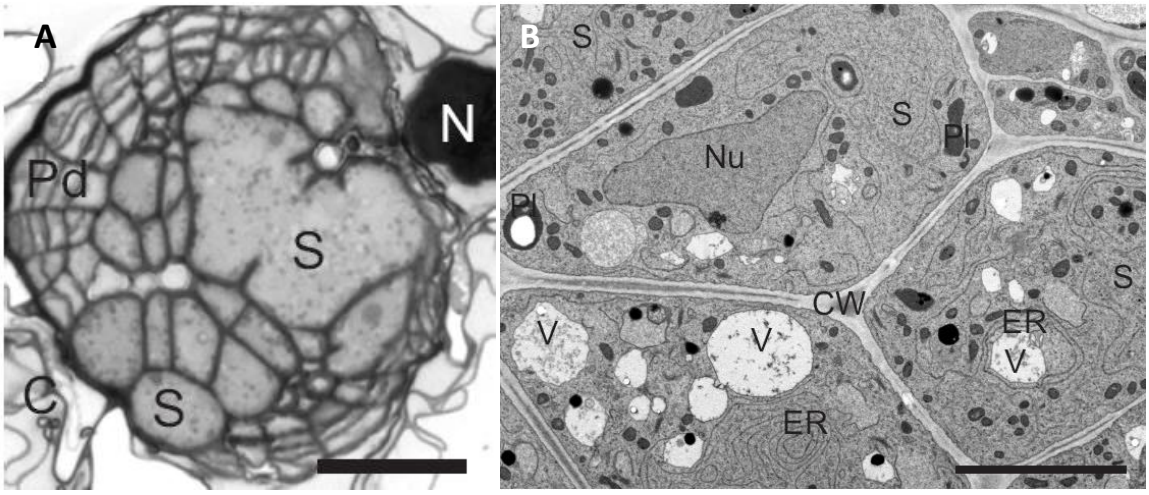

Figure 5: Light (A) and transmission electron microscopy (B) of 5 days old syncytium produced by *Heterodera schachtii* in *Arabidopsis* roots. Abbreviations: C-cortex, CW-cell wall, ER-cistern of endoplasmic reticulum, N-nematode, Nu-nucleus, Pd-peridermis-like tissue, Pl-plastid, S-syncytium, V-vacuole. Scale bars: 50 µm (Anjam et al., unpublished).

Upon establishment of the syncytium, nematode feeds from it and undergoes further two moulting stages J3 and J4 to become an adult. The J2s of cyst nematodes are sexually undifferentiated and after feeding their sex appears at the start of J3 or at late J2 phase. The adult male becomes worm form (Figure 6B) inside the cuticle sac and later on, comes out for fertilization. However female adopts pear shape formation (Figure 6A), stays connected and continue feeding from the feeding site. After fertilization, female turns to a brown cyst with few hundred eggs inside (reviewed by Bohlmann, 2015). The typical life cycle of cyst nematode is illustrated in Figure 7.

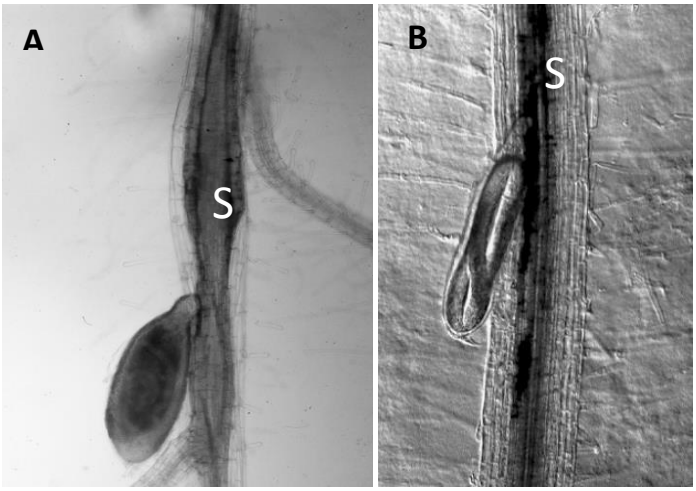

Figure 6: 12 days old adult female (A) and male (B) of *Heterodera schachtii* feeding from *Arabidopsis* root. S = syncytium (Golinowski et al., 1996).

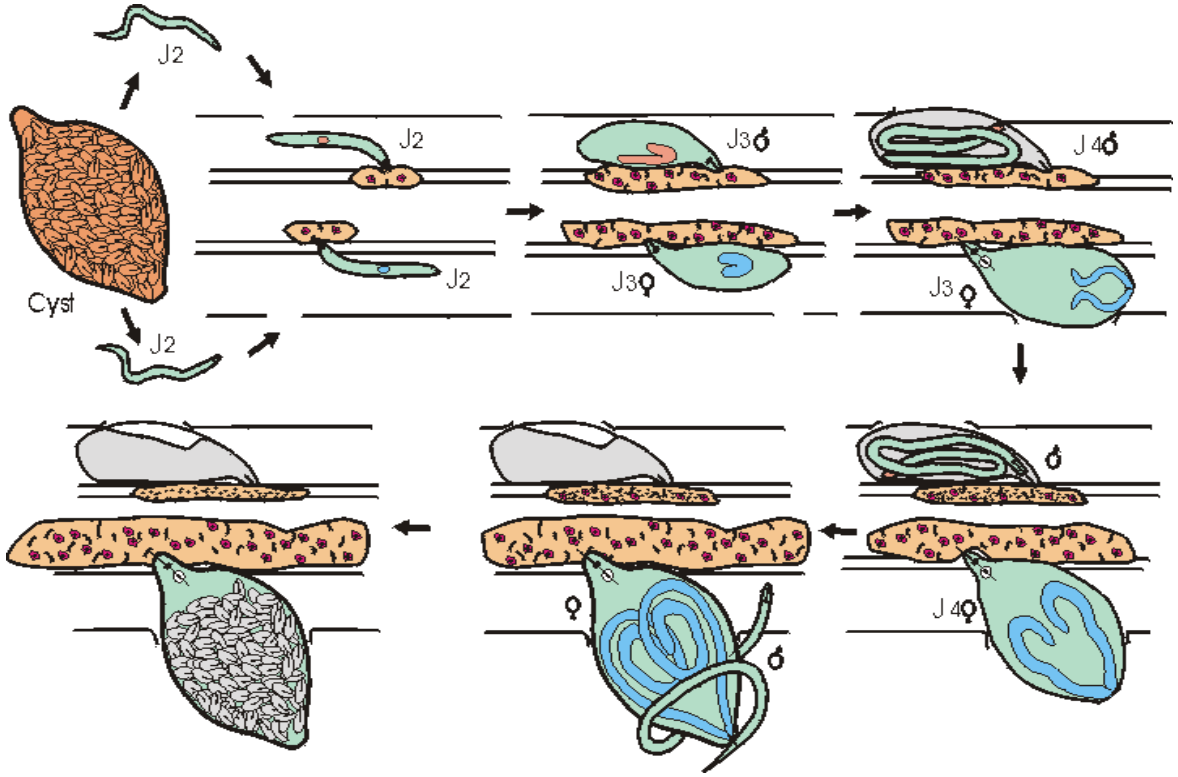

Figure 7: Schematic representation for the lifecycle of cyst nematodes (Courtesy of Florian M.W. Grundler).

In contrast to the male, the female requires 29 times more food during its life (Müller et al., 1981). Therefore, the syncytium associated to a female nematode is metabolically hyperactive and stays active for a longer period than it does for males. The observation that resistant cultivars of crop plants (for example sugar beet) support fewer females as compared to the susceptible ones indicates that environmental conditions play a role in sex

determination of cyst nematodes (Steele & Savitsky, 1981; Lelivelt & Hoogendoorn, 1993). Therefore, understanding and manipulation of the mechanism of sex determination in cyst nematodes have captured the attention of researchers since the beginning of 20th century. Mechanisms for sex determination in general in nematodes are quite diverse, ranging the gamut for all major sex determination mechanisms across the animal kingdom.

1.5. Sex determination in animals

Generally, in bisexual animals, depending upon their genetic constitution, the embryo (zygote) differentiates into a male or female. In the first step under genetic control, gonads are produced, which release sex hormones to direct the development of further sex-related phenotypes. However, the artificial manipulation of such hormones could alter sexual phenotypes. In this case, genes for controlling gonads or sex determination are randomly distributed on sex chromosomes and autosomes. In mammals, sex determination is controlled by sex chromosomes, where the male is heterogametic (XY), whereas the female contains a pair of equal sex chromosomes (XX). In humans, a person with the XXY condition of sex chromosomes is phenotypically a sterile male (Klinefelter's syndrome), whereas in "Turner's syndrome" (XO) the woman is sterile. This indicates that the Y chromosome plays a role in the development of male sexual appearance and functionality (Hunter, 1995). The X and Y chromosomes are unequal in size, and some part of the Y chromosome does not share homology with the X chromosome. This unequal region of the Y chromosome harbors genes considered essential to male fertility. However, in birds, as opposed to mammals, females are heterogametic (ZW) possessing an unequal pair of chromosomes, whereas males possess a ZZ genotype. The relationship between sexual phenotype and sex chromosome in birds is not fully clear due to unavailability of data on sex chromosomal abnormalities (Ellegren, 2000). In fruit flies (*Drosophila melanogaster*) XX is a female, and XY is a male; however, the Y chromosome does not exclusively control the male sex. In drosophila, XO is a fertile male, whereas XXY flies are fertile females (Cline, 1993). Molecular studies have concluded that the sex-lethal gene (*SXL*) controls sexual appearance in fruit flies, which is active when the ratio of X chromosome to the set of autosomes is 1:1, resulting in a female phenotype. The gene must be inactive to produce a male phenotype (Cline, 1993). In contrast to genetic control, the environment plays a significant role in sex differentiation in many animal species such as fish, reptiles, amphibians and nematodes.

In certain fresh water animals (*e.g.*, Cichild and Poleciliid fish), pH of water influences the sexual differentiation of gonads while in some others (*e.g.*, *Discoglussus pictus*) ionic ratio (K^+/Ca^{++}) of water is important for their sexual development. Moreover, in various classes of ectothermic vertebrates, the temperature has been shown to play a role in their sex determination. In some parasitic species of nematodes (*e.g.*, *Mermithidae*, *Meloidogyne* spp.) nutrition affects the sexual phenotype. Moreover, in amphipod, *Gammarus duebeni*, photoperiod seems to have an effect on sex differentiation. However, thus far, only temperature has clearly proven to be a determinant environmental factor influencing the sexual differentiation of gonads. In all species of crocodilians, the incubation temperature of eggs for a certain period of development determines sexual phenotype. There is a narrow range of incubation temperature that entirely (100%) changes phenotype from one sex to another and this range varies among species. In the European pond turtle (*Emys orbicularis*), incubation temperature below 28 $^{\circ}$C produces 100% male phenotype, whereas 100% of females are recovered at a temperature above 29 $^{\circ}$C (reviewed by Pieau et al., 1994; reviewed by Mittwoch, 1996). Regardless of sex chromosomes, temperature does indeed seem to have a critical effect on sex differentiation in a wide range of sexually dimorphic species.

1.6. Sex determination in nematodes

Most of the nematodes including plant-parasitic species are sexually dimorphic. The sex can be recognized phenotypically by primary and secondary sex characteristics. However, the mode of reproduction in nematodes could be amphimixis (cross-fertilization), automixis (self-fertilization) or parthenogenetic, depending upon the species. The male-to-female sex ratio is usually equal in nematode species that reproduce by amphimixis, whereas it varies in parthenogenetic and hermaphroditic species. Parthenogenetic species produce relatively few numbers of males (Triantaphyllou, 1973a). Interestingly, in hermaphroditic species, variable numbers of males have been observed albeit in some cases they are non-functional. In cases where males are functional, reproduction occurs partially by amphimixis and partially by automixis (Triantaphyllou, 1973b). The mechanisms by which this sexual differentiation occurs are extremely diverse in the phylum Nematoda. Nematodes show approximately all major mechanisms of sex determination, which are found across the animal kingdom. Genetic control of sex determination (like XX-XY or XX-XO chromosomes) is common in certain species, whereas environmental control is present in some other species (reviewed by Triantaphyllou, 1971). However, in certain nematodes, it remains unclear whether genetic or environment determines the sexual outcome. Even though sexual differentiation in these

cases is genetically controlled, the fitness of any sex to environmental conditions may decide the final outcome of the sex ratio.

1.6.1. Genetic sex determination (GSD)

Genetic sex determination is controlled by sex chromosomes (*e.g.*, XY) or by variation in chromosome numbers (*e.g.*, XO). In certain species, the presence of autosome sets or their balance to X-chromosome also triggers particular sex gonads in an individual (Steinmann-Zwicky et al., 1990; Heimpel & Boer, 2008). This type of sex determination is believed to be robustly controlled by the genetic composition of an embryo. The environment offers only a slight influence here. Other examples of genetic sex determination, where chromosomes distribution decide the final sex outcome of offspring, include XX – XO, ZW-ZZ, and NN-N. However, in certain cases the influence of the environment on post -embryogenesis events plays a major role in sex determination (reviewed by Goldstein, 1981).

Sex chromosomes are the unequal pair of chromosomes sharing partial homozygosity and they are generally known as X and Y. In the case of mammals, the female is homogametic (XX) and the male is heterogametic (XY), but in birds the opposite is true. In that case, the sex chromosomes are designated ZZ-ZW. The second type of sex chromosomes is XX-XO, where one sex has only one sex chromosome (X) along with autosomes and the other has a complete pair (XX).

In the majority of cases such as free-living and animal-parasitic nematodes, exhibit a mechanism of sex determination based on sex chromosomes, but such mechanism of sex determination remains unclear for plant-parasitic nematodes (reviewed by Goldstein, 1981). The system of XX-XY sex chromosomes occurs more often in animal-parasitic nematodes, for example, *Brugia pahangi*, *B. malayi*, *Trichuris muris*, *Haemonchus contortus*, *Ascaris lumbricoides* (Bremner, 1955; Goldstein, 1978; Sakaguchi et al., 1983; Spakulová et al., 1994). However, sex determination by a unequal number of sex chromosomes (XX-XO) is less common in animal-parasitic nematodes *e.g.*, *Strongyloides ratti* (Harvey & Viney, 2001). However, in the case of *Strongyloides ratti* the partner with XX chromosomes is parthenogenetic. Therefore, the nematodes reproduce both sexually and by parthenogenesis. Moreover, here the environment also seems to interact with gametogenesis because females produce a larger number of males when a host response is present (Harvey et al., 2000). The variation in sex determination in nematodes extends to multiple sex chromosomes controlling sexual phenotype, as reported in some animal-parasitic species. For example, *Ascaris incurve*

contains eight X chromosomes in germs cells and only one Y chromosomes. Therefore, a zygote acquires 42 chromosomes (26A + 16X) to be a female while 35 chromosomes (26A+8X+1Y) for a male (Goodrich, 1916).

In free-living nematodes, *C. elegans* is a well-studied model organism where the sex determination pathway has been described in detail. Sex determination in *C. elegans* occurs through the sex chromosomes (XX-XO). In this case, offspring with the XX genotype are hermaphrodites and those with XO are male. Hermaphrodites are somatically female and partially self-fertilize and reproduce by mating with males of XO genotype. However, in *C. elegans* X-linked dosage compensation is required for the sexual phenotype. The balance between autosomes and X chromosomes regulates the expression of master regulator gene *XOL1*, which dictates the pathway for sexual appearance. It promotes male characteristics, while inactivation of *XOL1* gives rise to female development (Meyer, 2006; Miller et al., 1988). Like *C. elegans*, the mechanism of sex determination in *Pristionchus pacificus* (an omnivorous nematode) is also controlled by an unequal number of X chromosomes that is XX-XO (Pires-Dasilva, 2007).

In contrast to the above-described examples of free-living and animal-parasitic nematodes, evidence for sex chromosomes in plant-parasitic nematodes are lacking. In general, cytological studies in sexually dimorphic species are very limited, and in the majority cases, they are restricted to females (reviewed by Triantaphyllou, 1971). However, on the basis of available reports, sex chromosomes in plant-parasitic species have not been recognized so far. Moreover, equal numbers of chromosomes are found in males and females (Triantaphyllou, 1971). Initially, it was assumed that sex chromosomes could be present in some species of *Heterodera* and *Meloidogyne* but it might be difficult to differentiate from autosomes because of their small size (1µ). However, later electron microscopic studies failed to produce any evidence for the presence of sex chromosomes (reviewed by Triantaphyllou, 1971; reviewed by Goldstein, 1981). Therefore, the role of the environment has drawn attention as the main player in the sexual differentiation of plant-parasitic nematodes.

1.6.2. Environmental sex determination (ESD)

In environmental sex determination, the sexual fate of an individual is influenced by the environment, independent of its genotypic constitution. Therefore, unlike GSD, in ESD the sex ratio of a certain species varies according to variation in environment. In nematode species where ESD is prevalent, environmental factors include nutritional availability,

temperature, hormones and the rate of infestation. In nematodes, studies on members of *Mermithidae* for the first time revealed evidence of environmental influence on sexual differentiation. Members of this family are the parasites of invertebrates and primarily insects. In several species, it was observed that when an insect was inoculated with single or few juveniles, in the majority of cases all of them developed into females. However, with a moderate infection density, the approximately equal ratio of females and males was recorded. In contrast, a high infection density of infecting juveniles in a single insect gave rise to all or mostly males (Petersen, 1972). In the entomopathogenic nematode *Heterorhabditis bacteriophora*, when researchers extended the starvation period of hatching juveniles more than 6 hours, the proportion of hermaphrodites increased. In smaller insects, the number of hermaphrodites increased but produced approximately equal numbers of females, hermaphrodites, and males in the case of injection of a single nematode. Sex differentiation in *H. bacteriophora* may depend on the supply of the nutritional source (Kahel-Raifer & Glazer, 2000). In animal-parasitic nematode *Strongyloides ratti*, the environment also seems to play a role in sex differentiation. However, environmental influence is limited to the time of gametogenesis only; after conception, sexual differentiation is genotypic (Harvey et al., 2000). The other examples of sex determination are found in plant-parasitic nematodes. The focus of research on these aspects of plant-parasitic nematodes arose due to their importance in pest management. Female nematodes are especially devastating because they cause more damage to the host plants owing to their high nutritional requirements of reproduction (Trudgill, 1967; Müller et al., 1981). The environmental control of the sex ratio of plant-parasitic nematodes has been reported in many species.

Meloidodera floridensis infects pine trees and reproduces by mitotic parthenogenesis. Triantaphyllou & Hirschmann (1973) kept the larvae of *Meloidodera floridensis* in tap water for 4 months and observed that 70% - 80% of them went through one or two moults to become male. Later on 50% of them became adult males. In natural conditions, 96% of the larvae infecting pine trees became female, whereas only 4% become male. Therefore Triantaphyllou & Hirschmann (1973) concluded that members of *Meloidodera floridensis* develop into females according to its genotype (thelytokous), but in starvation conditions, due to changes in gene expression or hormonal reasons, which may be controlled by feeding, they develop into males. Similarly, root-knot nematodes, *Meloidogyne incognita*, and *M. arenaria* do not produce many males under normal growth conditions suggesting that they are completely thelytokous (Triantaphyllou, 1963, 1973a). In *Meloidogyne incognita*, on the

basis of gonad anatomy, it was revealed that some female juveniles undergo sex reversal and proceed with further development as males. Sex reversal in an early period gives rise to males with one testis, which are almost indistinguishable from true males. More delayed sex reversal results in males with two testes of approximately equal size. To explain these patterns of development, it was assumed that sex differentiation is hormonally controlled and that the environment influences hormonal balance by affecting gene expression (Papadopoulou & Triantaphyllou, 1982). *M. arenaria* shows a similar pattern of sex determination which is influenced by the environment like *M. incognita* (Triantaphyllou, 1963, 1973a). Nevertheless, the majority of *Meloidogyne* species reproduce by parthenogenesis, where many males are also developed under certain environmental conditions. Laughlin et al. (1969) studied the effect of temperature on the sexual development of *Meloidogyne graminis*. They observed that the sex ratio was significantly altered with temperature. Specifically, at 21 °C and 16 °C, they observed no males in the population. However, they observed 80% males at 32 °C and 4% at 27 °C. Moreover, they observed male sex reversal and male intersex according to temperature. Later on, Webber and Fox (1971) observed different proportions of males from single egg mass isolates and single larvae and reasoned that variation was due to the different genetic potential of larvae to differentiate into males (reviewed by Triantaphyllou, 1973a). However, later studies found that variation in male numbers was due to the mode of reproduction. Higher numbers of males are produced when *Meloidogyne graminis* reproduces by amphimixis under adverse environmental conditions (Triantaphyllou, 1973b). In contrast to root-knot nematodes, cyst nematodes only reproduce bisexually. The role of environment in sexual differentiation in cyst nematodes is poorly understood.

1.7. Sex determination in cyst nematodes

Most important plant parasitic cyst nematodes are amphimictic. Several reports on sexual differentiation of cyst nematodes have been published, but the conclusions drawn are often contradictory. The first concept that sex differentiation in cyst nematode (*Heterodera schachtii*) could be regulated by the environment came from Molz's study in 1920. He observed imbalanced sex ratios under variable growth conditions of the host plant. He associated the high proportions of male differentiation to the unfavorable growing conditions of the host plant. However, Sengbusch (1927) contradicted Molz's conclusions and offered a different interpretation of the data. He suggested that variation in sex ratio was due to the differential death rate of females under unfavorable conditions because female need 35 times

more food than males. Later, Müller et al. (1981) confirmed that males stop feeding earlier than females and therefore consumes 29 times less food than females.

Variations in sex ratio due to the environment were also reported from potato cyst nematode. Ellenby (1954) confirmed that the sex ratio of *Heterodera rostochiensis* (now called *Globodera rostochiensis*) was different in the primary and lateral roots and varied with infection density. He correlated this with environmental influence on sex determination. Den Ouden (1960) supported this view when he recovered more females by infecting potato-seedlings with a single nematode (*H. rostochiensis*). Environmental influence on sex determination in potato cyst nematode was also supported by Trudgill (1967). He inoculated potato seedlings with single juveniles and found the male-to-female ratio approximately 0.89 and this ratio increased with the increasing density of invading nematodes. Furthermore, he removed the aerial parts of the inoculated potato seedlings and found an almost 5 times higher male-to-female ratio than in the control plant. This led him to conclude that sex determination of this nematode was influenced by the size of feeding site (giant cells) and the nutrients. He further concluded that a higher number of males are developed on secondary roots. In another study, Trudgill et al. (1967) tried to figure out genetic differences. He proposed that juveniles with a homozygous recessive genotype (aa) overcome resistance in *Solanum tuberosum* spp. antigena plants and become female. Juveniles with heterozygous (Aa) and dominant homozygous (AA) genotypes become males. Two years later, he endorsed these conclusions by experiments on three resistant and one susceptible potato cultivar inoculated with nine populations of potato cyst nematodes. He observed characteristic differences of sex ratios among different populations of nematodes (Trudgill & Parrott, 1969). Mugniery & Fayet (1984) also endorsed the hypothesis of epigenesis in sexual differentiation of *H. rostochiensis*. They studied the penetration of larvae with a higher inoculum load by putting them on excised root pieces of resistant and partial resistant cultivars. They observed that on the one hand larvae needed to induce giant cells for their development, and on other hand competition was strong, which made development difficult. Therefore, they ruled out the classical type of sexual differentiation. Meanwhile, the effect of infection density and invasion in secondary and tertiary roots on sexual ratio was also reported in the soybean cyst nematode (*Heterodera glycines*). In this case, variation in sex ratio was attributed to differential death rates of females under stress conditions (Koliopanos & Triantaphyllou, 1972). However, Evans and Fox (1977) found a 3:1 ratio of males to females in an Arkansas 1 isolate of *H. glycines* when applying only 1-2 juveniles to soybean

roots. They emphasized on alternative factors rather the classical genotypic mechanism of sex determination and differential death rate of females. The hypothesis they proposed was a polygenic control of sex determination as in *Meloidogyne graminis* or in mammals, where sexual phenotype appears as a result of genotype and sex hormones at the time of embryogenesis. The effect of temperature was also investigated in another study, but it did not show any effect on the sex ratio of *Heterodera glycines* (Melton et al., 1986). During this period, reports were also added from rice cyst nematodes. The experiments were designed almost in a similar way to observe the effect on sexual development either by increasing the infection density or removing the tops of the plants or both. It was concluded that the sex of *Heterodera oryzae* was genetically controlled but it was by epigenesis in *H. sacchari* (Cadet et al., 1975; Patrice et al., 1978). Regarding the cereal cyst nematode *H. avenae,* Kerry & Bridgeman (1980) drew conclusions about the differential death rate of females. They studied sex ratio by adding a single juvenile of different populations of *H. avenae* and found out that there was a variation in the invading ability of populations. Nevertheless, variation in the rate of invasion did not lead to changes in the proportion of male to female. Moreover, variation in sex ratio was observed on oats cv. Milford and cv. Sun II, but the number of males remained constant.

The story of sexual determination in sugar beet cyst nematode *Heterodera schachtii* linked to variable sex ratio contains several conflicting conclusions. A lot of work has been done to determine whether it is controlled by the environment or by genetics in terms of the underlying mechanism for the orientation of sexual development. As discussed earlier, Molz (1920) first time reported the environmental influence on sex determination of *Heterodera schachtii*. Sengbusch (1927) challenged this hypothesis, asserting that variation in sex ratio with regards to environmental change was in fact because of the differential death rate of females. In further reports, other environmental factors like nitrogen deficiency, restriction of water supply, lack of light and infection density was shown to affect sex ratio. Along with these results, it was suggested that sexual development was influenced by nutritional availability (Apel & Kämpfe, 1957; Kämpfe & Kerstan, 1964). However, conclusions presented in some of following reports contradicted this opinion. An experiment involving adding a single juvenile to sugar beet roots showed that male-to-female sex ratio was equal, as appears in genetically controlled sex determination (Kerstan, 1969). Moreover, it was explained that when sex ratio varies under variable environmental conditions, the male percentage remains constant, but the female percentage varies. The study associated the

phenomenon of female's survival with environmental or nutritional variations (Viglierchio & Johnson, 1969). The possibility of sex chromosomes in *H. schachtii* was addressed by Triantaphyllou (1974) when he conducted cytological studies of about 12 bisexual species of *Heterodera* including *H. schachtii*. It revealed equal numbers of chromosomes in males and females and no sex chromosomes were found. The other known mechanism of genetic sex determination is single or multi-locus sex determination, where alleles of one or more genes regulate sexual development (De Boer et al., 2008; Whiting, 1943).

The concept of single locus-complementary sex determination emerged in 1933 in Hymenoptera insects, when a researcher found that in addition to haploid, some diploid insects were also males (Whiting, 1933). The females were diploid and produced as a result of fertilization. In following studies a locus was highlighted, which, if present in the homozygous or hemizygous form, results in male development, while heterozygous form leads to the female formation (Stahlhut & Cowan, 2004; Van Wilgenburg et al., 2006; Whiting, 1943). However, such examples are not known in nematodes. Moreover, this possibility does not seem to occur in *H. schachtii*, which is strictly amphimictic and females cannot reproduce without fertilization. Moreover, there are several known genetic disorders in various animals where a mutation in a single gene alters the sexual phenotype. For example, in mice, autosomal dominant mutation (*sxr*) converts a genotypically female (XX) into a phenotypic male, albeit with smaller testis (Hodgkin & Brenner, 1977; Cattanach et al., 1971). Similarly, in *C. elegans* where the sex determination pathway has been mapped in great detail, single gene mutations have been linked to sex reversal (Hodgkin, 1983). Intriguingly, the primary sex determination mechanism in all these organisms is chromosomal.

Further evidence of environmental sex determination in *H. schachtii* came from Grundler (1991). In this case, experiments were performed under sterile conditions using monoxenic cultures to evaluate the role of nutrition in sexual differentiation. The underlying hypothesis assumed that changing the nutritional status of the host plant by changing exogenous sucrose supply may change nutritional status of the syncytium (feeding site), thus affecting juvenile development. The author expected that under good nutritional conditions more females should develop only if sexual development is environmentally controlled. Otherwise, a balanced sex ratio should result because plenty of nutrients can support both sexes equally. The data showed that indeed a higher number of females developed in good nutritional conditions, supporting the effect of the environment on the sexual outcome of nematodes.

However, under poor nutritional conditions, instead of more males, a lot of undeveloped juveniles were found and a balanced sex ratio was never found (Grundler et al., 1991). This study served as an important milestone to support the effect of environment on sexual differentiation. Based on these observations, one can conclude that the syncytium, which forms the nutritional environment for nematodes, should be somehow different in males and females. This hypothesis is supported by several other reports showing the differences in size of male- and female-associated syncytia (Kerstan, 1969; Müller et al., 1981; Caswell-Chen & Thomason, 1993). Furthermore, electron microscopy of male- and female-associated syncytia of adult nematodes showed ultrastructural differences (Sobczak et al., 1997), which reflects differences in biochemical signaling or molecular events between the two syncytia.

In the present studies, we assumed that male- and female-associated syncytia can be a source for exploring host genes, which may influence the sex determination of *H. schachtii*. Therefore, we planned to study a comparative transcriptome of both syncytia types. We selected *Arabidopsis thaliana* as a host plant because it has been extensively used for studies in plant sciences. The molecular information about this plant is available more than any other plant. Moreover, hybridisation gene chips are also commercially available for differential expression studies. However, there were certain associated challenges. The sample collection at a time point when nematodes have already become adult may not contain information of molecular events influencing sexual differentiation. Therefore, it was important to collect samples at an early time point when the sex of the nematodes was still under differentiation. However, sample collection at an early time point posed certain challenges. First, male and female nematodes can only be differentiated around 10 days post infection when they already become adults (dpi). We solved this problem by devising a strategy to predict the sex of nematodes at an earlier time point of 5 dpi. The strategy is based on the above-stated fact that the female nematodes consume 29 times more food than males; therefore, female development is faster than that for males and the associated syncytia of female is more hypertrophied than that for males (Caswell-Chen & Thomason, 1993; Kerstan, 1969; Muller et al., 1981). More detail about this strategy appears in Chapter 3. The second problem was isolating pure syncytial cells because syncytia at 5 dpi are usually small in size particularly for males. The dissected tissues may have contained a high quantity of surrounding uninfected cells, which could dilute the effect of expressed genes in comparative studies. Therefore, we used laser capture microdissection to isolate pure cells.

1.8. Laser capture microdissection (LCM)

Laser capture microdissection (LCM) allows for the isolation of RNA, DNA, proteins and metabolites from a heterogeneous cell population. In this technique, the laser is coupled with microscope focusing on a slide. The microscope helps to select the target cells from a micro-section placed on a slide, which is excised with a laser beam. Depending upon the instrument model, the excised cells are either collected by gravity or catapulted into an "adhesive cap" using a photonic pulse. This is a contact-free method of sample collection which is commonly adopted in more recent models. Alternatively, at the time of excision, a film of long chain polymers transiently melts exactly over the selected cells, which remains embedded after separation from the whole section (Curran et al., 2000; Reviewed by Ludwig & Hochholdinger, 2014).

The procedure of LCM involves longer steps of tissue preparation, embedding, and sectioning. For the successful application of LCM, good morphological preservation of tissues is required. Furthermore, the isolated RNA, DNA or proteins should be of high quality for downstream processing. The collected samples need to be immediately fixed in a suitable fixative because it is required for embedding and sectioning. For excision of targeted cells, 2-20 µm sections of sample tissues are adhered on slides. Therefore, tissue preparation is important for the morphological preservation of sections, required to identify a specific cell type. In immuno-histological studies, paraformaldehyde is usually used for tissue fixation. It is known for preserving a high quality of section morphology (Srinivasan et al., 2002). However, its use is avoided in experiments where RNA isolation is the objective because it cross-links with nucleic acid making its recovery difficult (Srinivasan et al., 2002; Kerk et al., 2003; Inada & Wildermuth, 2005; Klink et al., 2005). The alternative fixative is Farmer's solution (ethanol: acetic acid). This is preferred in the latter type of experiments. After tissue fixation, the next step is embedding of tissues using paraffin or OCT (optimum cutting temperature) medium for cryo-sectioning. In paraffin embedding, tissues are embedded in molten paraplast and sections are made at room temperature using a rotary microtome. This is a very long procedure and the majority of the steps are performed at room temperature, so RNA degradation could be high. Cryo-sectioning allows the whole procedure to be performed at a low temperature, which minimizes RNA degradation (Nakazono et al., 2003;

Barcala et al., 2010). Later steps involve adhering the sections to glass slides and removing the embedding material, followed by laser dissection and RNA isolation.

LCM had been widely used in medical sciences, but in plant sciences, the first time was when Nakazono et al. (2003) reported its application for the isolation of epidermis and vascular tissues of maize roots. They isolated RNA and successfully used it for microarray studies. Soon after, Kerk et al. (2003) optimized the procedure of LCM for RNA isolation from a variety of plant tissues using paraffin-embedded sections. Later on, the technique was also applied to study differential gene expression in the syncytial cells of soybean roots infected with cyst nematode *H. glycine* (Ithal et al., 2007; Klink et al., 2005; Klink et al., 2007). They used paraffin embedding for the processing of tissues and showed differential regulation of certain genes. However, in *Arabidopsis*, Barcala et al. (2010) used LCM for giant cells induced by root-knot nematode *Meloidogyne incognita*. They used cryo-sectioning, and the isolated RNA was amplified for microarray studies. This method was a good choice to follow in our experiments. However, during RNA isolation we encountered some issues related to its quality. Therefore, we had to optimize the protocol for isolation of quality RNA from syncytial cells in *Arabidopsis* roots. A detailed description has been given in Chapter 2.

The objective of the present study was to explore the genes of the host plant (*Arabidopsis*), which may play a role in the sex determination of *Heterodera schachtii*. It was assumed that transcriptomic studies of male- and female-associated syncytia at an early feeding stage could highlight the genes with a possible role in the sexual development of the nematode. Therefore to accomplish these studies, a methodology was developed and validated for sex prediction of nematodes at earlier feeding point. For RNA isolation from the pure syncytial material, LCM was used to avoid the contamination of non-infected tissues. The RNA isolated by this method was amplified and used for gene chip hybridization with the *Arabidopsis* genome. The details of this strategy have been described in Chapter 3. Furthermore, in Chapter 3, the data obtained from transcriptomic studies were analyzed with reference to transcriptional differences between male- and female-associated syncytia. The categories of genes showing prominent transcriptional differences between the two syncytia were discussed. On the basis of the transcriptomic data, some of the candidate genes were analyzed for their effect on the sexual differentiation of the nematodes by using the loss of function mutants of *Arabidopsis*. Moreover, to visualize differential expression between male- and female-associated syncytia, promoter::reporter lines of *Arabidopsis* were developed. The results of loss of function

mutants and promoter::reporter lines are also discussed in Chapter 3. Whereas, the general discussion in the context of present studies, has been described in Chapter 4.

1.9. References

Albonico, M., Crompton, D. W. T. & Savioli, L. Control strategies for human intestinal nematode infections. *Adv. Parasitol.* **42,** 277–341 (1999).

Angstadt, J. D., Donmoyer, J. E. & Stretton, A. O. Retrovesicular ganglion of the nematode *Ascaris*. *J. Comp. Neurol.* **284,** 374–88 (1989).

Apel, A. & Kämpfe, L. Beziehungen Zwischen Wirt Und Parasit Im Infektionsverlauf Von *Heterodera schachtii* Schmidt in Kurzfristigen Topfversuchen. *Nematologica* **2,** 131–143 (1957).

Barbercheck, M. E. Insect-parasitic nematodes for the management of soil-dwelling insects in *Entomological Notes*. (Department of Entomology, The Pennsylvania State University, 2005).

Barcala, M., García, A., Cabrera, J., Casson, S., Lindsey, K., Favery, B., García-Casado, G., Solano, R., Fenoll, C. & Escobar, C. Early transcriptomic events in microdissected *Arabidopsis* nematode-induced giant cells. *Plant J.* **61,** 698–712 (2010).

Bird, D. M. & Bird, A. F. Plant-parasitic nematodes: In *Parasitic Nematodes*: *Molecular Biology, Biochemistry and Immunology* (eds. Kennedy, M. W. & Harnett, W.) 139–166 (CABI, 2001).

Bird, D. M. & Digennaro, P. M. The complex armoury of plant-parasitic nematodes: In *Parasitic Nematodes*: *Molecular Biology, Biochemistry and Immunology* (eds. Kennedy, M. W. & Harnett, W.) 30–66 (CABI, 2013).

Blackburn, B. G. & Barry, M. Soil-transmitted helminths: Ascaris, Trichuris, and Hookworm infections: In *Water and Sanitation-Related Diseases and the Environment: Challenges, Interventions, and Preventive Measures* (ed. Selendy, J. M. H.) 81–93 (John Wiley & Sons, Inc., 2011).

Böckenhoff, A. & Grundler, F. M. W. Studies on the nutrient uptake by the beet cyst nematode *Heterodera schachtii* by in situ microinjection of fluorescent probes into the feeding structures in *Arabidopsis thaliana*. *Parasitology* **109,** 249-255 (1994).

Bohlmann, H. Introductory chapter on the basic biology of cyst nematodes. *Adv. Bot. Res.* **73,** 33–59 (2015).

Bremner, K. Cytological studies on the specific distinctness of the ovine and bovine 'Strains' of the nematode *Haemonchus contortus* (Rudolphi) cobb (NematodaL Trichostrongylidae). *Aust. J. Zool.* **3,** 312 (1955).

Burkhart, C. N. & Burkhart, C. G. Assessment of frequency, transmission, and genitourinary complications of *Enterobiasis* (pinworms). *Int. J. Dermatol.* **44,** 837–840 (2005).

Cadet, P., Merny, G. & Reversat, G. Factors affecting sex determination in *Heterodera oryzae* (Nematoda: *Tylenchoidea*). *Cah. O.R.S.T.O.M., Ser. Biol. Nematol.* **10,** 207–214 (1975).

Caswell-Chen, E. P. & Thomason, I. J. Root volumes occupied by different stages of *Heterodera schachtii* in sugarbeet, *Beta vulgaris*. *Fundam. Appl. Nematol.* **16,** 39–42 (1993).

Cattanach, B. M., Pollard, C. E. & Hawkes S. G. Sex-reversed mice: XX and XO males. *Cytogenetics* **10,** 318–337 (1971).

Chan, M. The global burden of intestinal nematode infections-fifty years on. *Parasitol. Today* **13,** 438–443 (1997).

Chitwood, B. G. The designation of official names for higher taxa of invertebrates. *Bull. Zool. Nomencl.* **15,** 860–895 (1958).

Cline, T. W. The Drosophila sex determination signal: how do flies count to two? *Trends Genet.* **9,** 385–390 (1993).

Cranshaw, W. & Zimmerman, R. Insect parasitic nematodes. (Fact Sheet No. 5.573, Extension, Colorado State University, 2013).

Curran, S., McKay, J. A., McLeod, H. L. & Murray, G. I. Laser capture microscopy. *Mol. Pathol.* **53,** 64–8 (2000).

De Boer, J. G., Ode, P.J., Rendahl, A. K., Vet, L. E., Whitfield, J. B. & Heimpel, G. E. Experimental support for multiple-locus complementary sex determination in the parasitoid *Cotesia vestalis*. *Genetics* **180,** 1525–35 (2008).

De Boer, J. M., Davis, E. L., Hussey, R. S., Popeijus, H., Smant, G. & Baum T. J. Cloning of a putative pectate lyase gene expressed in the subventral esophageal glands of *Heterodera glycines*. *J. Nematol.* **34,** 9–11 (2002).

De Ley, P. & Blaxter, M. Systematic Position and Phylogeny: In *The Biology of Nematodes* (ed. Lee, D. L.) 59-139 (Taylor & Francis e-Library, 2005).

De Ley, P. A quick tour of nematode diversity and the backbone of nematode phylogeny in *WormBook* (2006).

De Meutter, J., Vanholme, B., Bauw, G., Tytgat, T., Gheysen, G. & Gheysen G. Preparation and sequencing of secreted proteins from the pharyngeal glands of the plant parasitic nematode *Heterodera schachtii*. *Mol. Plant Pathol.* **2,** 297–301 (2001).

Decraemer, W. & Hunt, D. J. Structure and classification: In *Plant Nematology* (eds. Perry, R. N. & Moens, M.) 3–32 (CABI, 2006).

Den Ouden, H. A note on parthenogenesis and sex determination in *Heterodera rostochiensis* Woll. *Nematologica* **5,** 215–216 (1960).

Ellegren, H. Evolution of the avian sex chromosomes and their role in sex determination. *Trends Ecol. Evol.* **15,** 188–192 (2000).

Ellenby, C. Environmental determination of the sex ratio of a plant parasitic nematode. *Nature* **174,** 1016–1017 (1954).

Elmer, N. R. & Glen, N. A., Gerhard, S. A. & Austin, M. J. *Parasitology: The Biology of Animal Parasites*. (Lea and Febiger, 1961).

Escobar, C., Barcala, M., Cabrera, J. & Fenoll, C. Overview of root-knot nematodes and giant cells. *Adv. Bot. Res.* **73,** 1–32 (2015).

Evans, D. M. & Fox, J. A. The sex ratio of *Heterodera glycines* at low population densities. *J. Nematol.* **9,** 207–210 (1977).

Eves-van den Akker, S., Lilley, C. J., Ault, J. R., Ashcroft, A. E., Jones, J. T. & Urwin, P. E. The feeding tube of cyst nematodes: characterisation of protein exclusion. *PLoS One* **9,** (2014).

Fae, F. Worms - A review. *S. Afr. Pharm. J.* **77,** 38–48 (2010).

Gibbons, L. M. General organisation: In *The Biology of Nematodes* (ed. Lee, D. L.) 59-139 (Taylor & Francis e-Library, 2005).

Goldstein, P. Sex determination in nematodes: In *Plant Parasitic Nematodes* (eds. Zuckerman, B. M. & Rohde, R. A.) 37–60 (Academic Press, 1981).

Goldstein, P. Ultrastructural analysis of sex determination in *Ascaris lumbricoides* vat. suum. *Chromosom.* **66,** 59–69 (1978).

Golinowski, W., Grundler, F. M. W. & Sobczak, M. Changes in the structure of *Arabidopsis thaliana* during female development of plant-parasitic nematode *Heterodera schachtii*. *Protoplasma*. **194,** 103–116 (1996).

Goodrich, H. B. The germ cells in *Ascaris incurva*. *J. Exp. Zool.* **21,** 61–99 (1916).

Goverse, A., Biesheuvel, J., Wijers, G. J., Gommers, F. J., Bakker, J., & Schots, A. In planta monitoring of the activity of two constitutive promoters, CaMV 35S and TR2', in developing feeding cells induced by *Globodera rostochiensis* using green fluorescent protein in combination with confocal laser scanning microscopy. *Physiol. Mol. Plant Pathol.* **52,** 275–284 (1998).

Grundler, F. M. W., Marlies, B. & Wyss, U. Influence of changes in nurse cell system (syncytium) on sex determination and development of the cyst nematode *Heterodera schachtii*: Total amount of proteins and amino acids. *Phytopathology* **81,** 70–74 (1991).

Harvey, S. C. & Viney, M. E. Sex determination in the parasitic nematode *Strongyloides ratti*. *Genetics* **158,** 1527–1533 (2001).

Harvey, S. C., Gemmill, A. W., Read, A. F. & Viney, M. E. The control of morph development in the parasitic nematode *Strongyloides ratti*. *Proc. Biol. Sci.* **267,** 2057–63 (2000).

Heimpel, G. E. & de Boer, J. G. Sex determination in the *Hymenoptera*. *Annu. Rev. Entomol.* **53,** 209–230 (2008).

Hodgkin, J. A. & Brenner, S. Mutations causing transformation of sexual phenotype in the nematode *Caenorhabditis elegans*. *Genetic*s **86,** 275-287 (1977).

Hodgkin, J. Two types of sex determination in a nematode. *Nature* **304,** 267–268 (1983).

Hofmann, J., Elashry, A- N., Anwar, S., Erban, A., Kopka, J. & Grundler, F. M. W. Metabolic profiling reveals local and systemic responses of host plants to nematode parasitism. *Plant J.* **62,** 1058–1071 (2010).

Hunter, R. H. F. Mechanisms of sex determination: In *Sex determination, Differentiation and Intersexuality in Placental Mammals*. 22-63 (Cambridge University Press, 1995).

Inada, N. & Wildermuth, M. C. Novel tissue preparation method and cell-specific marker for laser microdissection of *Arabidopsis* mature leaf. *Planta* **221,** 9–16 (2005).

Ithal, N., Recknor, J., Nettleton, D., Maier, T., Baum, T. J., & Mitchum, M. G. Developmental transcript profiling of cyst nematode feeding cells in soybean roots. *Mol. Plant-Microbe. Interact.* **20**, 510–525 (2007).

Jasmer, D. P., Goverse, A. & Smant, G. Parasitic nematode interactions with mammals and plants. *Annu. Rev. Phytopathol* **41,** 245–70 (2003).

Jones, J. T., Haegeman, A., Danchin, E. G., Gaur, H. S., Helder, J., Jones, M. G., Kikuchi, T., Manzanilla-López, R., Palomares-Rius, J. E., Wesemael, W. M. & Perry, R. N. Top 10 plant-parasitic nematodes in molecular plant pathology. *Mol. Plant Pathol.* **14,** 946–961 (2013).

Kahel-Raifer, H. & Glazer, I. Environmental factors affecting sexual differentiation in the entomopathogenic nematode *Heterorhabditis bacteriophora*. *J. Exp. Zool.* **287,** 158–66 (2000).

Kämpfe, L. & Kerstan, U. Die Beeinflussung des Geschlechtsverhältnisses in der Gattung *Heterodera Schmidt*. *Nematologica* **10,** 388–398 (1964).

Kerk, N. M., Ceserani, T., Tausta, S. L., Sussex, I. M. & Nelson, T. M. Laser capture microdissection of cells from plant tissues. *Plant Physiol.* **132,** 27–35 (2003).

Kerry, B. R. & Bridgeman, M. R. The sex ratios of cyst-nematodes produced by adding single second-stage juveniles to host roots. *Nematologica* **26,** 209–213 (1980).

Kerstan, U. Die Beeinflussung des Geschlechterverhältnisses in der Gattung *Heterodera*. *Nematologica* **15,** 210–228 (1969).

Klink, V. P., Alkharouf, N., MacDonald, M. & Matthews, B. Laser capture microdissection (LCM) and expression analyses of *Glycine max* (soybean) syncytium containing root regions formed by the plant pathogen *Heterodera glycines* (soybean cyst nematode). *Plant Mol. Biol.* **59,** 965–979 (2005).

Klink, V. P., Overall, C. C., Alkharouf, N. W., MacDonald, M. H. & Matthews, B. F. Laser capture microdissection (LCM) and comparative microarray expression analysis of syncytial cells isolated from incompatible and compatible soybean (*Glycine max*) roots infected by the soybean cyst nematode (*Heterodera glycines*). *Planta* **226,** 1389–1409 (2007).

Koliopanos, C. N. & Triantaphyllou, A. C. Effect of Infection density on sex ratio of *Heterodera glycines*. *Nematologica* **18,** 131–137 (1972).

Laughlin, C. W., Williams, A. S. & Fox, J. A. The Influence of temperature on development and sex differentiation of *Meloidogyne graminis*. *J. Nematol.* **1,** 212–215 (1969).

Lee, D. L. Life cycles: In *The Biology of Nematodes* (ed. Lee, D. L.) 141-162 (Taylor & Francis e-Library, 2005).

Lelivelt, C. L. C. & Hoogendoorn, J. The development of juveniles of *Heterodera schachtii* in roots of resistant and susceptible genotypes of *Sinapis alba*, *Brassica napus*, *Raphanus sativus* and hybrids. *Netherlands J. Plant Pathol.* **99,** 13–22 (1993).

Ludwig, Y. & Hochholdinger, F. Laser microdissection of plant cells: In *Plant cell Morphogenesis: Methods and Protocols* (eds. Žárský, V.& Cvrcková, F.) 249–258 (Springer, Heidelberg, 2014).

Maykel, J. A. & Steele, S. R. Other benign colorectal disorders: In *The ASCRS Textbook of Colon and Rectal Surgery* (eds. David E. B., Patricia, L. R., Theodore, J. S., Anthony, J. S., Michael J. S. & Steven, D. W.) 565–596 (Springer, New York, 2011).

Melton, T. A., Jacobsen, B. J. & Noel, G. R. Effects of temperature on development of *Heterodera glycines* on *Glycine max* and *Phaseolus vulgaris*. *J. Nematol.* **18,** 468–474 (1986).

Meyer, B. J. Somatic sex determination in *C. elegans*: In *WormBook* (2006).

Miller, L. M., Plenefisch, J. D., Casson, L. P. & Meyer, B. J. *XOL-1*: A gene that controls the male modes of both sex determination and X chromosome dosage compensation in *C. elegans*. *Cell* **55,** 167–183 (1988).

Mittwoch, U. Sex-determining mechanisms in animals. *Trends Ecol. Evol.* **11,** 63–67 (1996).

Molz, E. Versuche zur Ermittlung des Einflusses aüsserer Faktoren auf des Geschlechtsverhältnis des Rübennematoden (*Heterodera schachtii* A. Schmidt). *Landw. Jb.* **54**, 769-91 (1920).

Mousley, A., McVeigh, P., Dalzell, J. J. & Maule, A. G. Nematode neuropeptide communication systems: In *Parasitic Nematodes: Molecular Biology, Biochemistry and Immunology* (ed. Kennedy, M. W.) 279–307 (2013).

Mugniery, D. & Fayet, G. Détermination du sexe de *Globodera rostochiensis* Woll. et influence des niveaux d'infestation sur la pénétration, le développement et le sexe de ce nérnatode. *Rev. Ndmatol*. **7,** 233–238 (1984).

Müller, J., Rehbock, K. & Wyss, U. Growth of *Heterodera schachtii* with remarks on amounts of food consumed. *Rev. Nematol.* **4,** 227–234 (1981).

Munn, A. E. & Munn, D. P. Feeding and Digestion: In *The Biology of Nematodes* (ed. Lee, D. L.) 415–461 (Taylor & Francis e-Library, 2005).

Nakazono, M., Qiu, F., Borsuk, L. A. & Schnable, P. S. Laser-capture microdissection, a tool for the global analysis of gene expression in specific plant cell types: identification of genes expressed differentially in epidermal cells or vascular tissues of maize. *Plant Cell* **15,** 583–96 (2003).

Nanda, J. C. & Stretton, A. O. W. In situ hybridization of neuropeptide-encoding transcripts afp-1, afp-3, and afp-4 in neurons of the nematode *Ascaris suum*. *J. Comp. Neurol.* **518,** 896–910 (2010).

Nicol, J. M., Turner, S. J., Coyne, D. L., Nijs, L., den Hockland, S. & Maafi, Z. T. Current nematode threats to world agriculture: In *Genomics and Molecular Genetics of Plant-Nematode Interactions* (eds. Jones, J., Gheysen, G. & Fenoll, C.) 21–43 (Springer, Netherlands, 2011).

Papadopoulou, J. & Triantaphyllou, A. Sex differentiation in *Meloidogyne incognita* and anatomical evidence of sex reversal. *J. Nematol.* **14,** 549–566 (1982).

Patrice, C., Georges, M. Influence of some factors on sex-ratio in *Heterodera oryzae* and *H. sacchari* (Nematoda : *Heterodesidae*). *Rev. Nematol.* **1,** 143–149 (1978).

Perry, R. N. & Moens, M. Introduction to plant-parasitic nematodes; modes of parasitism: In *Genomics and Molecular Genetics of Plant-Nematode Interactions* (eds. Jones, J., Gheysen, G. & Fenoll, C.) 3–20 (Springer, Netherlands, 2011).

Petersen, J. J. Factor effecting sex ratios of a Mermithid parasite of mosquitoes. *J. Nematol.* **4,** 83-87 (1972).

Pieau, C., Girondot, M., Desvages, G., Dorizzi, M., Richard-Mercier, N. & Zaborski, P. Environmental control of gonadal differentiation: In *The Differences between the Sexes* (eds. Short, R.V. & Balaban, E.) 433-448, (Cambridge University Press, 1994).

Pires-Dasilva, A. Evolution of the control of sexual identity in nematodes. *Semin. Cell Dev. Biol.* **18,** 362–370 (2007).

Platzer, E. G. Biological control of mosquitoes with mermithids. *J. Nematol.* **13,** 257–262 (1981).

Poinar, G. O. Mermithid (Nematoda) parasites of spiders and harvestme *N. J . Arachnol.* **13,** 121–128 (1985).

Pokharel, R. Importance of plant parasitic nematodes in Colorado crops (Fact Sheet No. 2.952) (Colorado Research Center, 2011).

Rafiq, M. S. *Tylenchida: parasites of plants and insects*. (CABI, 2000).

Robert W. Li. & Louis C. G. Gene expression in the bovine gastro-intestinal tract during nematode infection: In *Veterinary parasitology* (ed. LaMann, G. V.) 157-178 (Nova Biomedical Press Inc. New York, 2010).

Robinson, M. W. & Dalton, J. P. Zoonotic helminth infections with particular emphasis on fasciolosis and other trematodiases. *Philos. Trans. R. Soc. Lond. B. Biol. Sci.* **364,** 2763–76 (2009).

Sakaguchi, Y., Tada, I., Ash, L. R. & Aoki, Y. Karyotypes of *Brugia pahangi* and *Brugia malayi* (Nematoda: *Filarioidea*). *J. Parasitol.* **69,** 1090 (1983).

Sengbusch, R. Beitrag zur biologie des Rübennematoden *Heterodera schachtii*. *Z. Pflanzenkrankh* **37**, 86-102 (1927).

Siddique, S., Endres S., Atkins, J. M., Szakasits, D., Wieczorek, K., Hofmann, J., Blaukopf, C., Urwin P. E., Tenhaken, R., Grundler, F. M. W., Kreil D. P. & Bohlmann, H. Myo-inositol oxygenase genes are involved in the development of syncytia induced by *Heterodera schachtii* in *Arabidopsis* roots. *New Phytol.* **184,** 457–472 (2009).

Smant, G., Stokkermans, J. P., Yan, Y., de Boer, J. M., Baum, T. J., Wang, X., Hussey, R. S., Gommers, F. J., Henrissat, B., Davis, E. L., Helder, J., Schots, A. & Bakker, J. Endogenous cellulases in animals: isolation of beta-1, 4-endoglucanase genes from two species of plant-parasitic cyst nematodes. *Proc. Natl. Acad. Sci. U. S. A.* **95,** 4906–11 (1998).

Sobczak, M. & Golinowski, W. Cyst nematodes and syncytia: In *Genomics and Molecular Genetics of Plant-Nematode Interactions* (eds. Jones, J., Gheysen, G. & Fennol, C.) 61–81 (Springer, Netherlands, 2011).

Sobczak, M., Golinowski, W. & Grundler, F. M. W. Changes in the structure of *Arabidopsis thaliana* roots induced during development of males of the plant parasitic nematode *Heterodera schachtii*. *Eur. J. Plant Pathol.* **103,** 113–124 (1997).

Sommer, R. J. & Ogawa, A. The genome of *Pristionchus pacificus* and the evolution of parasitism: In *Parasitic Nematodes: Molecular Biology, Biochemistry and Immunology* (eds. Kennedy, M. W. & Harnett, W.) 86–98 (CABI, 2013).

Spakulová, M., Králová, I. & Cutillas, C. Studies on the karyotype and gametogenesis in *Trichuris muris*. *J. Helminthol.* **68,** 67–72 (1994).

Srinivasan, M., Sedmak, D. & Jewell, S. Effect of fixatives and tissue processing on the content and integrity of nucleic acids. *Am. J. Pathol.* **161,** 1961–1971 (2002).

Stahlhut, J. K. & Cowan, D. P. Single-locus complementary sex determination in the inbreeding wasp *Euodynerus foraminatus* Saussure (Hymenoptera: *Vespidae*). *Heredity* **92,** 189–196 (2004).

Steele, E. & Savitsky, H. Resistance of trisomic and diploid hybrids of *Beta vulgaris* and *B.*

procumbens to the sugarbeet nematode, *Heterodera schachtii* Arnold. *J. Nematol.* **13,** 352–357 (1981).

Steinmann-Zwicky, M., Amrein, H. & Nöthiger, R. Genetic control of sex determination in *Drosophila*. *Adv. Genet.* **27,** 189–237 (1990).

Szakasits, D., Heinen, P., Wieczorek, K., Hofmann, J., Wagner, F., Kreil, D. P. Sykacek, P., Grundler, F. M. W. & Bohlmann, H. The transcriptome of syncytia induced by the cyst nematode *Heterodera schachtii* in *Arabidopsis* roots. *Plant J.* **57,** 771–784 (2009).

Triantaphyllou, A. C. & Hirschmann, H. Environmentally controlled sex expression in *Meloidodera floridensis*. *J. Nematol*. **5,** 181–185 (1973).

Triantaphyllou, A. C. Environmental sex differentiation of nematodes in relation to pest management. *Annu. Rev. Phytopathol.* **11,** 441–462 (1973a).

Triantaphyllou, A. C. Gametogenesis and reproduction of *Meloidogyne graminis* and *M. ottersoni* (Nematoda: *Heteroderidae*). *J. Nematol.* **5,** 84–7 (1973b).

Triantaphyllou, A. C. Genetics and cytology: In *Plant Parasitic Nematodes* (eds. Zuckerman, B. M. & Mai, W. F.) 207–217 (Academic Press, Inc., 1971).

Triantaphyllou, A. C. Oogenesis and the chromosomes of twelve bisexual species of *Heterodera* (Nematoda : *Heteroderidae*). *J. Nematol.* **7,** 34-40 (1974).

Triantaphyllou, A. C. Polyploidy and parthenogenesis in the root-knot nematode *Meloidogyne arenaria*. *J. Morphol.* **113,** 489–499 (1963).

Trudgill, D. L. & Parrott, D. M. The behaviour of nine populations of the potato cyst nematode *Heterodera rostochiensis* towards three resistant potato hybrids. *Nematologica* **15,** 381–388 (1969).

Trudgill, D. L. The Effect of environment on sex determination in *Heterodera rostochiensis*. *Nematologica* **13,** 263–272 (1967).

Trudgill, D. L., Webster, J. M. & Parrott, D. M. The effect of resistant solanaceous plants on the sex ratio of *Heterodera rostochiensis* and the use of the sex ratio to assess the frequency and genetic constitution of pathotypes. *Ann. Appl. Biol.* **60,** 421–428 (1967).

Urwin, P. E., McPherson, M. J. & Atkinson, H. J. Enhanced transgenic plant resistance to nematodes by dual proteinase inhibitor constructs. *Planta* **204,** 472–479 (1998).

Urwin, P. E., Møller, S. G., Lilley, C. J., Mcpherson, M. J. & Atkinson, H. J. Continual green fluorescent protein monitoring of cauliflower mosaic virus 35S promoter activity in nematode-induced feeding cells in *Arabidopsis thaliana*. *Mol. Plant-Microbe Interact.* **394,** 394–400 (1997).

Van Wilgenburg, E., Gerard, D. & Leo, W. Single locus complementary sex determination in Hymenoptera: an "unintelligent" design? *Front. Zool.* **3,** 1 (2006).

Vanholme, B. Van Thuyne, W., Vanhouteghem, K., De Meutter. J., Cannoot, B. & Gheysen, G. Molecular characterization and functional importance of pectate lyase secreted by the cyst nematode *Heterodera schachtii*. *Mol. Plant Pathol.* **8,** 267–78 (2007).

Viglierchio, D. R. & Johnson, R. N. Sugarbeet nematode (*Heterodera schachtii*) reared on axenic *Beta vulgaris* root explants. *Nematologica* **15,** 129–143 (1969).

Wang, X., Meyers, D., Yan, Y., Baum, T., Smant, G., Hussey, R., & Davis, E. In planta localization of a beta-1,4-endoglucanase secreted by *Heterodera glycines*. *Mol. Plant. Microbe. Interact.* **12,** 64–7 (1999).

Whiting, P. Selective fertilization and sexdetermination in Hymenoptera. *Science* **78,** 537–538 (1933).

Whiting, P. W. Multiple alleles in complementary sex determination of Habrobracon. *Genetics* **28,** 365–82 (1943).

Wieczorek, K. Golecki, B., Gerdes, L., Heinen, P., Szakasits, D., Durachko, D. M., Cosgrove, D. J., Kreil, D. P., Puzio P. S., Bohlmann, H. & Grundler, F. M. W. Expansins are involved in the formation of nematode-induced syncytia in roots of *Arabidopsis thaliana*. *Plant J.* **48,** 98–112 (2006).

Wieczorek, K., Elashry, A., Quentin, M., Grundler, F. M. W., Favery, B., Seifert, G. J. & Bohlmann, H. A distinct role of pectate lyases in the formation of feeding structures induced by cyst and root-knot nematodes. *Mol. Plant-Microbe Interact.* **27,** 901–912 (2014).

Witty, M. J. Current strategies in the search for novel antiparasitic agents. *Int. J. Parasitol.* **29,** 95–103 (1999).

Wyss, U. & Grundler, F. M. W. Feeding behaviour of sedentary plant parasitic nematodes. *Neth. J. Pl. Path.* **98,** 165–173 (1992).

Publication 1

……

An improved procedure for isolation of high-quality RNA from nematode-infected *Arabidopsis* roots through laser capture microdissection

Muhammad Shahzad Anjam[1,2], Yvonne Ludwig[1], Frank Hochholdinger[1], Chisato Miyaura[3], Masaki Inada[3], Shahid Siddique[1], Florian M. W. Grundler[1]

[1]Institute of Crop Science and Resource Conservation (INRES), Molecular Phytomedicine, Karlrobert-Kreiten-Straße 13, D-53115 Bonn, Germany

[2]Institute of Molecular Biology and Bio‑technology, Bahauddin Zakariya University, Multan, Pakistan

[3] Department of Biotechnology and Life Science, and Global Innovation Research Organization, Tokyo University of Agriculture and Technology, 2-24-16 Nakacho, Koganei, Tokyo 184-8588, Japan.

*Corresponding author e-mail: grundler@uni-bonn.de

Published: 2016, *Plant Methods* 12 (25): 1-9

DOI: 10.1186/s13007-016-0123-9

Anjam et al. Plant Methods (2016) 12:25
DOI 10.1186/s13007-016-0123-9

Plant Methods

METHODOLOGY Open Access

An improved procedure for isolation of high-quality RNA from nematode-infected *Arabidopsis* roots through laser capture microdissection

Muhammad Shahzad Anjam[1,4], Yvonne Ludwig[2], Frank Hochholdinger[2], Chisato Miyaura[3], Masaki Inada[3], Shahid Siddique[1] and Florian M. W. Grundler[1*]

Abstract

Background: Cyst nematodes are biotrophs that form specialized feeding structures in the roots of host plants, which consist of a syncytial fusion of hypertrophied cells. The formation of syncytium is accompanied by profound transcriptional changes and active metabolism in infected tissues. The challenge in gene expression studies for syncytium has always been the isolation of pure syncytial material and subsequent extraction of intact RNA. Root fragments containing syncytium had been used for microarray analyses. However, the inclusion of neighbouring cells dilutes the syncytium-specific mRNA population. Micro-sectioning coupled with laser capture microdissection (LCM) offers an opportunity for the isolation of feeding sites from heterogeneous cell populations. But recovery of intact RNA from syncytium dissected by LCM is complicated due to extended steps of fixation, tissue preparation, embedding and sectioning.

Results: In the present study, we have optimized the procedure of sample preparation for LCM to isolate high quality of RNA from cyst nematode induced syncytia in Arabidopsis roots which can be used for transcriptomic studies. We investigated the effect of various sucrose concentrations as cryoprotectant on RNA quality and morphology of syncytial sections. We also compared various types of microscopic slides for strong adherence of sections while removing embedding material.

Conclusion: The use of optimal sucrose concentrations as cryoprotection plays a key role in RNA stability and morphology of sections. Treatment with higher sucrose concentrations minimizes the risk of RNA degradation, whereas longer incubation times help maintaining the morphology of tissue sections. Our method allows isolating high-quality RNA from nematode feeding sites that is suitable for downstream applications such as microarray experiments.

Keywords: Syncytium, LCM, Root, Arabidopsis, RNA degradation, Cyst nematode, Nematode

Background

Plant-parasitic nematodes (PPNs) are obligate biotrophs that cause significant damage to almost every economically important crop [27]. PPNs are classified based on their feeding habits as either ectoparasites or endoparasites. The endoparasitic root-knot (*Meloidogyne* spp.) and cyst nematodes (*Globodera* spp. and *Heterodera* spp.) are sedentary parasites of roots and the primary nematode pathogen of a wide range of crops. Infective stage juveniles (J2s) of cyst nematodes invade the host root and migrate intracellularly until they reach the vascular cylinder. There, these nematodes select an initial syncytial cell (ISC) and become sedentary. Within 24 h of the ISC selection the cells adjacent to the ISC appear hypertrophied and fused together due to local dissolution

*Correspondence: grundler@uni-bonn.de
[1] INRES - Molecular Phytomedicine, Rheinische Friedrich-Wilhelms-Universitaet Bonn, Karlrobert-Kreiten-Straße 13, 53115 Bonn, Germany
Full list of author information is available at the end of the article

of the cell walls [32]. Three days after ISC selection, the cells that have been incorporated into the syncytium are enlarged and exhibit the features of a typical syncytial cell such as condensed cytoplasm and enrichment of ribosomes, endoplasmic reticulum, mitochondria and plastids. The nuclei have become enlarged, and several smaller vacuoles are present in the cytoplasm. Moreover the outer cell walls thicken to withstand the high osmotic pressure within the syncytium [5]. The syncytium serves as the sole source of nutrients and water for the rest of the nematode's successive growth and development. A cocktail of secretions, which are synthesised in the oesophageal glands of the nematodes, are responsible for the modulation of the plant's defence and the developmental pathways that lead to the formation of a syncytium [8, 9, 12, 29]. Therefore understanding the function of host genes that are required for syncytium development is crucial for identifying novel targets for nematode resistance.

Compatible interaction is best studied between cyst nematode *Heterodera schachtii* and the model plant *Arabidopsis thaliana*. In recent years a lot of work with this particular pathosystem has shown that the development of the syncytium is accompanied by massive transcriptomic, metabolomic and proteomic changes [11, 13, 31]. Nevertheless isolating pure syncytial material and extracting good quality RNA from Arabidopsis roots for downstream application, such as microarray analyses, qPCR and RNA-seq is challenging. Puthoff et al. [25] used the entire root systems of cyst nematode-infected Arabidopsis plants to perform the first transcriptomic studies. However including non-infected cells dilutes the feeding cell specific mRNA expression profile [10, 31]. In a step forward, Szakasits et al. [31] tried to overcome this limitation by collecting the pure cytoplasm of feeding cells through micro-aspiration. But producing a sufficient amount of material for analysis using this technique is laborious. Moreover it works better on larger, well-developed syncytial cells as compared to syncytial tissues during the early stages of development. An alternative and promising technique for collecting pure cells is laser capture microdissection (LCM).

LCM is becoming a popular tool among cell biologists because it allows isolation of RNA, DNA, proteins and metabolites from a heterogeneous cell population. Current LCM techniques are based on two principles. In the "touch-free" approach, cells identified under a microscope are excised by a laser beam and removed from their tissue context by gravity or by catapulting them away with a photonic pulse. Alternatively, cells are fused to a plastic membrane and are subsequently removed mechanically from the remaining tissue (reviewed in Ludwig and Hochholdinger [22]).

Successful LCM requires good morphological preservations of tissues. Furthermore, isolated nucleic acids (RNA or DNA), proteins or metabolites must be of high quality to ensure their utility for downstream applications. Therefore, tissue preparation is the crucial step towards successful RNA isolation of samples generated by LCM. Since LCM requires micro-sections of 2–20 µm, samples must be fixed and embedded prior to sectioning and mounting them on the slides. During this multistep procedure, RNA integrity remains at high risk of degradation due to the presence of RNases. Samples for immuno-histological analyses are generally fixed in paraformaldehyde and embedded in paraffin to ensure well-preserved tissue morphology. In contrast, ethanol:acetic acid (EAA) solution is preferred for fixation in experiments involving RNA extraction because paraformaldehyde cross links with RNA and thus makes its recovery difficult [14, 17, 18, 30]. After fixation the tissues are embedded either in paraffin at room temperature or in an optimum cutting temperature (OCT) medium at −20 °C (cryosectioning). While OCT-embedded samples are sectioned through a cryomicrotome at −20 °C, the paraffin-embedded samples are sectioned at room temperature. Cryosectioning is often preferred over sectioning of paraffin-embedded samples because processing the tissue at a low temperature reduces the activity of RNases and increase yield [1, 23]. Nevertheless keeping the RNA intact during the various steps of the cryosectioning for LCM poses a challenge and entails fixing and processing tissues. For example, plant cells contain big vacuoles for water storage, which may form crystals because of fast freezing of samples during cryosectioning leading to the destruction of cellular structures. Similarly, it is challenging to maintain the histological preservation during cryosectioning so that the target cells can be distinguished from others cell types. Therefore a number of tissue fixation and embedding procedures have been developed to ensure optimised handling of tissues with different physical rigidity [4].

Nakazono et al. [23] were the first to report application of LCM in plant samples by isolating the epidermis and vascular tissue cells of maize plants, which were subsequently used in microarray studies. Soon after, Kerk et al. [17] presented an RNA isolation technique using the paraffin-embedded sections of a variety of plant tissues. Further the LCM procedure has been applied to isolate syncytial material from soybean roots infected with cyst nematode *H. glycines* [15, 18, 19]. These authors applied paraffin embedding to process the syncytial samples and showed that a number of genes are differentially regulated in these plants upon nematode infection. But the utility of this protocol for nematode-infected Arabidopsis roots remains questionable as it may lead to poor

quality RNA extraction. LCM was also used to capture giant cells and isolate RNA induced by root-knot nematodes in Arabidopsis, rice and tomato during different stages of infection [1, 3, 7, 16, 24, 26]. However no protocol describing the isolation of syncytial cells from Arabidopsis have been described so far. In the present study we optimised the LCM procedure for the isolation of syncytial cells from Arabidopsis roots in such a manner that their morphology can be preserved and high-quality RNA can be isolated for downstream applications such as microarray analyses.

Results

To assess the potential of a previously described giant cell RNA isolation protocol in Arabidopsis for its utility for syncytial samples, we grew Arabidopsis plants in KNOP medium and infected them with J2 nematodes of *H. schachtii*. Root segments containing syncytia were cut at 5 days post inoculation (dpi). The infected root segments were subsequently fixed in EAA (3:1) and processed for LCM as described previously [1, 23, 24]. However, RNA was heavily degraded in these samples and was unusable for downstream applications (data not shown).

To identify the crucial step in which the RNA was degraded, we hand-dissected root segments containing syncytia at 5 dpi and isolated RNA at three different steps (Table 1). The subsequent quality analysis revealed that the RNA was already degraded before embedding in OCT. Hence sections mounted on the slides already contained deteriorated RNA (Fig. 1a, b). Conversely the RNA isolated from syncytial tissues that were fixed but not treated for cryoprotection produced high-quality RNA (Fig. 1c). We concluded that the cryoprotection procedure needs to be modified to obtain good quality RNA.

Modification of cryoprotection steps yielded good quality RNA

To investigate whether RNA degradation might have occurred because of multiple incubations in different sucrose concentrations (10 % for 3 h, 15 % for 3 h and 34 % overnight) during cryoprotection; we modified the tissue preparation procedure by reducing the sucrose incubation steps. For this, root segments containing infected tissues were cut and fixed in EAA solution followed by a direct incubation in 15 % sucrose solution for 3 h (low concentration sucrose-treated samples). These samples were then left overnight in 34 % sucrose solution. Alternatively fixed tissues were directly incubated in 34 % for 5 h (high concentration sucrose-treated samples). Subsequently, tissues from low- and high-concentration sucrose-treated samples were embedded in OCT, cryosectioned and used for RNA isolation. While the RNA from low-concentration sucrose-treated tissues was

Table 1 An overview of influence of tissue fixation and embedding on RNA quality

Method	Fixation	Cryoprotection in sucrose	Embedding	RNA quality
A	Yes	Yes	Yes (OCT)	Degraded
B	Yes	Yes	No	Degraded
C	Yes	No	No	Good

A, B and C refers to three different steps from which RNA was isolated. (A) RNA was extracted from tissues following all steps of fixation, cryoprotection and embedding, however before LCM. (B) Tissue samples after fixation and cryoprotection but before embedding. (C) Control samples with fixation but without cryoprotection or embedding

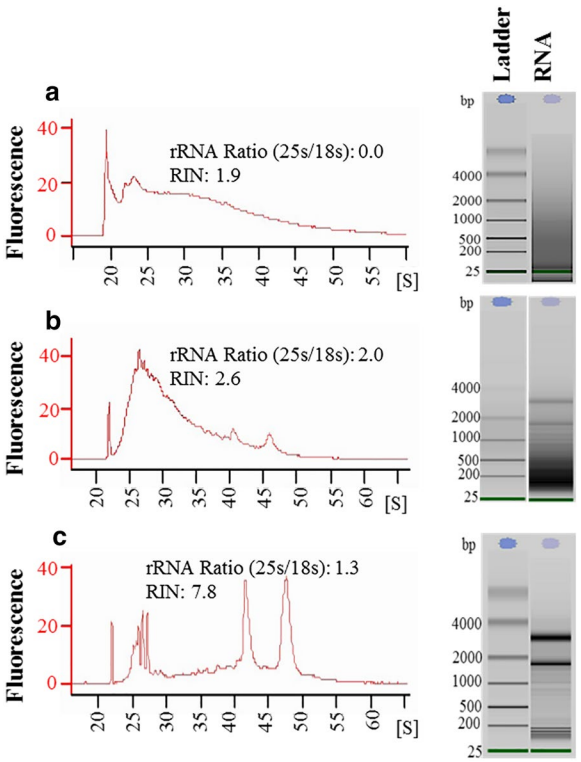

Fig. 1 Influence of tissue fixation and embedding on RNA quality. Electropherograms indicating the quality of RNA extracted from Arabidopsis root segments infected with nematodes at 5 dpi. **a** RNA was extracted from tissues following all steps of fixation, cryoprotection and embedding, however before LCM. Number of root pieces (containing syncytium) used for extraction: 10; RNA concentration: 3407 pg/µL. **b** Tissue samples after fixation and cryoprotection but before embedding. There is a splice between Ladder and RNA samples; however, both runs are from the same chip and were put together to facilitate visualization. Number of root pieces (containing syncytium) used for extraction: 15; RNA concentration: 4693 pg/µL. **c** Control samples with fixation but without cryoprotection or embedding. Number of root pieces (containing syncytium) used for extraction: approx. 25 RNA concentration: 1440 pg/µL. **a** The experiment was performed once. **b**, **c** The experiments were repeated three times and data from one representative experiment is provided. *S* seconds, *bp* base pair

heavily degraded (Fig. 2a), the sections from high-concentration sucrose-treated tissues showed high-quality RNA (Fig. 2b). Therefore these samples were further processed (mounting on slides, and removing OCT) to isolate syncytial sections through LCM. Subsequent RNA isolation showed a slight degradation in quality of RNA; however, both the quantity and quality of RNA was still reasonable to perform downstream applications (Fig. 2c). We concluded that incubating fixed samples directly in a 34 % sucrose solution for 5 h improves the RNA quality considerably.

Incubation in higher sucrose concentrations affected tissue morphology

Although incubating fixed samples directly in 34 % sucrose for 5 h resulted in improved RNA quality, the tissue morphology was poor (Fig. 3a, b). We reasoned that this might be due to shorter and direct incubation in high concentration sucrose, which may lead to sudden loss of tissue pressure. Therefore we increased the vacuum infiltration of samples in 34 % sucrose from 15 to 45 min followed by an overnight incubation at 4 °C. As a consequence, tissue morphology was improved to normal (Fig. 3c). The RNA quality of the samples was not affected by increasing the incubation time.

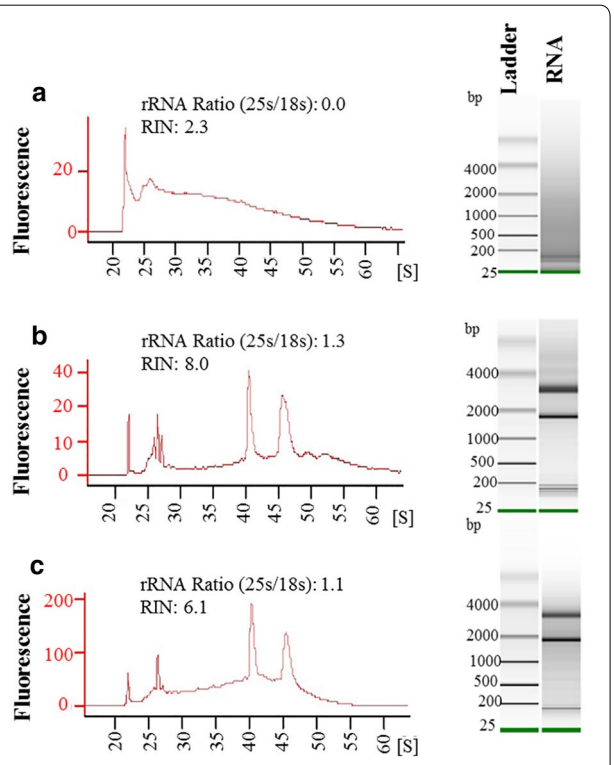

Fig. 2 Quality assessment of RNA isolation from samples after modifying the tissue preparation steps. **a** RNA isolated after direct incubation in 15 % sucrose solution (low sucrose concentration treated samples). Number of root pieces (containing syncytium) used for extraction: 10; RNA Concentration: 2514 pg/µL. **b** RNA isolated after direct incubation in 34 % sucrose (high sucrose concentration treated samples). Number of root pieces (containing syncytium) used for extraction: 10; RNA concentration: 2253 pg/µL. **c** RNA isolation from samples B after LCM. Number of syncytium used for cryosectioning: 30; RNA concentration: 6297 pg/µL. **a**–**c** The experiments were repeated three times and data from one representative experiment is provided. *S* seconds, *bp* base pair

Poly-L-lysine-coated glass slides strongly adhere to micro-sections

Different types of glass slides with diverse features are available. In this study, four types of slides were tested to obtain a strong tissue adherence: (a) polyethylene teraphthalate (PET)-membrane-coated slides, (b) polyethylene napthalate (PEN)-membrane-coated slides, (c) Superfrost® positively charged slides, and (d) poly-L-lysine-coated glass slides. We mounted 10 µm sections on PET- and PEN-membrane-coated glass slides and washed them with PBS buffer and 70 % ethanol to remove the OCT medium. The complete removal of the OCT medium is necessary for laser cutting. However during washing, all sections were washed away from the slides. We pre-treated the slides with UV light for 30 min to 4 h to enhance adherence, but the majority of the sections was still washed off during the washing step. Next we used Superfrost® positively-charged glass slides, on which tissue retention was greatly improved, while the use of poly-L-lysine-coated glass slides proved robust in holding the tissues during the washing step. Hence, in all subsequent experiments, we used poly-L-lysine-coated glass slides, and the laser capture machine was also calibrated to glass slides.

In vitro amplification of cDNA

To assess the quality of RNA isolated through our protocol for downstream applications, cDNA was synthesised from 5-days-old syncytial using NuGEN's Ovation Pico WTA System according to the manufacturers' instructions. Subsequent analysis showed that enough high quality cDNA was amplified (Fig. 4a–c). The amplified cDNA was used to perform further steps of hybridization with the GeneChip® Arabidopsis ATH1 Genome (Affymetrix UK Ltd). The data analysis showed that amplified cDNA was suitable for microarray experiments (data not shown). Whereas the detailed results from microarray will be presented elsewhere, we analysed the expression of six different genes (BGLU28, PGIP1, PDF1.4, WRKY76, Xylanase, and ß tubulin4) in 5-days-old syncytial samples by RT-PCR (see methods for details). These genes were selected based on intensity of expression in syncytium in our microarray data (data not shown). Under optimized PCR conditions, five out of six genes

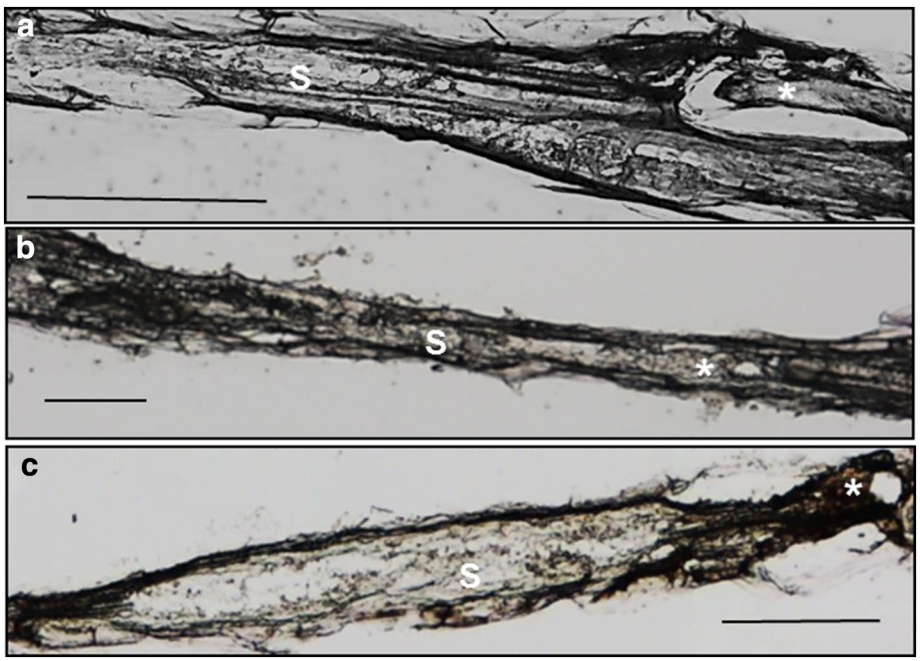

Fig. 3 Morphology of longitudinal syncytial samples (10 µm thin)upon different sucrose treatment. **a** Infected root segments upon direct incubation in 15 % sucrose solution (low sucrose concentration treated samples). **b** Infected root segments upon direct incubation in 34 % sucrose (high sucrose concentration treated samples). **c** Infected root segments upon direct overnight incubation in 34 % sucrose. *Asterisk* (*) nematode, *S* syncytium, *scale bar* 100 µM

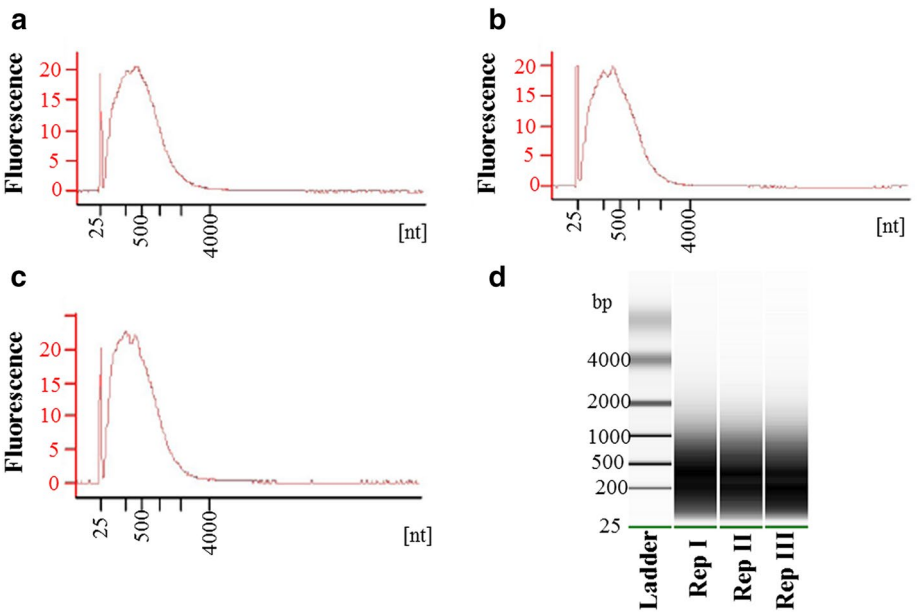

Fig. 4 Amplification of cDNA, where **a**–**c** represents three replications of syncytial samples processed after LCM. The virtual gel generated by an Agilent 2100 Bioanalyzer is shown in **d**. *nt* nucelotide, *bp* base pair

produced a single band of the expected size from LCM-derived syncytial RNA. However, WRKY76 showed an extra band in syncytial samples suggesting unspecific binding of primers (Fig. 5). Nevertheless, these results confirm that RNA isolated through LCM protocol as described in this manuscript can be used to study gene

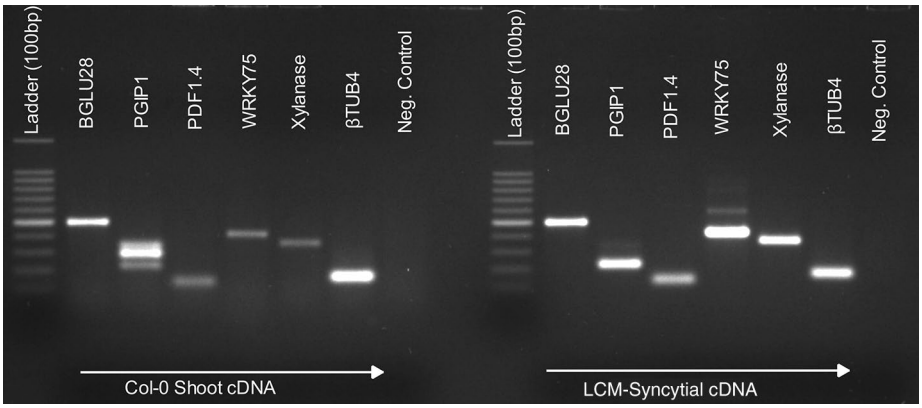

Fig. 5 Analysis of gene expression in uninfected leaf tissues and in 5-days-old syncytium by RT-PCR. Negative control is without template

expression in syncytium during early stages of nematode infection.

Discussion

After the successful use of LCM on animal and human tissues, it has become increasingly popular among plant scientists because of its ability to isolate a single cell-type from a heterogeneous population. The collected material can be used for a broad range of downstream molecular studies, for example, qPCR, RNAseq, microarray and proteomics. In contrast to animal cells the presence of a cell wall and large vacuole in plants necessitates modifications to preserve cell morphology and macromolecules, such as RNA and proteins. As the use of LCM in plant sciences expands, a variety of optimized protocols for specific cell-type harvest have been established. However in contrast to a typical plant cell with a large central vacuole, the cyst-nematode-induced syncytium is a distinctive structure surrounded by a thick cell wall that contains several smaller vacuoles. Therefore performing LCM on syncytial samples may necessitate certain modifications in existing protocols.

In this study we used a previously described protocol for LCM on giant cells induced by root-knot nematodes in Arabidopsis as a starting point [1]. However when we incubated the samples in various sucrose concentrations, the RNA in the samples was highly degraded (Fig. 1a). In contrast incubating samples directly in a 34 % sucrose solution preserved the RNA integrity, indicating that RNase activity may not completely stop at lower sucrose concentrations. A higher concentration of sugar minimise the availability of water in the tissues, which may reduce enzymatic activities including that of RNase. The cryoprotective use of higher sucrose concentrations (20 or 30 %) has already been reported in animal tissues when performing LCM and immunohistochemistry [6, 20, 21]. The use of an RNase inhibitor, for example, RNase later®, maintains high-quality RNA; however RNase later® severely compromised the morphology of the sections in some reports [2].

Although the 34 % sucrose concentration significantly increased RNA quality, the morphology of the sections was strongly compromised. We reasoned that this may be due to direct tissue incubation in a higher concentration sucrose solution (34 %), which may result in a rapid loss of water and thus shrunk tissues. Indeed tissue morphology was maintained through longer vacuum infiltration and an overnight incubation in a 34 % sucrose solution (see "Methods"). The slow intake of solution might have helped the cells maintain their shape.

After the morphology of the sections was satisfying, the embedding medium was removed completely by washing which is a perquisite for the laser beam to function properly. The commercially available OCT medium is water soluble and can be removed easily by washing with PBS buffer. However the root sections can also be washed away unless they adhere strongly to the slides. We tried membrane-covered slides (PET and PEN), which permit very fine dissection of target cells, and the targeted area can be catapulted as a single intact piece, but they proved very poor in holding root sections during the washing step. In contrast, Ramsay et al., [26] used PEN slides for the LCM of giant cells from tomato roots, and Barcala et al. [1] used Superfrost® positively-charged glass slides for giant cells in Arabidopsis roots. However we found that poly-L-lysine-coated glass slides robustly anchored the frozen sections of 5-day-old syncytia.

In conclusion, we have shown that fixation with EAA and a direct infiltration with 34 % sucrose, prior to embedding in OCT medium generates syncytial samples with well-preserved morphology that are suitable

to distinguish syncytial cells from uninfected surrounding tissue during LCM. Moreover, high quality RNA was extracted from LCM-processed syncytial samples, which was suitable for downstream applications such as microarrays analysis and RT-PCR. Importantly, we were able to analyse the RNA quality prior to amplification, which has not been shown previously [24]. Our protocol will help analysing gene expression during early stages of cyst nematode infection, which may help understanding genes and pathways that are important for nematode development. In addition, development of analytical tools such as syncytium-specific promoters will be greatly facilitated by application of this methodology.

Methods

Tissue preparation and sample collection

10-day-old *Arabidopsis thaliana* plants were grown on KNOP medium and inoculated with 60–70 juveniles of *Heterodera schachtii* as described previously [28]. Subsequently, 5-day-old infected root samples were hand-dissected and vacuum infiltrated in EAA solution (3:1) for 20 min. Afterwards, EAA solution was replaced with fresh solution and samples were incubated at 70 rpm on an undulating shaker at 4 °C for 1 h.

Cryoprotection

The fixative solution was replaced with a 34 % sucrose solution prepared in 0.01 M PBS buffer (treated with 0.1 % DEPC), pH 7.4. Safranin-O (0.01 % in water; Cat. No. S2255. Sigma-Aldrich, USA) was added to visualise the otherwise transparent tissues. Moreover, to facilitate solution penetration, a vacuum was applied for 45 min at 4 °C. Subsequently, samples were incubated in an undulating shaker at 4 °C for 24 h.

Embedding

The tissues were horizontally embedded in a tissue freezing medium, OCT (Polyfreeze®, Cat No. 25112. Poly Sciences, Germany) using Cryomold Tissue-Tek® (Cat No. E62534. EMS, USA). The embedded tissues were frozen by touching the back of cryomolds to liquid nitrogen. The embedded samples (OCT blocks) were stored at −80 °C until cryosectioning.

Cryosectioning and laser capture microdissection

The OCT blocks containing tissues were left inside a cryomicrotome (CM 1850 UV, Leica, Germany) pre-cooled to −20 °C for 15 min for acclimatisation before making sections. Longitudinal sections of 10 µm were mounted on poly-L-lysine-coated glass slides (Cat no. J2800AMNZ. Manzel Glaser, Germany). After collecting 10–15 sections on the cryomicrotome platform, a slide at RT was suddenly placed over the sections to adhere them. The slides with sections were stored in 70 % ethanol, which was already pre-chilled in the cryomicrotome.

For OCT removal and dehydration, the slides were treated twice with 70 % ethanol for 30 s each at RT, 95 % ethanol overnight at −20 °C and 99.8 % ethanol for 2 min at RT. After air drying the slides at RT for 2 min, the sections were immediately processed for LCM, and the remaining slides were stored in a box containing silica gel. The LCM captured syncytium cells were collected in RNAse-free adhesive caps (Cat. No. 415190-9211-001 Zeiss, Germany) using the following settings for PALM Microbeam laser capture (Zeiss, Germany). Energy: 55–57, Focus: 79–80, Cutting Program: "CloseCut+AutoLPC" RNA Extraction, Quality Assessment and Gene expression: 10 µl extraction buffer from the PicoPure® RNA isolation kit (Cat no. KIT0204, ThermoFisher Scientific, Germany) was added to an adhesive cap, incubated at 42 °C for 20 min. The extraction mixture was briefly spun down in a table centrifuge at 8000 rpm and was stored at −80 °C until RNA extraction. The later steps of RNA extraction followed the instructions provided in the kit by the manufacturer. The quality of the isolated RNA was tested with an Agilent 2100 Bioanalyzer using the Agilent RNA 6000 Pico kit (Cat. No. 5067-1513. Agilent, Germany).

Table 2 Primer sequences used in this study

Gene	Primer	Sequence	Product size	Locus
BGLU28	Forward	GCTACGACACT GGCAACAAA	501	AT2G44460
	Reverse	TGTGATTTGTTA CTCGCCATTG		
PGIP1	Forward	CCATTCCAA-GTTCTCTCTCT ACG	221	AT5G06860
	Reverse	AGCATCACCTT GGAGCTTGT		
PDF1.4	Forward	CTTCCT-TATAGCTT CCACTGAGAT	130	AT1G19610
	Reverse	AGCACGTTCCCA TCTCTTAC		
WRKY75	Forward	ATGGAGGGATAT-GATAATGGGTC	418	AT5g13080
	Reverse	GCATTTGAGTG AGAATAT-GCTCG		
Xylanase	Forward	CTGTTCTTGGT CGTCCCATT	360	AT1G10050
	Reverse	CGACAACGA ACGTTTTGAGA		
Beta tubulin 4	Yes	TTTCCGTACCC TCAAGCTCG	160	AT5G44340
		GTGAAGCCTTG CGAATGGGA		

cDNA synthesis was done with NuGEN's Ovation Pico WTA System (Cat. No. 3302-12. Nugen, USA) according to the manufacturers' instructions, starting with 1–50 ng of total RNA. NuGEN's Encore Biotin Module (Cat. No. 4200-12. Nugen, USA) was used to fragment 3.95 µg cDNA followed by Biotin-labelling according to the manufacturers' instructions. The gene expression was analysed through RT-PCR. Each sample contained 6 µL Master Mix, 1 µL template cDNA (1:20 dilution), 0.5 µL of forward and 0.5 µL of reverse primers (10 µM) and water in 20 µL of total reaction volume. Primers are given in Table 2.

Authors' contributions

MSA and YL performed experiments. MSA, SS and FMWG designed the research and wrote the paper. FH, CM, and MI provided technical support and helped editing the manuscript. All authors read and approved the final manuscript.

Author details

[1] INRES - Molecular Phytomedicine, Rheinische Friedrich-Wilhelms-Universitaet Bonn, Karlrobert-Kreiten-Straße 13, 53115 Bonn, Germany. [2] INRES - Crop Functional Genomics, Rheinische Friedrich-Wilhelms-Universitaet Bonn, Friedrich-Ebert-Allee 144, 53113 Bonn, Germany. [3] Department of Biotechnology and Life Science, and Global Innovation Research Organization, Tokyo University of Agriculture and Technology, 2-24-16 Nakacho, Koganei, Tokyo 184-8588, Japan. [4] Institute of Molecular Biology and Bio-technology, Bahauddin Zakariya University, Multan, Pakistan.

Acknowledgements

We thank Jennifer Topping and Keith Lindsey for technical training of Muhammad Shahzad Anjam.

Competing interests

The authors declare that they have no competing interests.

Funding

Muhammad Shahzad Anjam was supported by a grant from German Exchange Service (DAAD).

Received: 7 January 2016 Accepted: 19 April 2016
Published online: 26 April 2016

References

1. Barcala M, Garcia A, Cabrera J, Casson S, Lindsey K, Favery B, Garcia-Casado G, Solano R, Fenoll C, Escobar C. Early transcriptomic events in microdissected Arabidopsis nematode-induced giant cells. Plant J. 2010;61:698–712.
2. Bevilacqua C, Makhzami S, Helbling JC, Defrenaix P, Martin P. Maintaining RNA integrity in a homogeneous population of mammary epithelial cells isolated by laser capture microdissection. BMC Cell Biol. 2010;11:95.
3. Fosu-Nyarko J, Jones MGK, Wang Z. Functional characterization of transcripts expressed in early-stage *Meloidogyne javanica*-induced giant cells isolated by laser microdissection. Mol Plant Pathol. 2009;10:237–48.
4. Gautam V, Sarkar AK. Laser assisted microdissection, an efficient technique to understand tissue specific gene expression patterns and functional genomics in plants. Mol Biotechnol. 2015;57:299–308.
5. Golinowski W, Grundler FMW, Sobczak M. Changes in the structure of *Arabidopsis thaliana* during female development of the plant-parasitic nematode *Heterodera schachtii*. Protoplasma. 1996;194:103–16.
6. Haynes T, Luz-Madrigal A, Reis ES, Ruiz NPE, Grajales-Esquivel E, Tzekou A, Tsonis PA, Lambris JD, Del Rio-Tsonis K. Complement anaphylatoxin C3a is a potent inducer of embryonic chick retina regeneration. Nat Commun. 2013;4:2312.
7. He B, Magill C, Starr JL. Laser capture microdissection and real-time PCR for measuring mRNA in giant cells induced by *Meloidogyne javanica*. J Nematol. 2005;37:308–12.
8. Hewezi T, Baum TJ. Manipulation of plant cells by cyst and root-knot nematode effectors. Mol Plant Microbe Interact. 2013;26:9–16.
9. Hewezi T, Juvale PS, Piya S, Maier TR, Rambani A, Rice JH, Mitchum MG, Davis EL, Hussey RS, Baum TJ. The cyst nematode effector protein 10A07 targets and recruits host posttranslational machinery to mediate its nuclear trafficking and to promote parasitism in Arabidopsis. Plant Cell. 2015;27:891–907.
10. Hofmann J, Hess PH, Szakasits D, Blöchl A, Wieczorek K, Daxböck-Horvarth S, Bohlmann H, van Bel AJE, Grundler FMW. Diversity and activity of sugar transporters in nematode-induced root syncytia. J Exp Bot. 2009;60:3085–95.
11. Hofmann J, El Ashry A, Anwar S, Erban A, Kopka J, Grundler F. Metabolic profiling reveals local and systemic responses of host plants to nematode parasitism. Plant J. 2010;62:1058–71.
12. Holbein J, Grundler FMW, Siddique S. Plant basal defence to nematodes: an update. J Exp Bot. 2016. doi:10.1093/jxb/erw005.
13. Hütten M, Geukes M, Misas-Villamil JC, van der Hoorn RAL, Grundler FMW, Siddique S. Activity profiling reveals changes in the diversity and activity of proteins in Arabidopsis roots in response to nematode infection. Plant Physiol Biochem. 2015;14:36–43.
14. Inada N, Wildermuth MC. Novel tissue preparation method and cell-specific marker for laser microdissection of Arabidopsis mature leaf. Planta. 2005;221:9–16.
15. Ithal N, Recknor J, Nettleton D, Maier T, Baum TJ, Mitchum MG. Developmental transcript profiling of cyst nematode feeding cells in soybean roots. Mol Plant Microbe Interact. 2007;20:510–25.
16. Ji HL, Gheysen G, Denil S, Lindsey K, Topping JF, Nahar K, Haegeman A, De Vos WH, Trooskens G, Van Criekinge W, De Meyer T, Kyndt T. Transcriptional analysis through RNA sequencing of giant cells induced by *Meloidogyne graminicola* in rice roots. J Exp Bot. 2013;64:3885–98.
17. Kerk NM, Ceserani T, Tausta SL, Sussex IM, Nelson TM. Laser capture microdissection of cells from plant tissues. Plant Physiol. 2003;132:27–35.
18. Klink VP, Alkharouf N, MacDonald M, Matthews B. Laser capture microdissection (LCM) and expression analyses of *Glycine max* (soybean) syncytium containing root regions formed by the plant pathogen *Heterodera glycines* (soybean cyst nematode). Plant Mol Biol. 2005;59:965–79.
19. Klink VP, Overall CC, Alkharouf NW, MacDonald MH, Matthews BF. Laser capture microdissection (LCM) and comparative microarray expression analysis of syncytial cells isolated from incompatible and compatible soybean (Glycine max) roots infected by the soybean cyst nematode (*Heterodera glycines*). Planta. 2007;226:1389–409.
20. Krol J, Busskamp V, Markiewicz I, Stadler MB, Ribi S, Richter J, Duebel J, Bicker S, Fehling HJ, Schubeler D, Oertner TG, Schratt G, Bibel M, Roska B, Filipowicz W. Characterizing light-regulated retinal microRNAs reveals rapid turnover as a common property of neuronal microRNAs. Cell. 2010;141:618–31.
21. Kwon B, Houpt TA. A combined method of laser capture microdissection and X-Gal histology to analyze gene expression in c-Fos-specific neurons. J Neurosci Methods. 2010;186:155–64.
22. Ludwig Y, Hochholdinger F. Laser microdissection of plant Cells. In: Plant cell morphogenesis: methods and protocols. Methods Mol Biol. 2014;1080, 249–258.
23. Nakazono M, Qiu F, Borsuk LA, Schnable PS. Laser-capture microdissection, a tool for the global analysis of gene expression in specific plant cell types: identification of genes expressed differentially in epidermal cells or vascular tissues of maize. Plant Cell. 2003;15:583–96.
24. Portillo M, Lindsey K, Casson S, Garcia-Casado G, Solano R, Fenoll C, Escobar C. Isolation of RNA from laser-capture-microdissected giant cells at early differentiation stages suitable for differential transcriptome analysis. Mol Plant Pathol. 2009;10:523–35.
25. Puthoff DP, Nettleton D, Rodermel SR, Baum TJ. Arabidopsis gene expression changes during cyst nematode parasitism revealed by statistical analyses of microarray expression profiles. Plant J. 2003;33:911–21.
26. Ramsay K, Wang ZH, Jones MGK. Using laser capture microdissection to study gene expression in early stages of giant cells induced by root-knot nematodes. Mol Plant Pathol. 2004;5:587–92.
27. Sasser JN, Freckman DW. A world perspective on nematology—the role of the society. J Nematol. 1986;18:596.

28. Siddique S, Matera C, Radakovic ZS, Hasan MS, Gutbrod P, Rozanska E, Sobczak M, Torres MA, Grundler FMW. Parasitic worms stimulate host NADPH oxidases to produce reactive oxygen species that limit plant cell death and promote infection. Sci Signal. 2014;7:ra33.
29. Siddique S, Radakovic ZS, De La Torre CM, Chronis D, Novak O, Ramireddy E, Holbein J, Matera C, Hutten M, Gutbrod P, Anjam MS, Rozanska E, Habash S, Elashry A, Sobczak M, Kakimoto T, Strnad M, Schmulling T, Mitchum MG, Grundler FMW. A parasitic nematode releases cytokinin that controls cell division and orchestrates feeding site formation in host plants. Proc Natl Acad Sci USA. 2015;112:12669–74.
30. Srinivasan M, Sedmak D, Jewell S. Effect of fixatives and tissue processing on the content and integrity of nucleic acids. Am J Pathol. 2002;161:1961–71.
31. Szakasits D, Heinen P, Wieczorek K, Hofmann J, Wagner F, Kreil DP, Sykacek P, Grundler FMW, Bohlmann H. The transcriptome of syncytia induced by the cyst nematode *Heterodera schachtii* in Arabidopsis roots. Plant J. 2009;57:771–84.
32. Wyss U, Grundler FMW. *Heterodera schachtii* and *Arabidopsis thaliana*, a model host-parasite interaction. Nematologica. 1992;38:488–93.

Publication 2

……

Host factors influence the sex of nematodes parasitizing roots of *Arabidopsis thaliana*

Muhammad Shahzad Anjam[1,2], Christiane Matera[1], Syed Jehangir Shah[1], Elżbieta Różańska[3], Miroslaw Sobczak[3], Shahid Siddique[1], Florian M.W. Grundler[1]

[1]Institute of Crop Science and Resource Conservation (INRES), Molecular Phytomedicine, Karlrobert-Kreiten-Straße 13, D-53115 Bonn, Germany

[2]Institute of Molecular Biology and Bio‑technology, Bahauddin Zakariya University, Multan, Pakistan

[3]Department of Botany, Warsaw University of Life Sciences, PL-02787 Warsaw, Poland

*Corresponding author e-mail: grundler@uni-bonn.de

Host factors influence the sex of nematodes parasitizing roots of *Arabidopsis thaliana*

Muhammad Shahzad Anjam[1], Christiane Matera[1], Syed Jehangir Shah[1], Elżbieta Różańska[2], Miroslaw Sobczak[2], Shahid Siddique[1], Florian M.W. Grundler[1]

[1]Rheinische Friedrich-Wilhelms-University of Bonn, INRES – Molecular Phytomedicine, Karlrobert-Kreiten-Straße 13, D-53115 Bonn, Germany
[2]Department of Botany, Warsaw University of Life Sciences (SGGW), Warsaw, Poland
Corresponding author email: grundler@uni-bonn.de

Abstract

Plant-parasitic cyst nematodes are biotrophs that infect roots and cause physiological and structural modifications of host cells leading to the formation of syncytial nurse cells in the roots. Cyst nematodes are sexually dimorphic but the differentiation into male or female occurs only after feeding has started. Because male to female sex ratio is highly variable with culturing conditions and genotype of the host plant, it is assumed that environmental conditions play a decisive role in sex determination. Under favorable conditions, more females develop, whereas mainly male nematodes develop under adverse conditions. However, it is not clear, whether this phenomenon is due to epigenetic sex determination or differential mortality of the females. Here, we developed and validated a method to predict the sex of beet cyst nematode *Heterodera schachtii* during early stages of its parasitism in the host plant *Arabidopsis thaliana*. Root segments containing male-associated syncytia (MAS) or female-associated syncytia (FAS) were collected, syncytial cells were isolated by laser microdissection, and a comparative transcriptome analysis was performed. The data analysis revealed that genes belonging to categories of defense, nutrient deficiency and starvation were overrepresented in MAS as compared to FAS. On the other hand, gene categories related to metabolism, modification and biosynthesis of cell wall were overrepresented in FAS. We have used β-glucuronidase (GUS) analysis, qRT-PCR and loss-of-function mutants to characterize FAS- or MAS- specific candidate genes. In conclusion, our data demonstrate that various plant factors including immune response, nutrients availability, and structural modifications influence the sexual fate of cyst nematodes.

Introduction

Plant-parasitic nematodes are obligate biotrophic pathogens that attack almost all economically important crops. International surveys have revealed an annual overall loss in yield of 12.3%, which has reached up to 20% for some crops, such as banana (Sasser & Freckman, 1986). Most damage is caused by sedentary root-knot nematodes (*Meloidygyne* spp.), cyst nematodes (*Globodera* spp. and *Heterodera* spp.), and several migratory nematodes (*Pratylenchus* spp. and *Radopholus* spp.).

Cyst nematodes induce specialized syncytial feeding structures inside the roots of the host plant. Therefore, the infective second stage juveniles of cyst nematodes (J2) invade the roots in the elongation zone behind the root tip. Once inside the root, the nematode moves through different tissue layers towards the vascular cylinder without feeding. The stylet thrusts and release of cell wall degrading enzymes and other proteins from nematode's esophageal secretory glands aid the movement of nematodes inside the root. Upon reaching the vascular cylinder, the nematode probes single cells in order to select a suitable initial syncytial cell (ISC) (Golinowski et al., 1996; Sobczak et al., 1999). Once the ISC is selected, the nematode becomes sedentary and a cocktail of secretions is released into the ISC that manipulate plant defense and metabolic pathways leading to the development of syncytium. Subsequently, nematodes develop into males or females by undergoing moulting three times (J3, J4, and adults). Whereas the adult male nematodes leave the roots, the females remain sedentary, and produce eggs after fertilization. Finally, they die and turn into egg-protecting cysts (reviewed by Lilley et al., 2005). Because of their prolonged sedentary phase due to reproduction, female cyst nematodes were found to require on average 29 times more food as compared with males (Müller, 1981). Further, female associated syncytia (FAS) were bigger in size as compared male associated syncytia (MAS) (Golinowski et al., 1996; Sobczak et al., 1997).

Although cyst nematodes are dimorphic, yet the mechanism of sex determination is not clearly understood. It has been observed that environment strongly influences the sex ratio in cyst nematodes. Under favorable conditions with plenty of nutrients, the majority of the juveniles develop into females. However, when the juveniles are exposed to adverse conditions e.g., as seen in resistant plants, the percentage of females decreases considerably (Sobczak et al., 2005). Because the sex ratios in cyst nematodes vary considerably under different environmental conditions, it raises the question of whether the environmental factors determine the sex of cyst nematodes or whether it is determined purely by genetic factors.

A considerable amount of work has been carried out to clarify the role of environmental and genetic factors on the sex of cyst nematodes. The results, however, are not all in agreement. The first report on the variation of the sex ratio was provided by Molz (1920) for the sugar beet cyst nematode *Heterodera schachtii*. He found that the sex of this nematode is strongly influenced by the physiological state of the host plants leading to the suggestion of Environmental Sex Determination (ESD) in cyst nematodes. However, contrasting conclusions were drawn a few years later by Sengbusch (1927), who repeated some of Molz's experiments and suggested that the excessive percentages of males under unfavorable conditions result from a differential death rate of the female larvae (Sengbusch, 1927). This conclusion was based on his estimations that females require 35 times more food as compared to males. The debate took a new turn when Ellenby (1954) published the results of experiments with *H. rostochiensis* (syn. *Globodera rostochiensis*) on potato roots. He argued that if a variation in the sex ratio is due to the differential death rate of females, then such degraded worms should be present in roots. Accordingly, all those worms, which were not adult males, were counted as females. The results showed that the proportion of males to females increased strongly with an increased intensity in unfavourable environmental conditions, thus reinforcing the ESD view. Adding a single juvenile of *Globodera rostochiensis* to the host root resulted in an overwhelming majority of females in two independent studies, which was attributed to a decrease in competition for feeding site induction (Den Ouden, 1960; Trudgill, 1967). Grundler et al. (1991) performed a number of experiments by adding single juveniles of *H. schachtii* on *Brassica rapa* growing in a nutrient solution containing minerals and various concentrations of sucrose. They also found that the majority of juveniles develop as females under favourable conditions. Although single juvenile experiments provided a strong hint indicating that ESD plays a role in the sexual outcome of cyst nematodes, it also appeared that the number of males in majority of these experiments was rather constant, whereas the number of females fluctuated under different environmental and nutritional conditions.

The establishment of *Arabidopsis thaliana* as a host provided a model system that allowed robust molecular and genetic analyses of plant-nematode interactions (Sijmons et al., 1991). Commonly, transcriptome analysis is the first step towards identifying genes and pathways that underlie a biological phenomenon. Indeed, a transcriptome and proteome analysis of female-associated syncytia induced by *H. schachtii* in *Arabidopsis* roots was performed, which provided valuable insights into the molecular functioning of syncytium (Szakasits et

al., 2009: Hütten et al., 2015). However, it is technically challenging to perform such studies to compare the differences between male- and female-associated syncytium. Firstly, when the morphological features discriminative for the sex of the nematode become apparent, they are already sexually differentiated into males and females (Raski, 1950; Wyss, 1992); therefore, it is unlikely that a transcriptome analysis at this time-point would provide insights into the host factors that influence the sexual differentiation of nematodes. Secondly, the isolation of pure syncytial material during the early stages of syncytium development is challenging and laborious. Accordingly, novel approaches had to be developed to shed light on ESD in cyst nematodes. Here, we established and validated a strategy to predict the sex of *H. schachtii* juveniles during the early stages of infection when their sexual outcome is not yet apparent (Wyss, 1992). The transcriptome analysis of potential male- and female-associated syncytia could then be compared by isolating pure syncytial material via Laser Capture Microdissection (LCM). In this way, sets of genes that are differentially regulated between male- and female-associated syncytium during the early stages of syncytium development were identified. The following infection assays on knock-out mutants for differentially regulated genes provided new insights into plant factors that influence sexual differentiation of *H. schachtii*.

Results

J2 of females grow faster as compared to males

A number of studies have explored the role of the environment on the sexual outcome of cyst nematodes; however, the underlying molecular mechanism is not well understood. We therefore asked whether there is a difference in growth patterns between J2s males and females. We grew plants *in vitro* and inoculated them with nematodes as described in the Methods section. We marked the juveniles that had successfully established the ISC 24 hours after inoculation (24 hai), and monitored their growth daily over the following 5 days. The sex of the marked nematodes was finally resolved at 12 days post inoculation (12 dpi), and growth curves for males and females were calculated. Until 3 dpi, there was no difference in the average size between male and female juveniles; however, the female juveniles were significantly larger from 4 dpi, and grew faster, as compared to the male juveniles (Figure 1). These observations suggested that the sexual fate of the J2s may be determined during the first 4 – 5 days after infection. These results also suggested that it might be possible to predict

the sex of a juvenile during the early stages of infection, based on the differences in their sizes.

The sex of nematodes can be accurately predicted as early as 5 dpi

To assess whether we can predict the sex of J2 nematodes during the early stages of infection, we inoculated the plants with nematodes and marked successfully established nematodes at 24 hai. The development of nematodes was assessed at 4 dpi and the sex of the nematodes was predicted as male or female at 5 dpi (see Methods section for details). Afterwards, the predicted sex of juveniles was re-evaluated at 12 dpi, a time-point where morphological differences between males and females can be clearly differentiated. Whereas we were able to predict the sex of female nematodes with more than 90% accuracy, the sex of male nematodes was correctly predicted with approximately 85% accuracy. Thus, the sex of the juveniles can be predicted successfully during the initial stage of infection **(**Table 1 and Figure 2).

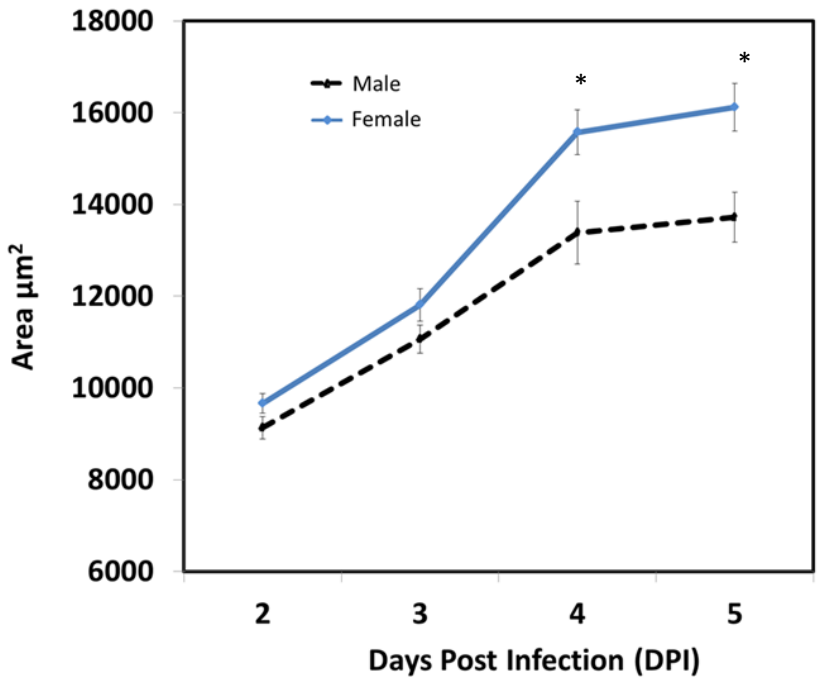

Figure 1: Development of *H. schachtii* J2s in *Arabidopsis* roots. The nematodes that established an ISC in roots were marked and their growth was monitored over next five days. The values represent average size of a nematode ± SE. Data were analyzed using Student´s *t-test* ($p < 0.05$). Asterisks represent the statistically significant difference.

Table 1: Sex prediction assays for *H. schachtii*. The experiment was repeated thrice independently and percentage of right prediction was calculated. N= number of nematodes, ± indicates standard deviation.

Nematode	Prediction (N)	Actual (N)	Success (%)
Male	76	66	86.3 ± 1.8
Female	125	115	91.2 ± 1.7

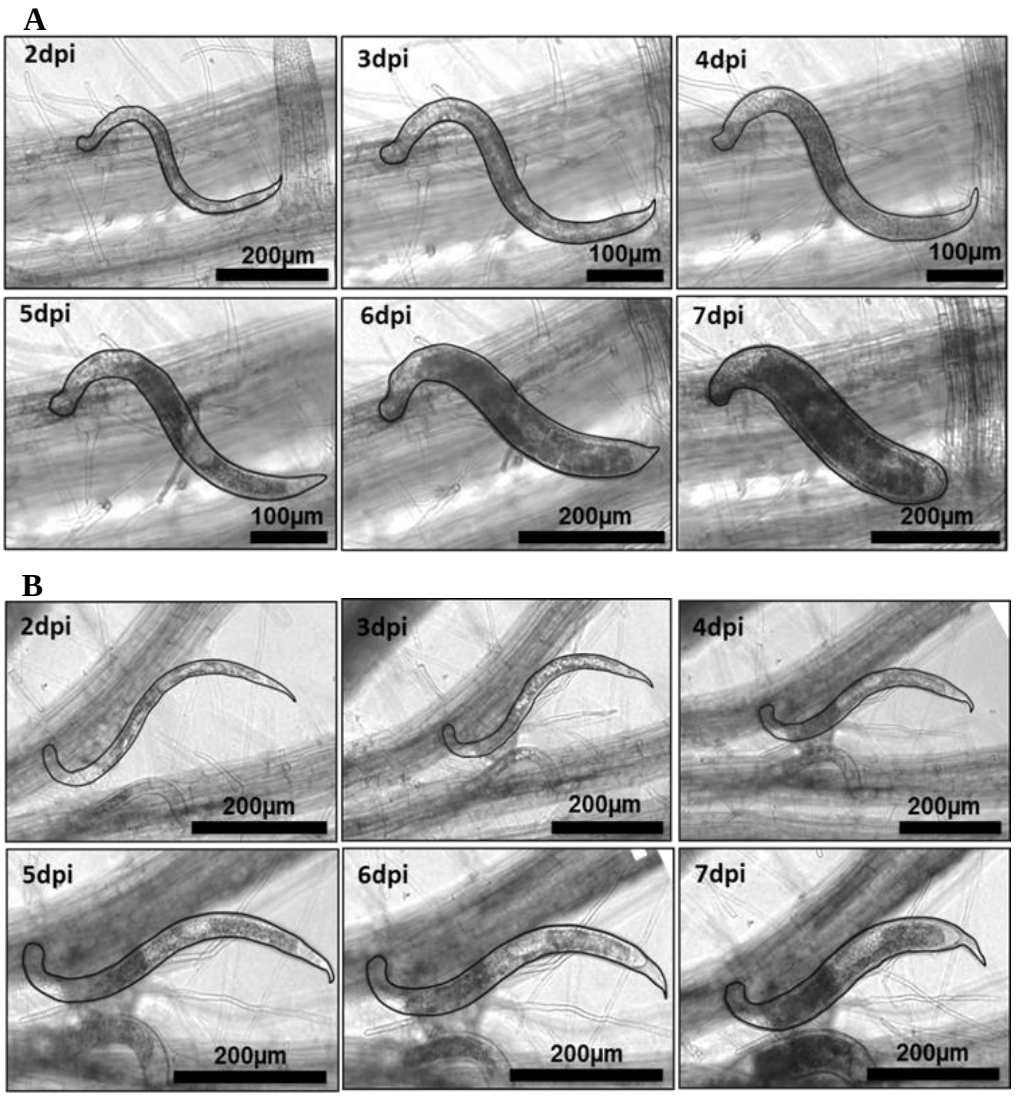

Figure 2: Development of female and male nematodes over period of time. (A): development of a female juvenile from 2 till 7 dpi. (B): development of a male juvenile from 2 till 7 dpi. Note: a line has been drawn around each nematode to make image prominent from other nematodes in the background.

Structural and cellular differences between FAS and MAS

To investigate cellular and ultrastructural differences between MAS and FAS, we predicted sex of the nematode at 5 dpi and dissected the root segments containing syncytium and attached nematode. The root segments were serially cross-sectioned and analyzed through light and transmission electron microscopy. We found that both syncytia expand via incorporation of hypertrophied vascular cylinder cells only, but they differed strongly in anatomy (Figure 3A-3J). MAS were shorter and composed of lower number of incorporated cells (Figure 3A-3E) than FAS (Figure 3F-3J). At the leading edge of syncytium, where new cells were incorporated into axially expanding syncytium, recently incorporated cells were only slightly hypertrophied in MAS (Figure 3A) whereas in FAS their hypertrophy was pronounced (Figure 3F). This difference was clearly recognizable also in submedian and median parts of both syncytia (Figure 3B and 3C versus Figure 3G and 3H). In the region close to the nematode head tip where the ISC had been selected, MAS usually had a crescent-like shape (Figure 3D) and many degraded cells were present. In contrast, FAS was located centrally inside the vascular cylinder (Figure 3I). Below the nematode head, in the juvenile migration region, the extent of destructions was very high around predicted male juveniles (Figure 3E), whereas almost undestroyed vascular cylinder was present next to predicted female juveniles (Figure 3J). Another anatomical feature differentiating both syncytia was the very weak development of peridermis-like secondary cover tissue around MAS (Figure 3A-3C versus Figure 3F-3I). It consisted of 3-4 continuous cell layers ensheathing FAS (Figure 3F-3H) and only 1-2 cells layers in MAS (Figure 3A-3C).

Serial sectioning of syncytia allowed us to localize heads and stylets of several predicted male and female juveniles. The equivocal identification of ISCs at this time point (5 dpi) was difficult due to extensive cell enlargement and translocations. However, it seems that juveniles always selected their ISCs in cells next to the xylem vessels (Figure 3I, 3K and 3L). FAS was induced among procambial cells (Figure 3I and 3K) whereas MAS was induced among pericyclic cells (Figure 3L).

Ultrastructural analysis showed that at 5 dpi FAS had electron-dense cytoplasm with strongly reduced volume of vacuoles (Figure 3M). Its protoplast contained enlarged and amoeboid nuclei, and numerous organelles. In contrast, MAS had less electron-dense cytoplasm almost completely devoid of rough ER cisternae, but small vacuoles were more numerous than in FAS (Figure 3N).

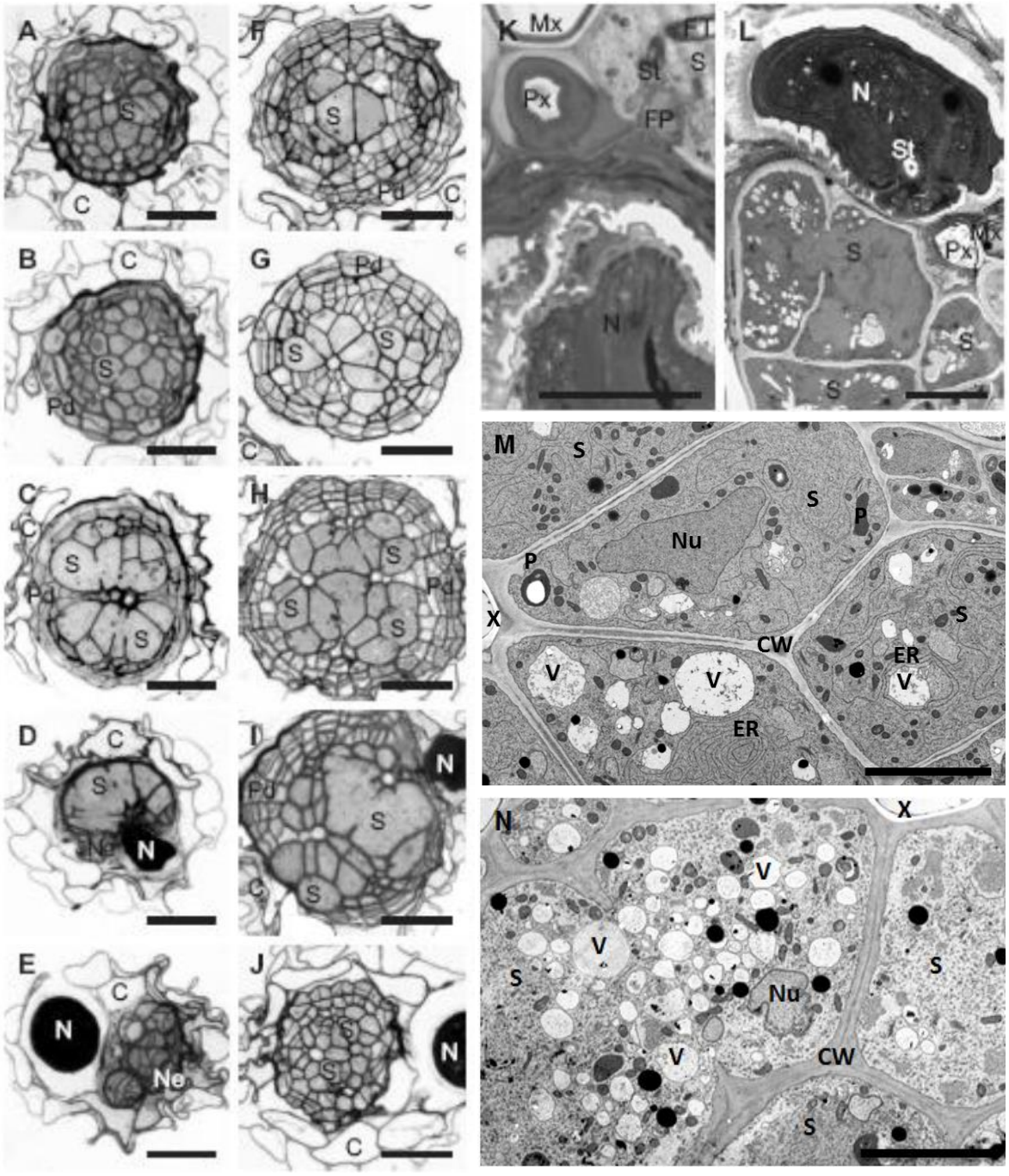

Figure 3: Anatomy and ultrastructure of syncytia associated with predicted male and female juveniles. Light (A-J) and transmission electron microscopy (K-N) images taken from cross sections of syncytia associated with male (A-E, L and N) and female (F-J, K and M) juveniles. The images were taken from sections made at the leading edge of syncytium (A and F), submedian region of syncytium (B and G), median region of syncytium (C, H, M and N), next to the nematode head (D, I, K and L) and along nematode migration path (E and J). Abbreviations: C-cortex, CW-cell wall, ER-cistern of endoplasmic reticulum, FP-feeding plug, FT-feeding tube, Mx-metaxylem vessel, N-nematode, Ne-necrosis, Nu-nucleus, Pd-peridermis-like tissue, Pl-plastid, Px-protoxylem vessel, S-syncytium, St-stylet, X-xylem, V-vacuole. Scale bars: 50 µm (A-J) and 5 µm (K-N).

FAS and MAS express transcriptional differences

To reveal changes in gene expression between FAS and MAS during early stages of infection, GeneChip analyses were performed. Plants were grown and inoculated with nematodes as described in the Methods section. Invading J2s that had successfully established the ISC (as defined by a cessation of stylet movements) were marked at 1 dai, and sex was predicted at 4 dai. Afterwards, root segments containing either potential MAS or FAS were dissected at 5 dpi. The samples were embedded in an optimum cutting medium (OCT) and pure syncytial material was isolated using Laser Capture Microdissection (LCM). Total RNA was extracted, labelled, amplified and hybridized with *Arabidopsis* ATH1 GeneChip® designed for detection of 24,000 genes. We compared the transcriptomes of FAS and MAS and found that 455 genes were differentially expressed (fold change >1.5) for a false discovery rate below 5% (Table S1). A detailed look at the transcriptome demonstrated that a higher number of genes showed increased transcript abundance in MAS (331), as compared to FAS (124). For the sake of simplicity, the terms FAS- or MAS-specific are used to describe genes that have an increased expression in FAS or MAS respectively, throughout this manuscript. A list of the 50 most strongly differentiated genes is given in Tables 2.

Defense- and nutrient stress-related genes are over-represented in MAS

To get an overall view of the processes that are altered between FAS and MAS, we performed a GO enrichment analysis of FAS- or MAS-specific genes by computing overlaps with 7041 previously defined data sets using PlantGSEA (Yi et al., 2013). Categories that were particularly enriched in genes upregulated in FAS include ‘polysaccharide biosynthetic processes’, ‘carbohydrate biosynthetic and metabolic processes’, ‘polysaccharide metabolic processes’, and many cell wall related biosynthetic and metabolic process categories (Figure 4A). On the other hand, this analysis identified categories of ‘response to stimulus, ‘response to stresses, ‘response to starvation’, ‘response to nutrition’, and ‘defense and innate immune response’, with a significant overrepresentation of MAS-specific genes (Figure 4B). The complete list of overrepresented categories in GO enrichment for FAS and MAS has been given in Supplementary Tables S2 and S3.

Next, we analyzed the organ-specific expression of 100 FAS-specific, and 100 MAS-specific genes, using the public microarray database Genevestigator (Zimmerman et al., 2004). We found that a number of these genes are not root-specific, but instead, shows maximum

expression in flowers (Supplementary Figure S1). Notably, we found a tendency for FAS-specific genes to show maximum expression in pistils (female reproductive organs in flower), as compared to those MAS-specific genes, which tended to have the highest expression levels in the stamens (male reproductive organ in flower) (Supplementary Figure S2).

An analysis of the expression of FAS-specific or MAS-specific genes in response to biotic infections was performed by Genevestigator and found that many of the MAS-specific genes are strongly induced in responses to biotic infections (Supplementary Figure S3). On the other hand, FAS-specific genes, showed little to no induction in response to biotic infections (Supplementary Figure S4). Further, we performed a similar analysis to evaluate the expression pattern of FAS-specific or MAS-specific genes in response to the nutrient stress. Whereas the FAS-specific genes were not or only slightly related to nutrient stress responses (Supplementary Figure S5), the MAS-specific genes showed a clear tendency to be induced by iron or sulphur deficiency. Interestingly, the expression of many of the MAS-specific genes was suppressed when seedlings were treated with sucrose or glucose (Supplementary Figure S6).

Table 2: List of top 50 genes differentially expressed between FAS and MAS. The data of FAS and MAS were compared with each other. The genes selected are differentially expressed with ajd. *p*-value <0.05.

Locus	Adj. *p*-value	Log_2	Fold change	Gene annotation
Genes upregulated in FAS compared to MAS				
At3g22120	0.003	3.75	13.46	CWLP (Cell Wall Plasma membrane Linker Protein)
At2g23170	0.026	1.97	3.92	GH3.3; indole-3-acetic acid amido synthetase
At3g21550	0.028	1.70	3.25	Protein of unknown function DUF679
At1g75900	0.049	1.57	2.97	Putative GDSL, Lipase
At4g00220	0.041	1.53	2.88	JLO (Jagged Lateral Organs)
At1g24020	0.001	1.53	2.88	MLP423 (MLP-Like Protein 423)
At5g57800	0.026	1.50	2.83	CER3 (Eceriferum 3)
At1g72970	0.037	1.49	2.81	HTH (Hothead)
At3g30180	0.030	1.43	2.70	BR6OX2 (Brassinosteroid-6-oxidase 2)
At5g15580	0.029	1.43	2.70	Encodes Longifolia (LNG1). Regulates leaf morphology by promoting cell expansion in the leaf-length direction
At5g48485	0.048	1.43	2.69	DIR1 (Defective In Induced Resistance 1)
At1g55260	0.041	1.41	2.65	LTPG6 (Glycosylphosphatidylinositol-Anchored Lipid protein Transfer 6)
At3g20520	0.001	1.40	2.64	SVL3 (SHV3-Like 3)
At4g39330	0.041	1.40	2.64	CAD9 (Cinnamyl Alcohol Dehydrogenase 9)
At5g02760	0.022	1.37	2.58	Involved in: protein amino acid dephosphorylation
At5g48350	0.023	1.35	2.55	3'-5' Exonuclease activity

At1g25450	0.013	1.29	2.44	KCS5 (3-Ketoacyl-Coa Synthase 5)
At1g13420	0.033	1.24	2.36	ST4B (Sulfotransferase 4B)
At3g58190	0.042	1.24	2.36	LBD29 (Lateral Organ Boundaries-Domain 29)
At3g15050	0.036	1.22	2.34	IQD10 (IQ-domain 10); Calmodulin binding
At2g38080	0.030	1.18	2.27	IRX12 (Irregular Xylem 12)
At3g30270	0.004	1.17	2.26	AGL79 (Agamous-Like 79); transcription factor
At1g73780	0.011	1.16	2.24	Bifunctional inhibitor/lipid-transfer protein
At1g68530	0.021	1.15	2.22	KCS6 (3-Ketoacyl-Coa Synthase 6)
At3g62020	0.04	1.15	2.21	GLP10 (Germin-Like Protein 10)

Genes upregulated in MAS compared to FAS

At5g10180	0.01	1.31	2.47	AST68; Sulphate transmembrane transporter
At4g38420	0.01	1.31	2.48	sks9 (SKU5 Similar 9); oxidoreductase
At2g41730	0.03	1.33	2.51	Molecular function not known
At4g36110	0.02	1.33	2.51	Sugar like auxin responsive protein
At3g21520	0.002	1.36	2.57	Encodes a protein is directly or indirectly involved in membrane fission during breakdown of the ER and the tonoplast during leaf senescence and in membrane fusion during vacuole biogenesis in roots
At1g70880	0.03	1.36	2.57	Polyketide cyclase/ Involved in defence response
At1g08080	0.01	1.39	2.62	ACA7 (Alpha Carbonic Anhydrase 7)
At5g06860	0.002	1.45	2.73	PGIP1 (Polygalacturonase Inhibiting Protein 1)
At5g02780	0.01	1.45	2.73	Glutathione transferase , found two loci
At1g64660	0.02	1.46	2.76	ATMGL (*Arabidopsis thaliana* Methionine Gamma-Lyase)
At3g49780	0.02	1.50	2.82	ATPSK4 (Phytosulfokine 4 Precursor)
At2g34610	0.004	1.52	2.88	Unknown Protein
At5g26220	0.03	1.60	3.03	ChaC-like family protein, molecular function unknown
At1g21100	0.02	1.62	3.08	O-methyltransferase family protein; Functions in: methyltransferase activity
At2g30770	0.09	1.66	3.17	CYP71A13 (Cytochrome P450, family 71, subfamily A, Polypeptide 13)
At2g43510	0.01	1.73	3.32	ATTI1; Serine-Type Endopeptidase Inhibitor
At5g59530	0.01	1.76	3.38	2-Oxoglutarate (2OG) and Fe(II)-dependent Oxygenase superfamily protein
At3g56980	0.05	1.90	3.72	BHLH039; Transcription factor
At5g04150	0.004	1.94	3.85	BHLH101; Transcription factor
At3g08860	0.03	2.03	4.08	Encodes a protein that is predicted to have beta-alanine aminotransferase activity
At3g49580	0.01	2.06	4.17	LSU1 (Response to Low Sulphur 1)
At1g12030	0.01	2.10	4.27	Protein unknown function
At1g19610	0.004	2.11	4.33	PDF1.4 (Plant Defensin 1.4)
At3g60140	0.01	3.21	9.28	DIN2 (Dark inducible 2)
At2g44460	0.03	4.30	19.75	BGLU28 (Beta glucosidase 28)

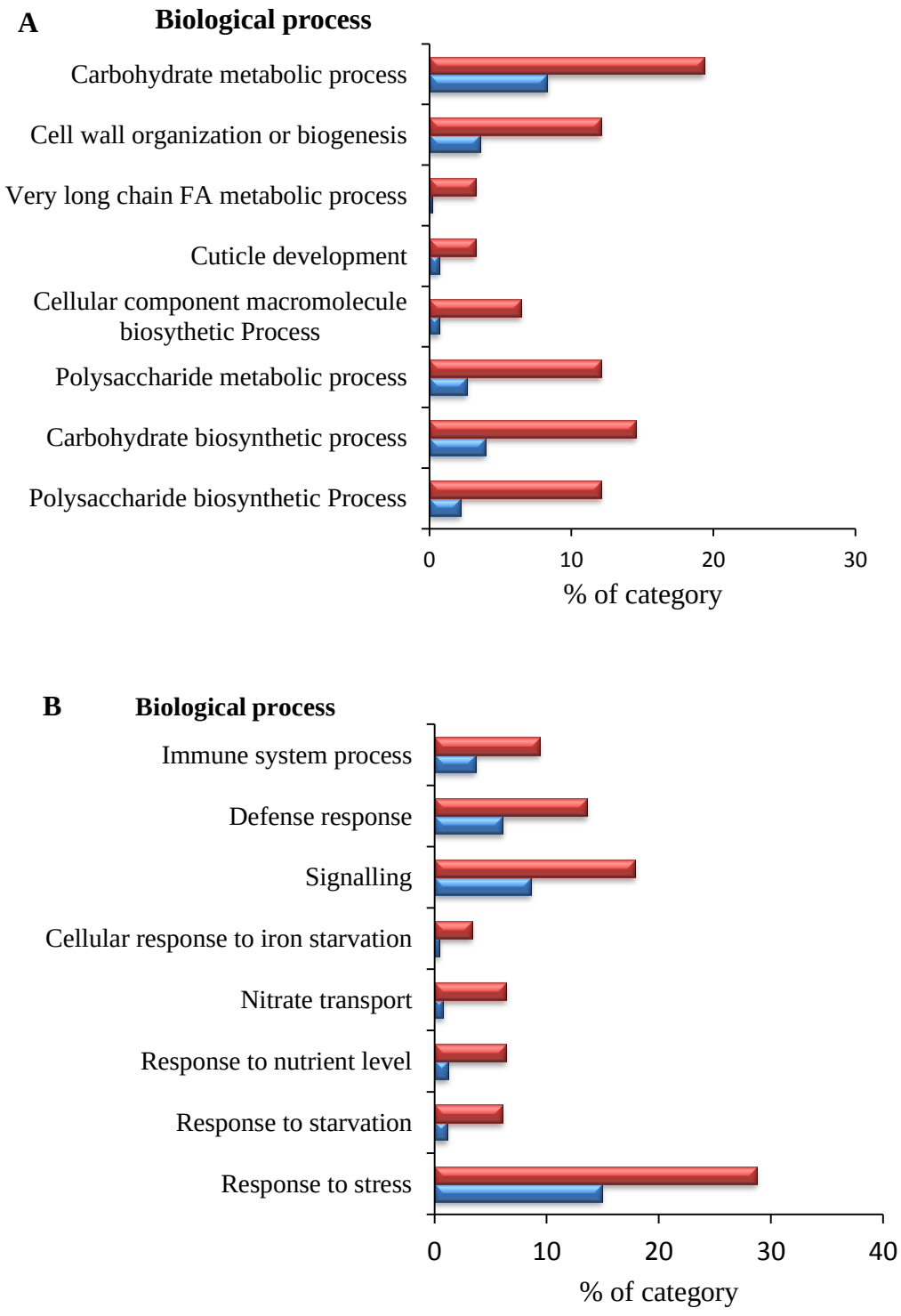

Figure 4: Preferential regulation in gene ontology categories with relevance to FAS and MAS. Preferential regulation of differentially expressed genes for selected GO categories of the domain 'biological process'. The percentage of expected and actual genes found in the examined subset is shown on the *x*-axis. The blue bar represents the expected set of whole *Arabidopsis* genome matching to respective category and red bar indicates the set of differentially regulated genes in current study. All the gene sets shown have FDR <0.05 and Fold change <1.5. (A) Over-representation of FAS preferentially upregulated genes (124) with respect to MAS. (B) Over-representation of MAS preferentially upregulated genes (331) with respect to FAS.

Validation of GeneChip data by quantitative RT-PCR

The expression of eight FAS-specific and/or MAS-specific genes was further validated using quantitative RT-PCR. Our analysis showed the same trend in qPCR examinations as that indicated by microarrays (Table 3). However, fold change for some candidate genes (*CWLP1*, cell wall plasma membrane linker protein; *GH3.3*, indole-3-acetic acid-amido synthetase; *PGIP1*, polygalacturonase inhibitor protein 1*;* and *LNG1*, longefolia 1) was much higher as compared to microarray.

Table 3: Validation of microarray data by qRT-PCR

		Fold Change* (Female vs Male)	
Locus	**Gene Name**	**Microarray**	**RT-qPCR**
At2g44460	BGLU28	-19.75	-18.02±10.24
At2g23170	GH3.3	3.92	8.72±1.74
At3g22120	CWLP1	13.46	36.25±12.25
At5g06860	PGIP1	-2.72	-5.95±2.47
At5g06870	PGIP2	-1.86	-2.82±0.97
At1g19610	PDF1.4	-4.33	-1.31±0.97
At1g55260	LTPG6	2.65	2.94±1.24
At5g15580	LNG1	2.58	6.05±1.20

* The fold change of FAS and MAS when compared to each other. The ΔCT value of each gene was calculated by deduction of mean C_T value of each gene from mean C_T of internal control (*β*-tubulin). For comparison, ΔCT of FAS samples was deducted from ΔCT value of MAS.

Promoter::GUS analysis

We generated promoter::GUS lines to analyse the spatio-temporal expression of two highly expressed candidate genes, one each for FAS (*CWLP1*,) and MAS (*BGLU28*, B-glucosidase 28). Three homozygous independent lines were selected and assessed further. Finally, one representative line for each gene was infected with nematodes and stained for GUS activity at 5 and 12 dpi (Figure 5). At 5 dpi, we predicted sex of the nematode either male or female and performed GUS staining. In *pCWLP1::GUS* plants, we found that the majority of the FAS showed a moderate-to-high GUS staining at 5 as well as 12 dpi. Only weak staining was detected in MAS (Figure 5). For *pBGLU28::GUS*, FAS showed a weak GUS staining, whereas MAS were stained strongly. For *pCWLP1::GUS*, whereas FAS showed a weak GUS staining, MAS showed a strong GUS staining. For *pCWLP1::GUS*, a slight GUS staining was detected in the vascular cylinder, however, in both *pCWLP1::GUS* and *pBGLU28::GUS*, faint GUS staining was detected at root tips of uninfected control plants (Figure 6).

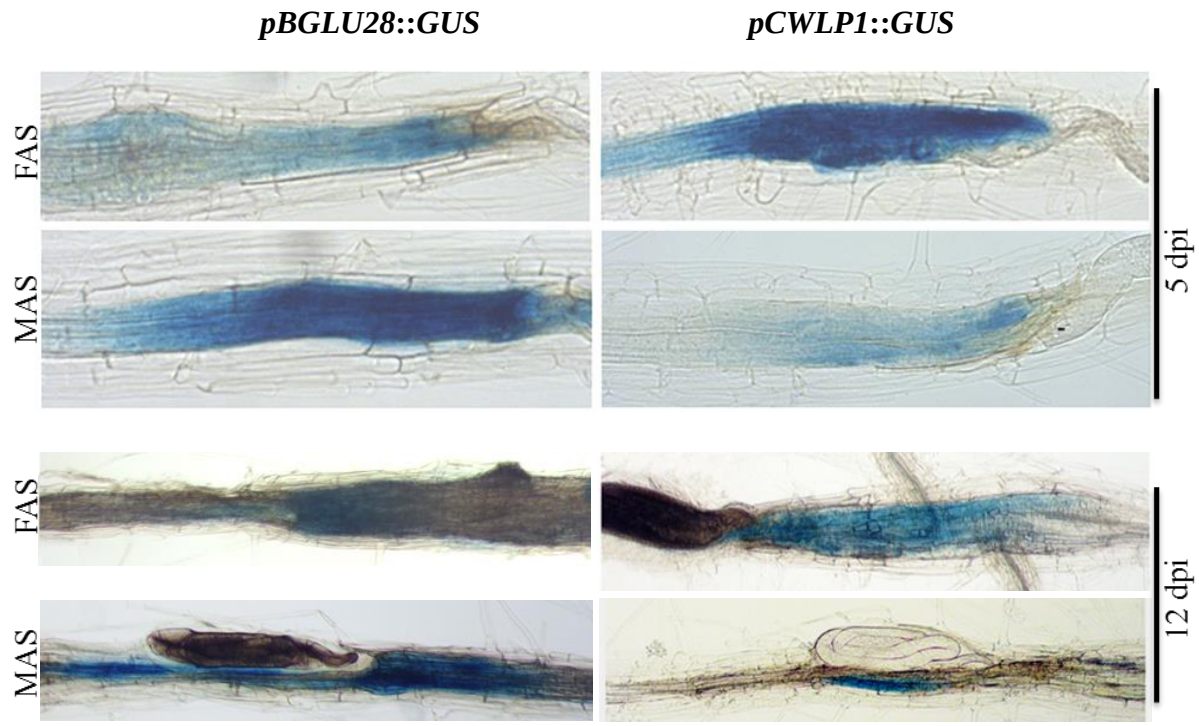

Figure 5: GUS staining of FAS and MAS at 5 and 12 dpi. The figures on the left side represent *pBGLU28*::*GUS* line and on the right side represent *pCWLP1*::*GUS* line of *Arabidopsis*.

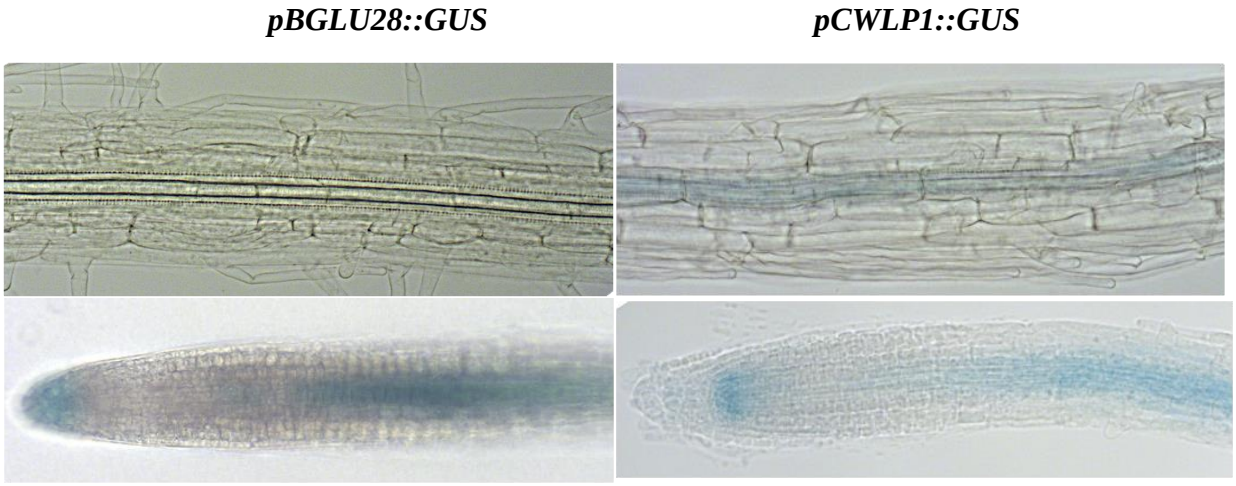

Figure 6: GUS staining in non-infected roots

Knocking-out host candidate genes alters the sexual fate of nematodes

Although our transcriptomic data provided information regarding the differences between FAS and MAS, it was not clear which genes/pathways are involved in ESD of nematodes. To investigate this, we selected eight FAS-specific genes (*CWLP1, Cell wall-plasma membrane linker protein 1*; *MLP423, MLP-like protein 423; SHVL3, Glycerophosphodiester phosphodiesterase GDPD like 5*; *LAC11, Laccase 11*; *LNG1, Longifolia 1*; *IRX12, Irregular xylem 12*; *LTPG, Glycosylphosphatidylinositol-anchored lipid protein transfer 6*) and three

MAS-specific genes (*BGLU28*; *BGLU30/DIN2*; *BHLH101*, Basic helix-loop-helix transcription factor) for further characterization using loss-of-function T-DNA mutants (Supplementary Table S4 and Supplementary Figures S7). Two weeks after inoculation, plants were screened for development of males and female. We found that out of 8 mutant lines for FAS, two lines, *lng1* and *irx12*, showed a significant reduction in number of females and a significant increase in number of males as compared to Col-0. In addition to *lng1* and *irrx12*, *lptg6* also showed a significant decrease in number of females as compared to Col-0, but the number of males did not change significantly (Figure 7A). We also found that size of syncytia but not the size of females in *ltpg6*, *irx12* and *lng1* mutants was significantly reduced in comparison to Col-0 plants (Figure 7B-C). In contrast to mutants for FAS genes, no changes in mutant lines for MAS genes were detected.

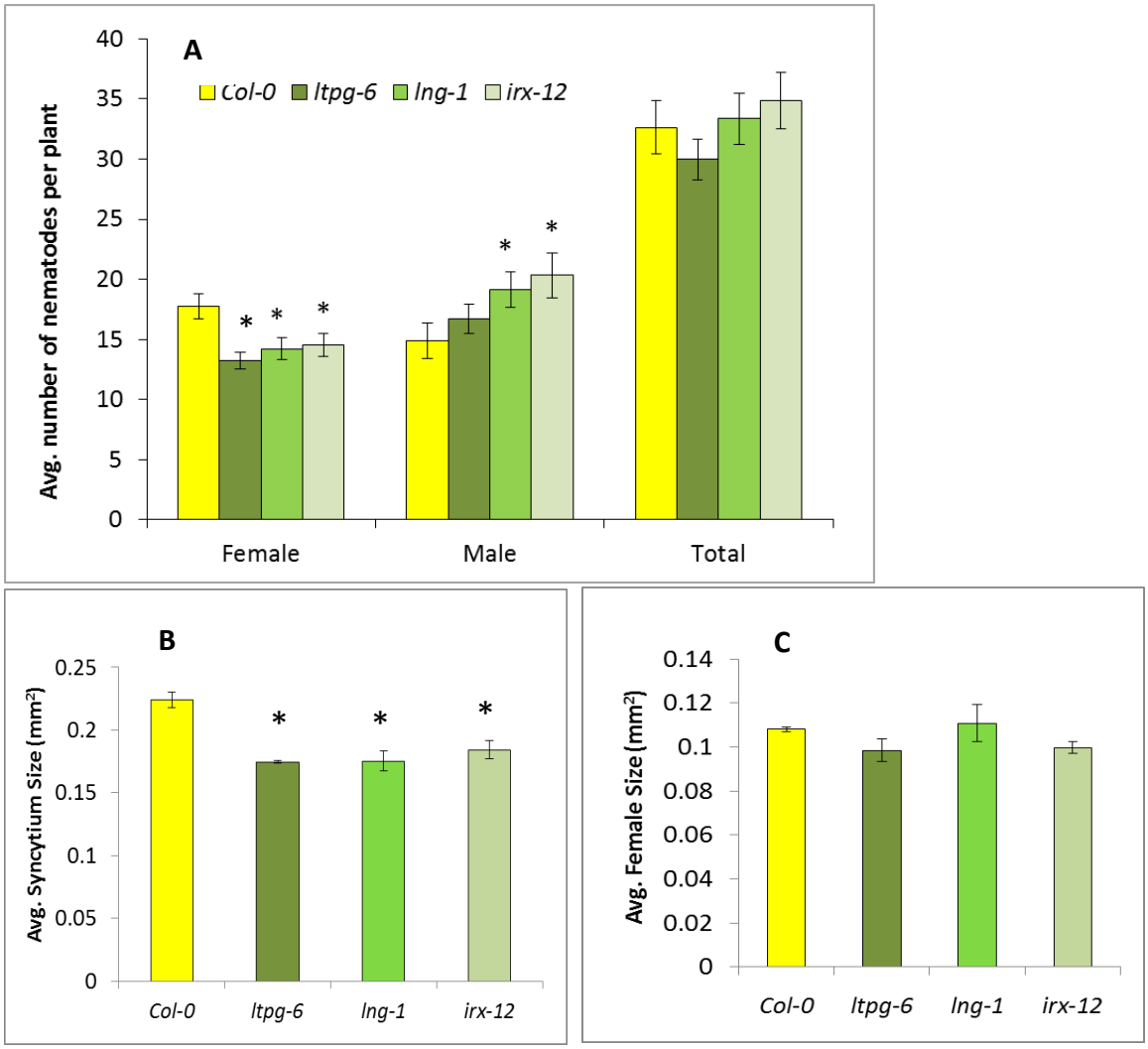

Figure 7: Nematode infection assays in *Arabidopsis* mutant lines. (A) An average number of males, females and total nematodes are presented. (B) Average syncytium size. (C) Average female size. Bars represent mean ± SE. Data was analyzed using student's *t-test*. Asterisks represent significant difference at $P < 0.05$, corresponding to Col-0.

Discussion

The effect of environment on sexual outcome of cyst nematode has long been debated (Molz, 1920; Sengbusch, 1927; Ellenby, 1954; Den Ouden, 1960; Trudgill, 1967). Nevertheless, mechanistic details underlying ESD of cyst nematodes remained elusive. A problem in performing such an analysis has been the fact that sexual dimorphism of the sedentary cyst nematodes is not recognizable until the end of J2 developmental stage (Wyss, 1992). Here we developed and validated a strategy that can predict the sex of cyst nematodes during early stages of infection with high certainty. Our analysis showed that those J2 nematodes, which were developing at the fastest rate during 5 dpi became females. Conversely, the nematodes that were slow in gaining their body size became mainly males. The difference between male and female juveniles is also reflected in the development of their respective syncytia. For example, MAS has been shown to remain smaller in size than FAS at various developmental stages and FAS reaches about 10 times larger volume than MAS (Kerstan, 1969; Endo, 1964; Endo, 1965). Interestingly, Müller and co-worker's study on comparative food consumption by male and female juveniles from roots of *B. napus* found that female in total consumes 29 times more food than male **(**Müller et al., 1981**)**. Based on our data and previous literature, we concluded that the difference in food consumption and related size of syncytia associated with male and female juveniles leads to the difference in body volume development between the sexes.

Anatomical and ultrastructural differences between FAS and MAS

On-section microscopic examination showed that FAS and MAS clearly differ in their anatomical organization. MAS were smaller in diameter and length in comparison to FAS (Endo 1964; Golinowski et al., 1996; Sobczak et al., 1997). Smaller dimensions correspond to smaller volume of the syncytium, thus to smaller volume of protoplast on which the juveniles feed. On the other hand, smaller syncytia have also proportionally reduced surface of the interface to the vascular cylinder's conductive elements thus the influx of nutrients to MAS seems to be also reduced. Predicted male juveniles usually migrated inside the vascular cylinder for long distances and caused very extensive destructions of its cells. It poses a question if the continuity of xylem and phloem conductive elements was maintained or disrupted. If the conductive system was disrupted, the MAS were located at its termini and there was no continuous current of xylem or phloem sap flowing along them. At the cellular level, the most obvious differences between MAS and FAS concerned to the presence of

numerous small vacuoles in the former and cisternae of rough ER in the latter. In general, cisternal rough ER is implicated in biosynthesis of proteins predicted for secretion, whereas small vacuoles, in conjunction with low electron density of syncytial cytoplasm, might indicate protoplast degradation related to defense response or programmed cell death. Above described set of structural differences clearly indicates that MAS faces physiological problems related to nutrients availability or defense responses of syncytial protoplast resembling those observed in resistant plant-nematode interactions (Endo, 1965; Trudgill 1991; Sobczak et al., 2005).

Transcriptome comparison between FAS and MAS

Earlier transcriptomic studies of syncytia induced in roots of soybean and *Arabidopsis* revealed that nematodes trigger massive changes in key pathways of host transcriptome including pathways of hormonal regulation, cell wall architecture, cytoskeleton and dedifferentiation of cells, supporting the syncytium to function as metabolically highly active cells (Puthoff et al., 2003; Ithal et al., 2007a and b; Szakasits et al., 2009). Metabolite profiling also revealed an accumulation of certain amino acids, phosphorylated metabolites and specific sugars inside the syncytia (Hofmann & Grundler, 2006; Hofmann et al., 2007 and 2010; Siddique et al., 2014). However, these studies were conducted exclusively on FAS or a mixture of FAS and MAS. We hypothesized that there may be differential transcriptional regulations between FAS and MAS that in turn influence the sexual differentiation of juveniles. Therefore, here, we performed a microarray analysis to compare the transcriptome of MAS and FAS at 5 dpi.

Cell wall modification in FAS and MAS

Starting from a single cell, syncytium undergoes extensive expansion by local dissolution of the cell wall of neighboring cells (Grundler et al., 1998; Wieczorek et al., 2006 and 2014; Davies et al., 2012). The outer wall of the syncytium is thickened to withstand increased turgor pressure inside the cell (Böckenhoff and Grundler, 1994; Siddique et al., 2012). Further, syncytial cell walls facing xylem vessels develop numerous cell wall ingrowths to enhance surface area for absorption of more nutrients and water (Golinowski et al., 1996; Offler et al., 2003). All these changes in cell wall structure contribute to meet the growing demand of food for fast developing nematodes. Indeed, microarray data published by Puthoff et al. (2003) at 3 days after inoculation and Szakasits at al. (2009) at 5 and 15 days after

inoculation also showed high upregulation of genes for 'cell wall biosynthesis and modifications'. Our results however, for the first time indicate that FAS undergoes a stronger upregulation of genes for 'cell wall biosynthesis, metabolism and modifications' as compared to MAS. Considering that female nematodes require comparatively more food and grow much faster in comparison to males (Müller et al., 1981; Golinowski et al., 1996; Sobczak et al., 1997; Hofmann et al., 2007), it is plausible that genes belonging to the category 'cell wall modification' showed an increase in transcript abundance in FAS as compared to MAS. Such a differential expression of cell wall genes may support differential nutritional requirement between FAS and MAS. This hypothesis is also supported by previous studies where FAS has been shown to contain more conspicuous cell wall ingrowths (transfer cells) and cell wall openings as compared to MAS (Golinowski et al., 1996, Sobczak et al., 1997).

Immune responses

Nematodes invasion of the root and subsequent migration towards the vascular cylinder cause cellular damage and activate plant defense responses (Holbein et al., 2016; Teixeira et al., 2016; Mendy et al., 2017). Previous analyses showed that the nematodes use their stylets to secrete a variety of molecules (effectors) that suppress the defense responses in the infected plant cells, leading to the formation of a functional feeding site (Hewezi & Baum, 2013). However, the transcriptome analysis presented in this study showed that several genes that are activated upon infection against a variety of pathogens are expressed more abundantly in MAS as compared with FAS. Particularly relevant is a set of genes with role in plant basal defence against pathogens. Among them are members of polygalacturonase-inhibiting protein gene family (*PGIP1* and *PGIP2*), which are involved in perception and activation of damage-associated defense responses. Both *PGIP1* and *PGIP2* are more strongly expressed in MAS as compared to FAS and our recent work demonstrated that loss-of-function *pgip1* mutants show a significant increase in average number of females and a corresponding decrease in average number of males as compared to Col-0 (Shah et al 2017, manuscript under review). Likewise, several host secondary metabolism genes such as phytoalexin deficient (*PAD3*), indole glucosinolate o-methyltransferase 1 (*IGMT1*) and cytochrome P450 91A1 (*CYP81D1*) are significantly upregulated in MAS as compared to FAS. Intriguingly, we have also found that PGIP-mediated changes in host susceptibility to cyst nematodes involve activation of genes encoding enzymes for host secondary metabolism (Shah et al 2017, manuscript under review). Other defense-related genes that are more abundantly expressed in MAS include

Plant defensins (*PDF1.4*, *PDF2.1*), transcription factors (*WRKY75*, *WRKY61*, *WRKY28*), receptor like proteins/kinases (*LRRRLK-At2g24130*, *LECRK-V.6-At3g59730*, *PERK2-At3g24400*, *AtRLP22-At2g32660*, *LECRK-V.7-At3g59740*, *LYK4-At2g23770*, *LRRRLK-At5g37450*) and MAP kinase singalling cascade components (substrate of the MAPK kinases- *At1g80180*, *MAPKKK16*, MPK3/6-Targeted VQP).

Altogether these results hinted that ESD in cyst nematodes is influenced by the extent to which host defence responses are avoided / suppressed. We propose that some of the nematodes may be able to effectively suppress or avoid the defence response during the initial stages of infection leading to the conditions that are favourable for a female development. In cases, where defence responses could be established by the plant, male development was induced. Alternatively, it can be argued that sex of the beet cyst nematode is genetically pre-determined and male nematodes just do not effectively suppress the defence responses below a minimum level that is required for a female development. However, the fact that knocking out key defense response genes such as *PGIP1* increases the number of females and decreases the number of males makes it unlikely that sex of the nematode is pre-determined.

Nutritional status

Syncytia are strong sinks and the only source of nutrients for nematodes throughout their live span of several weeks. These sinks are symplasmically isolated during the initial phase of development to support cellular organization. However, secondary plasmodesmata are established with surrounding phloem during next few days of syncytium development to support the high demand of assimilates for rapidly growing juveniles (Hofmann & Grundler 2006; Hoth et al., 2008). Intriguingly, the presence of plasmodesmata has been shown to occur only between FAS and surrounding phloem, whereas intake of nutrients in MAS is largely supported by membrane-localized transporters (Hofmann & Grundler, 2006; Siddique & Grundler, 2015). Our data showed that a number of FAS-specific genes show maximum expression in flower's pistil (Supplementary Figure S1). Conversely, a number of MAS-specific genes were found to have maximum expression in stamen pollen grains (Supplementary Figure S2). Similar to syncytium, ovary and pollen are sinks for nutrients. Whereas ovules are connected to the surrounding phloem during early stages via plasmodesmata, the plasmodesmata connecting pollen to nutritive tissue degenerate as the pollen cells mature and carbohydrates import occurs via plasma membrane localized

transport proteins (Sager & Lee, 2004; Stadler et al., 1999; Ruan et al., 2012). Based on these observations, we propose that source-sink interaction of FAS and MAS resemble with that of ovule and pollen respectively, which may explain the overlapping expression of FAS-specific and MAS-specific genes with that of ovule and pollen grain respectively.

We also found that a number of genes induced by sulphur deficiency, iron deficiency, or starvation were upregulated in MAS as compared with FAS. These observations raise the question whether availability of certain essential elements influences sexual differentiation of the nematodes. We propose that nematodes associated with syncytia that are unable to provide them optimal composition of nutrients may develop as males. This hypothesis is supported by earlier studies suggesting that deficiency of essential elements like phosphorous, nitrogen and potassium significantly increase the number of males on the host plant (Kämpfe & Kerstan, 1964). Alternatively, it is possible that nematode juveniles provoke a local host defence response during migration and establishment of ISC and an inability to effectively suppress or overcome these defence responses may lead to a restrictions in nutrients supply, leading to the development of males. More work will be needed to investigate this hypothesis.

Functional characterization of candidate genes

Irregular Xylem 12

Our transcriptome data showed that Irregular Xylem Phenotype 12 (*IRX12*) is one of the most strongly upregulated genes in FAS as compared to MAS. *IRX12* is strongly expressed in vascular bundles and has been found to be involved in constitutive lignification of the *Arabidopsis* stem by regulating phenylpropanoid metabolism (Brown et al., 2005; Berthet et al., 2011). Knock-out mutant for *IRX12* has been characterized by exhibiting irregular xylem morphology due to negative pressure produced by water transportation (Brown et al., 2005). The phenotype arises due to defective cellulose and lignin biosynthesis, which otherwise would provide resistance against compressive forces. The phenotype is also an indicator of secondary cell wall malformation (Turner & Somerville, 1997; Jones et al., 2001). The phenotype intensity of irregular or distortion of xylem vessels in *IRX12* has been found to be from mild to severe within the vascular bundles of the same plant (Brown et al., 2005). Moreover, *IRX12* has also been found providing mechanical strength to xylem vessels (Yokoyama & Nishitani, 2006). The results from our infection assays on knock-out mutant

irx12 showed a reduction in numbers of females, whereas the numbers of males were increased significantly as compared to wild type. Because *irx12* mutants are known for defects in lignin biosynthesis and mild reduction in cellulose during secondary cell wall formation of xylem (Yokoyama & Nishitani, 2006; Hao & Mohnen, 2014), we suggest that upregulation of *IRX12* in FAS is required for increased thickening of syncytial cell wall, which would in turn support expanding syncytia tolerating high turgor pressure. In absence of IRX12, impairment in cell wall thickening may restrict proper enlargement of syncytia leading to development of more males.

Alternatively, impairment in secondary cell wall synthesis might lead to activation of plant defense pathways that restrict further development of female nematodes and favor development of more males. This hypothesis is supported by previous studies where knocking-out cell wall biosynthesis genes such as *IRX5* and *IRX3* conferred enhanced resistance against necrotrophic and vascular pathogens (Ellis et al., 2002; Hernández-Blanco et al., 2007; Ramos et al., 2013).

Glycosylphosphatidylinositol-anchored lipid transfer protein 6 (*LTPG6*)

Non-specific lipid transfer proteins (nsLTPs) are plant-specific proteins encoded by large gene families. One of the major types includes LTPGs, where the transcript additionally encodes a C-terminal signal sequence, which leads to addition of glycosylphosphatidylinositol (GPI)-anchor via post-translational modification (Debono et al., 2009). Although *in vivo* role of these proteins has not yet been clearly determined, *in vitro,* they have been shown to bind and transport lipid molecules (Carvalho & Gomes, 2007; Lee et al., 2009). Therefore, it is assumed that *in vivo,* LTPGs are involved in lipid transport to the plant surface (Edstam & Edqvist, 2014). Several members of LTPGs including LTPG6 have also been found in phloem exudates of *Arabidopsis* secreted upon inoculation with *Pseudomonas syringae* pv. tomato. These observations led to the suggestions that *LTPGs* may be involved in systemic acquired resistance (SAR); however, no such role for *LTPGs* has been yet established (Carella et al., 2016). Nevertheless, knock-out mutant for some *LTPGs* in *Arabidopsis* has been reported to have reduced fertility due to infertile ovules, an inability to restrict the uptake of tetrazolium salt, and decreased levels of ω-hydroxy fatty acids in seed coat. These authors suggested that *LTPGs* may be involved in biosynthesis or deposition of suberin or sporopollenin (Edstam & Edqvist, 2014).

Our pathogenicity assays with *ltpg6* mutants showed that although numbers of female nematode were significantly decreased, but there was no significant increase in the number of male nematodes. Moreover, size of FAS was also significantly decreased in *ltpg6* as compared to Col-0. Although, it is hard to identify a role for *LTPG6* in plant-nematode interaction based on current data, it may be that *LTPG6* is involved in suberin biosynthesis and deposition around feeding site. This is supported by recent studies where a role of suberin in syncytium formation is described (Holbein et al. unpublished). However, further characterization will be required to understand role of *LTPG6* in nematode development.

Longifolia 1 (LNG1)

The infection assays on *lng1* mutant revealed that numbers of female nematodes were significantly reduced and numbers of male nematode were significantly increased. Moreover, syncytia sizes were also significantly reduced in *lng1* as compared to wild-type *Arabidopsis*. The *LNG* gene family consists of only two genes, *LNG1* and *LNG2*, in *Arabidopsis*. Indigenously, they are expressed in various plant organs, including leaves, flowers, and lateral roots where the cellular expression has been localized in cytosol and nucleus. The *lng1* overexpression mutants were observed to have extremely long leaf, elongated floral organs, and elongated siliques. Moreover, it was observed that *LNG1* and *LNG2* regulate leaf morphology by promoting longitudinal polar cell elongation (Lee et al., 2006). Kerstan (1969) studied female and male development of *H. schachtii* with respect to root and giant cell (syncytium) diameter and found that a certain minimum size of syncytium is required for female development. Therefore, we suggest that in *LNG* knock-out plants the size and probably shape of the syncytial cell is reduced which may be less supportive to females. Therefore, more males developed. Further studies involving a double mutant of both LNG genes may provide more insight into the role of *LNGs* in syncytium and nematode development.

Conclusion

In context of crop damage, population dynamics, and nematode management through host plants, the sex ratio of cyst nematodes is of fundamental importance. It not only influences the population rate in the next generation but also affects the intensity of crop damage, which is usually proportional to the number of females. Therefore, understanding the factors behind sexual differentiation could be helpful in developing conceivable methods to exploit the sex

ratio in the favour of males. In the present study, the plant host factors driving the sexual differentiation of the cyst nematode *H. schachtii* have been explored at the molecular level. We conclude that a number of factors including intensity of immune responses, availability of nutrients and selection of ISC may contribute to the development of nematodes as females or males. We also identified more than four hundred genes that are differentially expressed between MAS and FAS. We found that knocking out some of the differentially regulated genes alters the male-to-female sex ratio of beet cyst nematode. In future, it will be important to extend this screening to identify additional host mutants with a strong influence on the sex ratio. It will also be critical to further investigate the mechanism by which these host genes influence sex of other cyst nematode species. Exploitation of cyst nematode sex-related host genes may provide additional resources for development of resistant cultivars.

Materials and Methods

Plant growth conditions

Arabidopsis seeds were surface sterilised using 0.7% NaOCl (v/v) for 5 minutes followed by three successive washings with sterile water. The sterilised seeds were grown in Petri dishes containing Knop medium supplemented with 2% (w/v) sucrose. The plates were incubated in growth room at 25 °C, with an alternating period of sixteen hours of light and eight hours of dark under sterile conditions. More details regarding this have been described earlier (Siddique et al., 2014; Siddique et al., 2015).

Nematode measurement, prediction and infection assay

Arabidopsis plants were grown under conditions as described above. 10-days-old plants were infected with freshly hatched J2s of *Heterodera schachtii* as previously described (Siddique et al., 2012). The J2s hatching was stimulated by keeping cysts in $ZnCl_2$. For relative growth, the J2s that invaded and established in the lateral roots at 24 hours after inoculation (hai) were marked with permanent markers on petri dishes and imaged daily for the next five days. Their feeding establishment was defined when a nematode stopped stylet movements. The average size of a nematode was measured as has been previously described (Siddique et al., 2014). For each experiment, 40 - 50 nematodes were measured and the experiments were repeated three times. An empirical curve was drawn across average measurements and the sex of the nematodes was re-evaluated at 12 dpi. Similarly, for prediction assays J2s established feeding sites in lateral roots were marked at 24 hai and observing their relative

development were predicted at 4 and 5 dpi. The only juveniles associated with single syncytium were considered for prediction. The sex of predicted juveniles was confirmed at 12 dpi. For infection assays, the numbers of males and females were counted. Moreover, the average size of females and the average size of syncytium at 14 days post infection was measured as described previously (Siddique et al., 2014).

Sample collection, processing and microarray

Root segments containing putative MAS or FAS were collected in a Farmer's fixative solution on ice. The fixative was vacuum infiltrated into samples for twenty minutes followed by an incubation period at 4 °C in an undulating shaker for 2 h. For cryo-protection, the tissues were incubated in a 34% sucrose solution (prepared in PBS buffer) at 4 °C in an undulating shaker after 45 minutes of vacuum infiltration. The fixed syncytia were embedded in an optimum cutting medium (OCT) (Polyfreez®) using Tissue´Tek® cryo molds. Sections of 10 µm were cut and the total RNA was extracted as described previously (Anjam et al., 2016). The quality of extracted RNA was controlled using Nanodrop and bioanalyzer (Agilent Technologies, USA). A cDNA synthesis was performed with NuGEN´s Applause 3'-Amp System (Cat. No. 5100), according to the manufacturer's instructions, and started with 100 ng of total RNA. NuGEN's Encore Biotin Module (Cat. No. 4200-12) was used to fragment 3.95 µg cDNA followed by Biotin-labelling according to the manufacturer's instructions. Hybridization, washing, and scanning, were performed according to the Affymetrix 30 GeneChip Expression Analysis Technical Manual (Affymetrix, Santa Clara, CA, USA). Three chips were hybridized for control and infected samples, with each microarray representing an independent, biological replicate. Primary data analysis was performed with Affymetrix software Expression Console v1.* using the MAS5 algorithm.

Statistical analysis of microarray data

Affymetrix .CDF and .CEL files were loaded into the Windows GUI program RMAExpress (http://rmaexpress.bmbolstad.com/) for the purpose of background correction, normalization (quantile) and summarization (median polish). After normalization, computed Robust Multichip Average (RMA) expression values were exported as log scale to a text file. Probe set annotations were performed by downloading Affymetrix mapping files matching array element identifiers to AGI loci from ARBC (www.arabidopsis.org). Data was analyzed using Student's *t-test* ($P<0.05$). The results tables include adj-P-values as indicators of statistical

significant difference after correction for multiple testing to control a false discovery rate (Benjamini & Hochberg, 1995).

The gene set enrichment analysis (GSEA) of FAS and MAS data was performed using PlantGSEA tool kit as described by Yi et al. (2013). The genes with fold change >1.5 and P-value <0.05 were selected for enrichment analysis in GO (gene ontology) annotations of domain 'biological process'. We compared expected and actual percentage of gene enrichment in selected subcategories. The number of *Arabidopsis* genes used for calculating expected enrichment was 27029. GSEA used these genes from TAIR database annotated into 7041 GO gene sets (Yi et al., 2013; Swarbreck et al., 2007). The actual enrichment was calculated from 124 FAS and 331 MAS genes. The expression of top 100 FAS and MAS genes in different anatomical parts, under nutrient and biotic stress conditions, was analyzed by genevestigator.

Genotyping and expression analysis of knock-out mutants

Single T-DNA inserted knock-out mutants for selected genes (Supplementary Table S4) were ordered from the relevant stock center. The homozygosity of SALK mutant lines (NASC, The European *Arabidopsis* Stock Centre, www.arabidopsis.info) was confirmed via PCR using primers given in Table S5. The homozygous mutants of SALK and GABI-KAT lines (University of Bielefeld, Germany, www.gabi-kat.de) were confirmed to be completely absent for expression of required gene through RT-PCR with gene specific primers given in Table S5.

Development of promoter-reporter lines and GUS analysis

Promoter regions upstream of the 5' UTR of *LPTG-6* (1361 bp), *BGLU28* (1471 bp) and *CWLP-1* (1214 bp) were amplified by Gateway PCR using *Arabidopsis* Col-0 genomic DNA as template using primer given in Supplementary Table S6. Subsequently, promoters were cloned via gateway cloning upstream of *GUS* gene in pMDC162. *Promoter::GUS* constructs were introduced into *Agrobacterium tumefaciens* GV3101 for transformation of *Arabidopsis* Col-0 plants by the floral dip method (Bent & Clough, 1998). Transformed plants were selected on KNOP without sucrose containing 20 $\mu g\ ml^{-1}$ hygromycin, 50 $\mu g\ ml^{-1}$ carbencillin and 10 $\mu g\ ml^{-1}$ Mancozeb, then transferred to soil for seed collection. T3 homozygous lines were generated and analyzed for GUS expression. *Arabidopsis* seeds were

surface-sterilized with NaOCl (0.7%) for 3 minutes followed by three successive washings of sterile water. Seedlings were grown vertically on KNOP medium supplemented with 2% (w/v) sucrose in 10-cm square Petri dishes. Roots of 12-days-old plants were inoculated with 60-70 sterile J2s of *H. schachtii*. The GUS expression was analyzed at 1, 3, 5, and 12 dpi. Four plants from each of three transgenic lines per construct were analyzed at each time-point. Root systems were separated from aerial tissue and submerged in 100 mM Na_3PO_4 buffer (pH 7.0) containing 10 mM EDTA, 0.01% (v/v) Triton X-100, 0.5 mM $K_3(Fe(CN)_6)$, 0.5 mM $K_4(Fe(CN)_6)$ and 1 mg ml^{-1} 5-bromo-4-chloro-3-indolyl glucuronide (X-gluc; Melford Laboratories Ltd, Ipswich, UK). Tissue was vacuum-infiltrated for five minutes then incubated in the dark for 16 h at room temperature. Stained tissue was mounted in glycerol and viewed using bright field optics on a Leica DMRB microscope and images were captured.

Real time PCR

The validation of the GeneChip data using Real-Time qPCR was performed according to Siddique et al. (2014). As described previously, RNA from LCM-derived MAS or FAS was isolated and cDNA was amplified. Transcriptome abundance for candidate genes was analyzed using StepOne Plus Real-Time PCR System (Applied Biosystems, USA). Each sample contained 10 µl of Fast SYBR Green qPCR Master Mix with uracil-DNA, glycosylase, and 6-carboxy-x-rhodamine (Invitrogen), 2 mM $MgCl_2$, 0.5 µl each of forward and reverse primers (10 µM), 2 µl of complementary DNA (cDNA), and water in 20 µl of total reaction volume. Samples were analyzed in three technical replicates. β-Tubulin and ubiquitin were used as internal controls. Relative expression was calculated by the Pfaffl's method (Siddique et al., 2014), where the expression of the candidate gene was normalized to the internal control to calculate fold change. Primer sequences for all genes are provided in Supplementary Table S7.

Anatomy and ultrastructure

Arabidopsis Col-0 plants were grown and inoculated aseptically with freshly hatched J2s of *H. schachtii* as described above. Root segments containing putative MAS or FAS were dissected at 5 days post inoculation (dpi), processed for light and transmission electron microscopy, and examined as described by Golinowski et al. (1996) and Sobczak et al. (1997).

Accession numbers

This work included microarrays data, which will be make publicly available through Array Express upon acceptance of manuscript.

Acknowledgments

The authors are thankful to Keith Lindsey and Jennifer Topping for help with LCM. We also acknowledge the excellent contribution of Stefan Neumann, Gisela Sichtermann and Thomas Gerhardt for help maintaining nematode culture.

References

Anjam, M. S., Ludwig, Y., Hochholdinger, F., Miyaura, C., Inada, M., Siddique, S. & Grundler, F.M.W. (2016) An improved procedure for isolation of high-quality RNA from nematode-infected *Arabidopsis* roots through laser capture microdissection. *Plant Methods* 12, 1-9.

Benjamini, Y. & Hochberg, Y. (1995) Controlling the false discovery rate: a practical and powerful approach to multiple testing. *J. R. Stat. Soc. Series B Stat. Methodol.* 57, 289–300.

Bent, A. F. & Clough, S. J. (1998) In *Plant Molecular Biology Manual* 17–30 (Springer Netherlands).

Berthet, S., Demont-Caulet, N., Pollet, B., Bidzinski, P., Cézard, L., Le Bris, P., Borrega, N., Hervé, J., Blondet, E., Balzergue, S., Lapierre, C. & Jouanin, L. (2011) Disruption of Laccase4 and 17 results in tissue-specific alterations to lignification of *Arabidopsis thaliana* stems. *Plant Cell* 23, 1124–37.

Böckenhoff, A. & Grundler, F. M. W. (1994) Studies on the nutrient uptake by the beet cyst nematode *Heterodera schachtii* by in situ microinjection of fluorescent probes into the feeding structures in *Arabidopsis thaliana*. *Parasitology* 109, 249-255.

Brown, D. M., Zeef, L. A. H., Ellis, J., Goodacre, R. & Turner, S. R. (2005) Identification of novel genes in *Arabidopsis* involved in secondary cell wall formation using expression profiling and reverse genetics. *Plant Cell* 17, 2281–95.

Carvalho, A. de O. & Gomes, V. M. (2007) Role of plant lipid transfer proteins in plant cell physiology—A concise review. *Peptides* 28, 1144–1153.

Davies, L. J., Lilley, C. J., Paul Knox, J. & Urwin, P. E. (2012) Syncytia formed by adult female *Heterodera schachtii* in *Arabidopsis thaliana* roots have a distinct cell wall molecular architecture. *New Phytol.* 196, 238–246.

Debono, A., Yeats, T. H., Rose, J. K. C., Bird, D., Jetter, R., Kunst, L. & Samuels, L. (2009) *Arabidopsis* LTPG is a glycosylphosphatidylinositol-anchored lipid transfer protein required for export of lipids to the plant surface. *Plant Cell* 21, 1230–8.

Den Ouden, H. (1960) A note on parthenogenesis and sex determination in *Heterodera rostoschiensis* Woll. *Nematologica* 5, 215-216.

Edstam, M. M. & Edqvist, J. (2014) Involvement of GPI-anchored lipid transfer proteins in the development of seed coats and pollen in *Arabidopsis thaliana*. *Physiol. Plant.* 152, 32–42.

Ellenby, C. (1954) Environmental determination of the sex ratio of a plant parasitic nematode. *Nature* 174, 1016-1017.

Ellis, C., Karafyllidis, I., Wasternack, C. & Turner, J. G. (2002) The *Arabidopsis* mutant *cev1* links cell wall signaling to jasmonate and ethylene responses. *Plant Cell* 14, 1557–66.

Endo, B. (1965) Histological responses of resistant and susceptible soybean varieties, and backcross progeny to entry and development of *Heterodera glycines*. *Phytopathology* 55, 375–381.

Endo, B. (1964) Penetration and development of *Heterodera glycines* in soybean roots and related anatomical changes. *Phytopath*ology 54, 79–88.

Golinowski, W., Grundler, F. M. W. & Sobczak, M. (1996) Changes in the structure of *Arabidopsis thaliana* during female development of the plant-parasitic nematode *Heterodera schachtii*. *Protoplasma* 194, 103–116.

Grundler, F. M. W., Marlies, B. & Urs, W. (1991) Influence of changes in the nurse cell system (syncytium) on sex determination and development of the cyst nematode *Heterodera-schachtii* - total amounts of proteins and amino-acids. *Phytopathology* 81, 70-74.

Grundler, F. M. W., Sobczak, M. & Golinowski, W. (1998) Formation of wall openings in root cells of *Arabidopsis thaliana* following infection by the plant-parasitic nematode *Heterodera schachtii*. *Eur. J. Plant Pathol.* 104, 545–551.

Hewezi, T & Baum, T.J. (2013) Manipulation of plant cells by cyst and root-knot nematode effectors. *Molecular Plant-Microbe Interactions* 26:9-16.

Hao, Z. & Mohnen, D. (2014) A review of xylan and lignin biosynthesis: Foundation for studying *Arabidopsis* irregular xylem mutants with pleiotropic phenotypes. *Crit. Rev. Biochem. Mol. Biol*. 43, 212-241.

Hernández-Blanco, C., Feng, D. X., Hu, J., Sánchez-Vallet, A., Deslandes, L., Llorente, F., Berrocal-Lobo, M., Keller, H., Barlet, X., Sánchez-Rodríguez, C., Anderson, L. K., Somerville, S., Marco, Y. & Molina, A. (2007) Impairment of cellulose synthases required for *Arabidopsis* secondary cell wall formation enhances disease resistance. *Plant Cell* 19, 890–903.

Hofmann, J. & Grundler, F. M. W. (2006) Females and males of root-parasitic cyst nematodes induce different symplasmic connections between their syncytial feeding cells and the phloem in *Arabidopsis thaliana*. *Plant Physiol. Biochem.* 44, 430–433.

Hofmann, J., Elashry, A. N., Anwar, S., Erban, A., Kopka, J. & Grundler, F. M. W. (2010) Metabolic profiling reveals local and systemic responses of host plants to nematode parasitism. *Plant J.* 62, 1058-71.

Hofmann, J., Szakasits, D., Blöchl, A., Sobczak, M., Daxböck-Horvath, S., Golinowski, W., Bohlmann, H. & Grundler, F. M. W. (2007) Starch serves as carbohydrate storage in nematode-induced syncytia. *Plant Physiol.* 146, 228–235.

Hoth, S., Stadler, R., Sauer, N. & Hammes, U. Z. (2008) Differential vascularization of nematode-induced feeding sites. *Proceedings of the National Academy of Sciences*105, 12617-12622.

Holbein, J., Grundler, F. M. W. & Siddique, S. (2016) Plant basal resistance to nematodes: an update. *J. Exp. Bot.* 67, 2049–61.

Hütten, M., Geukes, M., Misas-Villamil, J. C., van der Hoorn, R. A., Grundler, F. M., & Siddique, S. (2015) Activity profiling reveals changes in the diversity and activity of proteins in Arabidopsis roots in response to nematode infection. Plant Physiology and Biochemistry 97, 36-43.

Ithal, N., Recknor, J., Nettleton, D., Hearne, L., Maier, T., Baum, T. J. & Mitchum, M. G. (2007a) Parallel genome-wide expression profiling of host and pathogen during soybean cyst nematode infection of soybean. *Mol. Plant Microbe Interact.* 20, 293–305.

Ithal, N., Recknor, J., Nettleton, D., Maier, T., Baum, T. J. & Mitchum, M. G. (2007b) Developmental transcript profiling of cyst nematode feeding cells in soybean roots. *Mol. Plant Microbe Interact.* 20, 510–525.

Jones, L., Ennos, A. R. & Turner, S. R. (2001) Cloning and characterization of irregular xylem4 (IRX4): a severely lignin-deficient mutant of *Arabidopsis*. *Plant J.* 26, 205–216.

Kämpfe, L. & Kerstan, U. (1964) Die Beeinflussung Des Geschlechtsverhältnisses in Der Gattung *Heterodera* Schmidt. *Nematologica* 10, 388-398.

Kerstan, U. (1969) Die Beeinflussung Des Geschlechterverhältnisses in Der Gattung *Heterodera*. *Nematologica* 15, 210–228.

Lee, S. B., Go, Y. S., Bae, H. –J., Park, J. H., Cho, S. H., Cho, H. J., Lee, D. S., Park, O. K., Hwang, I. & Suh, M. C. (2009) Disruption of glycosylphosphatidylinositol-anchored lipid transfer protein gene altered cuticular lipid composition, increased plastoglobules, and enhanced susceptibility to infection by the fungal pathogen *Alternaria brassicicola*. *Plant Physiol.* 150, 42–54.

Lee, Y. K., Kim, G. –T., Kim, I.-J., Park, J., Kwak, S.-S., Choi, G. & Chung, W.-I. (2006) Longifolia1 and Longifolia2, two homologous genes, regulate longitudinal cell elongation in *Arabidopsis*. *Development* 133, 4305–4314.

Lilley, C. J., Atkinson, H. J. & Urwin, P. E. (2005) Molecular aspects of cyst nematodes. *Mol. Plant Pathol.* 6, 577–588.

Mendy, B., Wang'ombe, M.W., Radakovic, Z., Holbein, J., Ilyas, M., Chopra, D., Holton, N., Zipfel, C., Grundler, F.M.W. & Siddique, S. (2017) *Arabidopsis* leucine-rich repeat receptor–like kinase NILR1 is required for induction of innate immunity to parasitic nematodes. *PLoS Pathogens*. doi: 10.1371/journal.ppat.1006284 (*in press*).

Molz, E. (1920) Versuche zur Ermittlung des Einflusses aüsserer Faktoren auf des Geschlechtsverhältnis des Rübennematoden (*Heterodera schachtii* A. Schmidt). *Landw. Jb.* 54, 769-91.

Müller, J., Rehbock, K. & Wyss, U. (1981) Growth of *Heterodera schachtii* with remarks on amounts of food consumed. *Rev. Nematol.* 4, 227–234.

Offler, C. E., McCurdy, D. W., Patrick, J. W. & Talbot, M. J. (2003) Transfer cells : Cells specialized for a special purpose. *Annu. Rev. Plant Biol.* 54, 431–454.

Pfafel, M. W. (2001) A new mathematical model for relative quantification in real-time RT-PCR. Nucleic Acids Research 29:e45.

Puthoff, D. P., Nettleton, D., Rodermel, S. R. & Baum, T. J. (2003) *Arabidopsis* gene expression changes during cyst nematode parasitism revealed by statistical analyses of microarray expression profiles. *Plant J.* 33, 911–921.

Ramos, B., González-Melendi, P., Sánchez-Vallet, A., Sánchez-Rodríguez, C., López, G. & Molina, A. (2013) Functional genomics tools to decipher the pathogenicity mechanisms of the necrotrophic fungus *Plectosphaerella cucumerina* in *Arabidopsis thaliana*. *Mol. Plant Pathol.* 14, 44–57.

Raski, D. J. (1950) The life history and morphology of the sugar beet nematode, *Heterodera schachtii* Schmidt. *Phyatopathology* 40, 135–152.

Rahman, M.B., & Joslyn, M.A. (1953a) The Hydrolysis of pectic acid by purified fungal polygalacturonase. *Food Res* 18:308-318.

Ruan, Y.-L., Patrick, J. W., Bouzayen, M., Osorio, S. & Fernie, A. R. (2012) Molecular regulation of seed and fruit set. *Trends Plant Sci.* 17, 656–665.

Sager, R., & Lee, J. Y. (2014) Plasmodesmata in integrated cell signalling: insights from development and environmental signals and stresses. *Journal of experimental botany*, eru365.

Sasser, J. N. & Freckman, D. W. (1986) A world perspective on nematology - the role of the society. *J. Nematol.* 18, 596-596.

Sengbusch, R. (1927) Beitrag zur biologie des Rübennematoden *Heterodera schachtii*. *Z. Pflanzenkrankh* 37: 86-102.

Siddique, S. & Grundler, F. M. W. (2015) In *Advances in Botanical Research* (eds. Escobar, C. & Fenoll, C.) 73, 119–138 (Elsevier Ltd.).

Siddique, S., Endres, S., Sobczak, M., Radakovic, Z. S., Fragner, L., Grundler, F. M., Weckwerth, W., Tenhaken, R., & Bohlmann, H. (2014) Myo-inositol oxygenase is important for the removal of excess myo-inositol from syncytia induced by *Heterodera schachtii* in *Arabidopsis* roots. New Phytologist 201, 476-485.

Siddique, S., Matera, C., Radakovic, Z. S., Shamim H. M., Gutbrod, P., Rozanska, E., Sobczak, M., Torres, M. A. & Grundler, F. M. W. (2014) Parasitic worms stimulate host NADPH oxidases to produce reactive oxygen species that limit plant cell death and promote infection. *Science Signaling* 7, ra33.

Siddique, S., Radakovic, Z. S., De L. T., Carola M., Chronis, D., Novák, O., Ramireddy, E., Holbein, J., Matera, C., Hütten, M., Gutbrod, P., Anjam, M. S., Rozanska, E., Habash, S., Elashry, A., Sobczak, M., Kakimoto, T., Strnad, M., Schmülling, T., Mitchum, M. G. & Grundler, F. M. W. (2015) A parasitic nematode releases cytokinin that controls cell division and orchestrates feeding site formation in host plants. *Proc. Natl. Acad. Sci. USA* 112, 12669–12674.

Siddique, S., Sobczak, M., Tenhaken, R., Grundler, F. M. W. & Bohlmann, H. (2012) Cell wall ingrowths in nematode induced syncytia require UGD2 and UGD3. *PLoS One* 7, e41515.

Sijmons, P. C., Grundler, F. M. W., von Mende, N., Burrows, P. R. & Wyss, U. (1991) *Arabidopsis thaliana* as a new model host for plant-parasitic nematodes. *Plant J.* 1, 245-254.

Sobczak, M., Golinowski, W. & Grundler, F. M. W. (1997) Changes in the structure of *Arabidopsis thaliana* roots induced during development of males of the plant parasitic nematode *Heterodera schachtii*. *Eur. J. Plant Pathol.* 103, 113–124.

Sobczak, M., Avrova, A., Jupowicz, J., Phillips, M. S., Ernst, K., Kumar, A. (2005) Characterization of susceptibility and resistance responses to potato cyst nematode (*Globodera* spp.) infection of tomato lines in the absence and presence of the broad-spectrum nematode resistance Hero gene. *Mol. Plant Microbe Interact.* **18**, 158–168 .

Sobczak, M., Golinowski, W., Grundler, F. M. W. (1999) Ultrastructure of feeding plugs and feeding tubes formed by *Heterodera schachtii*. Nematology. 1, 363–374.

Stadler, R., Truernit, E., Gahrtz, M. & Sauer, N. (1999) The AtSUC1 sucrose carrier may represent the osmotic driving force for anther dehiscence and pollen tube growth in *Arabidopsis*. *Plant J.* 19, 269–278.

Szakasits, D., Heinen, P., Wieczorek, K., Hofmann, J., Wagner, F., Kreil, D. P., Sykacek, P., Grundler, F. M. W. & Bohlmann, H. (2009) The transcriptome of syncytia induced by the cyst nematode *Heterodera schachtii* in *Arabidopsis* roots. *Plant J.* 57, 771–784.

Teixeira, M.A., Wei, L. & Kaloshian, I. (2016) Root-knot nematodes induce pattern-triggered immunity in *Arabidopsis thaliana* roots. *New Phytologist* 211, 276-287

Trudgill, D. L. (1991) Resistance to and tolerance of plant parasitic nematodes in plants. *Annu. Rev. Phytopathol.* 29, 167–192.

Trudgill, D. L. (1967) The effect of environment on sex determination in *Heterodera rostochiensis*. *Nematologica* 13, 263-72.

Turner, S. R. & Somerville, C. R. (1997) Collapsed xylem phenotype of *Arabidopsis* identifies mutants deficient in cellulose deposition in the secondary cell wall. *Plant Cell* 9, 689–701.

Wieczorek, K., Elashry, A., Quentin, M., Grundler, F. M. W., Favery, B., Seifert, G. J. & Bohlmann, H. (2014) A distinct role of pectate lyases in the formation of feeding structures induced by cyst and root-knot nematodes. *Mol. Plant-Microbe Interact.* 27, 901–912.

Wieczorek, K., Golecki, B., Gerdes, L., Heinen, P., Szakasits, D., Durachko, D. M., Cosgrove, D. J., Kreil, D. P., Puzio, P. S., Bohlmann, H. & Grundler, F. M. W. (2006) Expansins are involved in the formation of nematode-induced syncytia in roots of *Arabidopsis thaliana*. *Plant J.* 48, 98–112.

Wyss, U. (1992) Observations on the feeding behaviour of *Heterodera schachtii* throughout development, including events during moulting. *Fundam. Appl. Nematol.* 15, 75–89.

Yokoyama, R. & Nishitani, K. (2006) Identification and characterization of *Arabidopsis thaliana* genes involved in xylem secondary cell walls. *J. Plant Res.* 119, 189–194.

Yi, X., Du, Z. & Su, Z. (2013) PlantGSEA: a gene set enrichment analysis toolkit for plant community. *Nucleic acids research*. 41(W1):W98-W103.

Zimmermann, P., Bleuler, S., Laule, O., Martin, F., Ivanov, N.V., Campanoni, P., Oishi, K., Lugon-Moulin, N., Wyss, M., Hruz, T. & Gruissem, W. (2014) ExpressionData - A public resource of high quality curated datasets representing gene expression across anatomy, development and experimental conditions. *BioData Mining* 7:18.

General discussion

The sex determination of cyst nematodes, whether under the influence of genetics or the environment, has been a matter of debate since the beginning of the 20th century. Although, cyst nematodes are strictly amphimictic, unlike many other bisexual organisms, the juveniles of cyst nematodes are sexually indistinguishable. Their sexual organs differentiate during the start of 3rd molting stage after feeding on the host plant. Molz (1920) for the first time showed that existence of favorable environmental conditions, in which plenty of food is available for nematodes, lead to a high female to male ratio and vice versa (Molz, 1920). Later on, Sengbusch (1927) repeated some of the Molz's experiments but reached contradictory conclusions. He estimated that females required 35 times more food for development than did males. Hence, he proposed that the variation in sex ratio in Molz's experiments was because of the differential death rate of females under adverse environmental conditions. These contradictory claims commenced a discussion about the role of environment on the sexual outcome of the cyst nematodes. Many studies were conducted to answer this intriguing question and the scope of experiments was also extended to other cyst nematodes like potato, soybean and rice cyst nematodes (Ellenby, 1954; Apel & Kämpfe, 1957; Den Ouden, 1960; Kämpfe & Kerstan, 1964; Koliopanos & Triantaphyllou 1972; Triantaphyllou, 1973; Kerry & Bridgeman, 1980; Müller et al., 1981; Seinhorst, 1986). However, the results were not all in agreement. Meanwhile, an attempt to identify the sex chromosomes in different species of *Heterdoera* also did not yield any positive results (Triantaphyllou, 1975). Thus the questions pertaining to the role of environment in cyst nematode experiments remained mostly unanswered.

The major clue to environmental sex determination in cyst nematode *Heterodera schachtii* came from the studies of Grundler et al. (1991) when single juveniles were infected in rich and adverse nutritional conditions. It was found that under favorable conditions, about 90% of the juveniles were developed as females, supporting the hypothesis of epigenetic sex determination. To the contrary, however, adverse nutritional conditions did not lead to higher numbers of male development but more stagnant juveniles were obtained at J2 and J3 developmental stages. Microscopic studies of genital primordium indicated that 85% of stagnated J2/J3 juveniles were females whose further development was inhibited by the change in the food supply and quality (Grundler et al., 1991). Later on, Lelivelt & Hoogendoorn (1993) also endorsed these conclusions by showing that despite a similar

inoculum level, certain resistant cultivars induced more than double the male to female sex ratio than did the susceptible lines. As syncytium is the ultimate source of food supply for nematode development, therefore, further studies focussed on the differences between male- and female-associated syncytia for example differences in anatomy, ultrastructure, symplasmic connections and contents of proteins and amino acids (Grundler et al., 1991; Golinowski et al., 1996; Sobczak et al., 1997; Hofmann and Grundler, 2006). The differences in the structural composition of the two syncytia and their symplasmic connections with vascular tissues indicated that female-associated syncytia are designed to meet higher food requirements than male. Based on these data, we hypothesized in the present study that there would be differential transcriptional events inside the syncytia associated with the two sexes, which may ultimately lead to structural differences and sexual differentiation of the juveniles.

To pick the earliest possible time point when nematodes can be predicted for their future sex, the rate of development of infected juveniles was measured over the course of development. Because a female nematode consumes 29 times more food than a male, it was assumed that putative female juveniles would grow at a faster rate than males. As the results indicate (Figure 1, Chapter 3), there was a clear difference in the rate of development between the male and female nematodes at 5 dpi. The nematodes that attained greater size ($\geq$16000 μm^2) during first 5 dpi eventually differentiated into females. Conversely, a majority of juveniles with the size <14000 μm^2 at 5 dpi became male. The results are supported by previous studies in *Heterodera glycines* where the higher development of females at an exponential rate of 31 ± 10% during 5 dpi had been observed (Atkinson & Harris, 1989). Further, males of the beet cyst nematode have been shown to require 60 times less space in the host root for their development as compared to females. The mean estimated volume of MAS in sugar beet root was 0.002 mm^3 while FAS was 0.026 mm^3 (Caswell-Chen & Thomason, 1993). Based on these data, we concluded that although sexual phenotype of these nematodes appears later, they begin differing from each other in their size and development during early stages of feeding. Accordingly, we further explored the anatomical and ultrastructural differences between MAS and FAS.

Anatomical and ultrastructural differences

The light microscopic analyses of both MAS and FAS at 5 dpi showed that FAS exhibited pronounced hypertrophy as compared to MAS. It was also found that FAS expanded longitudinally and was surrounded by 1-2 more layers of actively dividing peridermis-like

cells in comparison to MAS. Moreover, FAS was mostly induced in procambial cells facing xylem vessels, whereas MAS was induced in pericyclic cells. Therefore, it was suggested that male juveniles get relatively less nutrient supply due to induction of initial syncytial cell (ISC) in the outer region of the vascular cylinder (Sobczak et al., 1997). A detailed study has also shown that FAS establish a profound cytoplasmic connection with sieve cells via plasmodesmata; however, such a connection is not present between MAS and sieve elements (Hofmann & Grundler, 2006; Hofmann et al., 2009; Siddique et al., 2012). It indicated that to meet high food requirements, female-syncytia on one hand, establish a profound cytoplasmic connection with sieve cells (Bockenhoff et al., 1996; Golinowski et al., 1996; Sobczak et al., 1997; Hofmann & Grundler, 2006) and on the other hand they expand the syncytium volume by incorporation of peridermis-like cells. Recently, the role of phytohormone cytokinin has been implicated in facilitating cell division in cells surrounding the syncytium (Siddique et al., 2015). Interestingly, transgenic lines actively degrading cytokinin (PYK10::CKX3) supported a significant increase a proportion of males as compared to wild-type (Siddique et al., 2015). Based on these observations, it is plausible that cytokinin signaling may also play a role in determining the sexual fate of the nematodes.

Furthermore, it was observed that there was an enhanced necrosis close to the initial syncytial cell in MAS, which indicates an activation of local plant defense responses. This hypothesis is supported by Sobczak et al. (1997). Before, Lelivelt & Hoogendoorn (1993) also observed an increased necrosis at the site of larval penetration and proposed it for reason of resistance to *Heterodera schachtii* in the roots of resistant *Sinapis alba*. The necrotic phenomenon was also observed around syncytial component cells in roots of resistant cultivar "Forrest" of soybean against *Heterodera glycines* (Kim et al., 1987).

Moreover, ultrastructural studies indicated that FAS contains much more electron-dense cytoplasm than the male, and consisted of a high frequency of parallel arrangements of rough ER and an abundance of subcellular organelles showing a very active metabolism and protein synthesis in comparison to the male. These results are quite similar to earlier studies on 5 days old syncytium induced by *H. glycines* in susceptible soybean roots (Kim et al., 1987). However, Golinowski et al. (1996) pointed out a high accumulation of smooth ER in the female syncytium at J3/J4 stages, which was suggested to be there for the synthesis of non-proteinaceous molecules such as lipid bodies. These molecules are in general much more abundant in FAS as compared to MAS (Golinowski et al., 1996; Sobczak et al., 1997;

Sobczak & Golinowski, 2011). The structure of endoplasmic reticulum changes from rough to smooth during syncytium development (Golinowski et al., 1996). Nevertheless, the presence of a large number of rough ER in FAS in current study indicates that MAS may be less actively involved in protein synthesis. In summary, FAS and MAS start differing from each other at earlier feeding stages where FAS actively incorporate surrounding cells for its expansion, while MAS comprise of a few hypertrophied cells.

Altogether, these observations suggested for a differential expression of host genes between MAS and FAS, which may lead to the above described structural differences. Therefore, transcriptomic of MAS and FAS was performed to resolve the underlying molecular mechanisms, which may contribute to the sexual differentiation of these nematodes.

Analysis of differential gene expression between MAS and FAS

The transcriptomic studies have indicated that male- and female-associated syncytia strongly differ at the transcriptional level as early as 5 dpi. A detailed GO analysis showed that a number of genes related to organization, biosynthesis, and modification of cell wall were specifically overrepresented in FAS in comparison to MAS. A number of studies have shown previously that development of syncytium is accompanied by drastic changes in cell wall structures. On one hand, cell walls with neighboring cells are locally dissolved to enlarge the syncytium (Wieczorek et al., 2006; Wieczorek et al., 2008). On the other hand, outer cell walls of the syncytium are thickened to withstand increased turgor pressure inside the cell (Golinowski et al., 1996; Siddique et al., 2012). Further, cell walls of syncytium facing xylem vessels develop numerous cell wall ingrowths (transfer cells) to increase the surface area for absorption of food and water. All these changes in cell wall contribute to meet growing demand for food for fast developing nematodes. Considering that female nematodes require comparatively more food and grow much faster as compared to males (Müller et al., 1981; Golinowski et al., 1996; Sobczak et al., 1997; Hofmann et al., 2007), it is plausible that genes belonging to the category of cell wall modification showed an increase in transcript abundance in FAS as compared to MAS. Such a differential expression of cell wall genes may support differential nutritional requirement between FAS and MAS. These data is also supported by previous studies where FAS has been shown to contain more conspicuous cell wall ingrowths and cell wall openings as compared to MAS (Sobczak & Golinowski, 2011). Microarray data published by Puthoff et al. (2003) at 3 days after inoculation and Szakasits et al. (2009) at 5 and 15 days after inoculation syncytia induced in *Arabidopsis* roots by beet

cyst nematode also confirmed high upregulation of genes for cell wall biosynthesis and modifications. However, these data had been collected irrespective of male and female. Present results on the other hand for the first time indicate that FAS undergoes a more strong regulation of genes for cell wall metabolism and modifications as compared to MAS.

The other prominent difference was found on the side of MAS where heat map of 100 strongly overexpressed genes indicated that a number of genes responding to biotic stress were overexpressed. Defense related genes including, *PGIPs*, transcription factors (e.g. *WRKYs*, *BHLH101*, *BHLH039*) and general stress-responsive genes (e.g., *glutathione S transferase*) were upregulated in MAS. In previous studies, *PGIPs*, *WRKYs* and *glutathione-s-transferase* have been shown overexpressing in syncytia induced in soybean root upon infection with *H. glycines* (Mahalingam et al., 1999; Klink et al., 2007). Beet cyst nematode suppresses the expression of several *WRKY* transcription factors for successful parasitism (Ali et al., 2014). Moreover, *PGIP* gene family has been reported providing resistance to plants against virulent fungus species which produces PGs to degrade pectin component of plant cell wall (Toubart et al., 1992; Berger et al., 2000; Gazendam et al., 2004; Nguema-Ona et al., 2013). However, *PGIP1* has been shown playing role in defense against pea cyst nematode, *Heterodera goettingiana* (Veronico et al., 2011). The overexpression of *PGIPs* was also observed in syncytium induced by *Heterodera glycines* in roots of soybean (Mahalingam et al. 1999; Ithal et al. 2007a). Although, PGs have been isolated from root-knot and soybean cyst nematode (Mahalingam et al. 1999; Jaubert et al. 2002; Danchin et al. 2010), the interaction of these PGs with plant *PGIPs* has not been confirmed so far. Recently it has been shown that *pgip1* mutant of *Arabidopsis* reduced numbers of female and increased males when infected with beet cyst nematodes, however, no effect was observed against root-knot nematodes (Shah et al., submitted).

Furthermore, a number of genes induced by sulfur deficiency, iron deficiency or starvation were upregulated in MAS as compared with FAS. These data suggest that nematodes associated with syncytium that cannot provide them enough energy and nutrients develop as a male. Generally, nutrients or essential elements are relatively less available to MAS because unlike FAS, they are symplasmically isolated from sieve elements (Hofmann & Grundler, 2006). The upregulation of genes encoding transporters of sulfate, iron, and nitrate in the transcriptome of MAS further strengthens the hypothesis. Likewise, earlier studies reported

that deficiency of essential elements like phosphorous, nitrogen and potassium significantly increase the number of males on the host plant (Kämpfe & Kerstan, 1964).

Based on the present data, it is suggested that nematode juveniles provoke a local host defense response during migration and establishment of ISC. The majority of the juveniles that can suppress or overcome these defense responses successfully induce rapidly expanding syncytium and may become females. On the other hand, the majority of the juveniles that cannot suppress or overcome these defense responses may induce syncytium that does not provide enough nutrients, leading to the development of males. It can be speculated that starved juveniles may find it difficult to overcome local plant defense and ultimately develop into males.

Analysis of regulation of selected genes

The promoter::GUS analyses were conducted to confirm the specificity of gene expression to FAS or MAS. Therefore, transgenic lines of *Arabidopsis* expressing *GUS* gene under *CWLP1* and *BGLU28* promoters were produced. *CWLP1* is strongly upregulated in FAS and *BGLU28* is in MAS. The *GUS* expression was assessed with representative lines transformed with *pCWLP1::GUS* and *pBGLU28::GUS*. In the *Arabidopsis* developmental map (http://bar.utoronto.ca), *CWLP1* has been shown natively expressing primarily in aerial parts, particularly in leaves, but also shows strong expression in ovary. However, it does not show expression in roots except for a few cells in the meristematic zone of the root tip. In the case of *BGLU28*, it primarily expresses in rosette leaves and developing seeds. However, in roots, it has a weak expression in elongation zone and around the pericycle. The GUS staining experiment on *pCWLP1::GUS* and *pBGLU28::GUS* lines infected with nematodes showed that syncytia were specifically stained in both of the lines at 5 dpi and 12 dpi (Figure 5, Chapter 3). It was also found that for *pCWLP1::GUS* line, a majority of the syncytia associated with females were stained at 5 and 12 dpi. However, MAS were also occasionally stained. In comparison to *pCWLP1::GUS*, we found that MAS were strongly stained at 5 dpi in *pBGUL28::GUS* lines. Nevertheless, occurring of this GUS staining in MAS for *pBGLU28::GUS* was decreased at 12 dpi. This decrease in stained MAS syncytia at 12 dpi is most likely due to the fact that J4 males stop feeding and the syncytia start degenerating at this stage. However, hardly any strong GUS staining was observed for *pBGLUG28::GUS* in FAS.

In conclusion, present expression analyses endorse differential gene expression between MAS and FAS as revealed by microarrays. It also demonstrated that the *CWLP1* and *BGLU28* promoters could be used for FAS- or MAS-specific expression of proteins that could inhibit the development of the syncytium.

Functional analysis of selected genes

The ten *Arabidopsis* homozygous knockout mutants for genes, which were highly upregulated in FAS and MAS used in infection assays. It was found that in three mutant lines *irx12*, *ltpg6*, and *lng1*, the numbers of female were significantly reduced. Likewise, the size of female-syncytia was significantly reduced in all these mutants in comparison to wild type plants. Moreover, in the case of *irx12* and *lng1* numbers of the male were also significantly decreased. These genes were significantly upregulated in FAS as compared to MAS. In general, the strong expression of *IRX12* and *LNG1* is found in vascular tissues and leaf petioles respectively (Jones et al., 2001; Brown et al., 2005; Lee et al., 2006; Berthet et al., 2011). However, *LTPG6* strongly expresses in flower pistil and stem epidermis (http://bar.utoronto.ca/efp_arabidopsis/cgi-bin/efpWeb.cgi).

Previous studies have shown that knock-out mutants for *IRX12* lead to irregular xylem phenotype due to impairment of cellulose and lignin biosynthesis (Hao & Mohnen, 2014; Yokoyama & Nishitani 2006). As *IRX12* is involved in constitutive lignification and cellulose deposition of the secondary cell wall, it provides mechanical strength to xylem cells against compressive forces generated during water transportation (Turner & Somerville, 1997; Jones et al., 2001; Brown et al., 2005). It is suggested that upregulation of *IRX12* in FAS required for thickening of the syncytium cell wall to withstand against increased turgor pressure inside the syncytium (Böckenhoff & Grundler, 1994; Davies et al., 2012). The loss of function may restrict the proper expansion of the syncytium required for the female development and ultimately resulted in the development of more numbers of the male. The alternative reason for the reduction in female numbers on *irx12* could be due to activation of defense response resulting as impairment of secondary cell wall biosynthesis, inside the syncytium. Because alteration in secondary cell wall biosynthesis activate novel defense pathway and generate hostile conditions for the pathogens. Therefore *irx3* and *irx5* mutants have shown enhanced resistance against vascular pathogens (Ellis et al., 2002; Hernández-Blanco et al., 2007; Ramos et al., 2013).

However, *lng1* probably limits the development of juvenile to the female by restricting the proper expansion or morphology of the syncytium. Previously, *LNG1* had been characterized for regulating leaf morphology via promoting longitudinally polar cell elongation (Lee et al., 2006). Previous studies about the volume of the male- and female-syncytia had shown that a minimum size of the syncytium is necessary for female development (Kerstan, 1969) and therefore it requires more root volume than a male (Caswell-Chen & Thomason, 1993).

The *in vivo* role of *LTPG6* has been not yet clearly understood. However, *in vitro* studies have led to the conclusion that they are involved in the transport of lipid molecules to the plant surface (Carvalho & Gomes, 2007; Lee et al., 2009; Edstam & Edqvist, 2014). LTPs also have been found playing role in signaling against biotic and abiotic stresses (Jung et al., 2005; Guo et al., 2013; Liu et al., 2015)**.** *Arabidopsis* knockout mutants of *LTPG6* have been shown for reduced fertility due to infertile ovules, inability to restrict tetrazolium salt and decreased levels of omega-hydroxy fatty acids in the seed coat. Moreover, it has been suggested that *LTPGs* are involved in biosynthesis or deposition of suberin or sporopollenin (Edstam & Edqvist, 2014)**.** The role of *LTPG6* could be expected in syncytium formation through suberin biosynthesis. Our results have shown that syncytium size in *ltpg6* was significantly reduced. It is supported by recent studies where the role of suberin has been explored in syncytium development (Holbein et al., unpublished). However, further characterization of *LTPG6* is needed to define its role in the plant-nematode interaction.

In context of crop damage and population dynamics, the sex ratio of cyst nematodes is of fundamental importance. It not only influences the population rate in the next generation but also affects the intensity of crop damage, which is usually proportional to number of females. Therefore, understanding the factors behind sexual differentiation could be helpful in developing conceivable methods to exploit the sex ratio in the favour of males. In the present study, the plant host factors leading the sexual differentiation of the cyst nematode *Heterodera schachtii* have been explored at the molecular level. We have identified more than four hundred genes that are differentially expressed between male- and female-associated syncytia. We also found that knocking out some of the differentially regulated genes alters the male-to-female sex ratio of cyst nematodes. In future, it will be important to extend this screening to identify additional host mutants with a strong influence on the sex ratio. It will also be critical to investigate the role of these host genes in influencing sex of

other cyst nematode species. Exploitation of cyst nematode sex-related host genes may provide additional resources for development of resistant cultivars.

References

Ali, M. A., Wieczorek, K., Kreil, D. P. & Bohlmann, H. The beet cyst nematode *Heterodera schachtii* modulates the expression of WRKY transcription factors in syncytia to favor its development in *Arabidopsis* roots. *PLoS One* **9,** 1–17 (2014).

Apel, A. & Kämpfe, L. Beziehungen Zwischen Wirt Und Parasit Im Infektionsverlauf Von *Heterodera Schachtii* Schmidt in Kurzfristigen Topfversuchen. *Nematologica* **2,** 131–143 (1957).

Atkinson, H. J. & Harris, P. D. Changes in nematode antigens recognized by monoclonal antibodies during early infections of soybean cyst nematode, *Heterodera glycines*. *Parasitology* **98,** 479–487 (1989).

Berger, D., Oelofse, D., Arendse, M. ., Du Plessis, E. & Dubery, I. . Bean polygalacturonase inhibitor protein-1 (PGIP-1) inhibits polygalacturonases from *Stenocarpella maydis*. *Physiol. Mol. Plant Pathol.* **57,** 5–14 (2000).

Berthet, S., Demont-Caulet, N., Pollet, B., Bidzinski, P., Cézard, L., Le Bris, P., Borrega, N., Hervé, J., Blondet, E., Balzergue, S., Lapierre, C. & Jouanin, L. Disruption of Laccase4 and 17 results in tissue-specific alterations to lignification of *Arabidopsis thaliana* stems. *Plant Cell* **23,** 1124–37 (2011).

Böckenhoff, A. & Grundler, F. M. W. Studies on the nutrient uptake by the beet cyst nematode *Heterodera schachtii* by in situ microinjection of fluorescent probes into the feeding structures in *Arabidopsis thaliana*. *Parasitology* **109,** 249-255 (1994).

Brown, D. M., Zeef, L. A. H., Ellis, J., Goodacre, R. & Turner, S. R. Identification of novel genes in *Arabidopsis* involved in secondary cell wall formation using expression profiling and reverse genetics. *Plant Cell* **17,** 2281–95 (2005).

Carvalho, A. de O. & Gomes, V. M. Role of plant lipid transfer proteins in plant cell physiology—A concise review. *Peptides* **28,** 1144–1153 (2007).

Caswell-Chen, E. P. & Thomason, I. J. Root volumes occupied by different stages of *Heterodera schachtii* in sugarbeet, *Beta vulgaris*. *Fundam. Appl. Nematol.* **16,** 39–42 (1993).

Danchin, E. G. J., Rosso, M., Vieira, P., de Almeida-Engler, J., Coutinho, P. M., Henrissat, B. & Abad, P. Multiple lateral gene transfers and duplications have promoted plant parasitism ability in nematodes. *Proc. Natl. Acad. Sci. U. S. A.* **107,** 17651–6 (2010).

Davies, L. J., Lilley, C. J., Paul Knox, J. & Urwin, P. E. Syncytia formed by adult female *Heterodera schachtii* in *Arabidopsis thaliana* roots have a distinct cell wall molecular architecture. *New Phytol.* **196,** 238–246 (2012).

Den Ouden, H. A note on parthenogenesis and sex determination in *Heterodera rostochiensis* Woll. *Nematologica* **5,** 215–216 (1960).

Edstam, M. M. & Edqvist, J. Involvement of GPI-anchored lipid transfer proteins in the development of seed coats and pollen in *Arabidopsis thaliana*. *Physiol. Plant.* **152,** 32–42 (2014).

Ellenby, C. Environmental determination of the sex ratio of a plant parasitic nematode. *Nature* **174,** 1016–1017 (1954).

Ellis, C., Karafyllidis, I., Wasternack, C. & Turner, J. G. The *Arabidopsis* mutant *cev1* links cell wall signaling to jasmonate and ethylene responses. *Plant Cell* **14,** 1557–66 (2002).

Gazendam, I., Oelofse, D. & Berger, D. K. High-level expression of apple PGIP1 is not sufficient to protect transgenic potato against *Verticillium dahliae*. *Physiol. Mol. Plant Pathol.* **65,** 145–155 (2004).

Golinowski, W., Grundler, F. M. W. & Sobczak, M. Changes in the structure of *Arabidopsis thaliana* during female development of the plant-parasitic nematode *Heterodera schachtii*. *Protoplasma* **194,** 103–116 (1996).

Grundler, F. M. W., Marlies, B. & Wyss, U. Iinfluence of changes in nurse cell system (syncytium) on sex determination and development of the cyst nematode *Heterodera schachtii*: total amount of proteins and amino acids. *Phytopathology* **81,** 70–74 (1991).

Guo, C., Ge, X. & Ma, H. The rice OsDIL gene plays a role in drought tolerance at vegetative and reproductive stages. *Plant Mol. Biol.* **82,** 239–253 (2013).

Hao, Z. & Mohnen, D. A review of xylan and lignin biosynthesis: Foundation for studying *Arabidopsis* irregular xylem mutants with pleiotropic phenotypes. *Crit. Rev. Biochem. Mol. Biol.* **49,** 212–41 (2014).

Hernández-Blanco, C., Feng, D. X., Hu, J., Sánchez-Vallet, A., Deslandes, L., Llorente, F., Berrocal-Lobo, M., Keller, H., Barlet, X., Sánchez-Rodríguez, C., Anderson, L. K., Somerville, S., Marco, Y. & Molina, A. Impairment of cellulose synthases required for *Arabidopsis* secondary cell wall formation enhances disease resistance. *Plant Cell* **19,** 890–903 (2007).

Hofmann, J. & Grundler, F. M. W. Females and males of root-parasitic cyst nematodes induce different symplasmic connections between their syncytial feeding cells and the phloem in *Arabidopsis thaliana*. *Plant Physiol. Biochem.* **44,** 430–433 (2006).

Hofmann, J., Hess, P., Szakasits, D., Blöchl, A., Wieczorek, K., Daxböck-Horvath, S., Bohlmann, H., van Bel, A. J. E. & Grundler, F. M. W. Diversity and activity of sugar transporters in nematode-induced root syncytia. *J. Exp. Bot.* **60,** 3085–95 (2009).

Hofmann, J., Szakasits, D., Blöchl, A., Sobczak, M., Daxböck-Horvath, S., Golinowski, W., Bohlmann, H. & Grundler, F. M. W. Starch serves as carbohydrate storage in nematode-induced syncytia. *Plant Physiol.* **146,** 228–235 (2007).

Ithal, N., Recknor, J., Nettleton, D., Hearne, L., Maier, T., Baum, T. J. & Mitchum, M. G. Parallel genome-wide expression profiling of host and pathogen during soybean cyst nematode infection of soybean. *Mol. Plant-Microbe Interact.* **20,** 293–305 (2007b).

Ithal, N., Recknor, J., Nettleton, D., Maier, T., Baum, T. J. & Mitchum, M. G. Developmental transcript profiling of cyst nematode feeding cells in soybean roots. *Mol. Plant. Microbe. Interact.* **20,** 510–525 (2007a).

Jaubert, S., Laffaire, J.-B., Abad, P. & Rosso, M.-N. A polygalacturonase of animal origin isolated from the root-knot nematode *Meloidogyne incognita*. *FEBS Lett.* **522,** 109–112 (2002).

Jones, L., Ennos, A. R. & Turner, S. R. Cloning and characterization of irregular xylem4 (IRX4): a severely lignin-deficient mutant of *Arabidopsis*. *Plant J.* **26,** 205–216 (2001).

Jung, H. W., Kim, K. D. & Hwang, B. K. Identification of pathogen-responsive regions in the

promoter of a pepper lipid transfer protein gene (CALTPI) and the enhanced resistance of the CALTPI transgenic *Arabidopsis* against pathogen and environmental stresses. *Planta* **221,** 361–373 (2005).

Kämpfe, L. & Kerstan, U. Die Beeinflussung Des Geschlechtsverhältnisses in Der Gattung *Heterodera* Schmidt. *Nematologica* **10,** 388-398 (1964).

Kerry, B. R. & Bridgeman, M. R. The sex ratios of cyst-nematodes produced by adding single second-stage juveniles to host roots. *Nematologica* **26,** 209–213 (1980).

Kerstan, U. Die Beeinflussung Des Geschlechterverhältnisses in Der Gattung *Heterodera*. *Nematologica* **15,** 210–228 (1969).

Kim, Y. H., Rioos, R. D. & Kim, K. S. Structural changes associated with resistance of soybean to *Heterodera glycines*. *J. Nematol.* **19,** 177–187 (1987).

Klink, V. P., Overall, C. C., Alkharouf, N. W., MacDonald, M. H. & Matthews, B. F. Laser capture microdissection (LCM) and comparative microarray expression analysis of syncytial cells isolated from incompatible and compatible soybean (*Glycine max*) roots infected by the soybean cyst nematode (*Heterodera glycines*). *Planta* **226,** 1389–1409 (2007).

Koliopanos, C. N. & Triantaphyllou, A. C. Effect of infection density on sex ratio of *Heterodera glycines*. *Nematologica* **18,** 131–137 (1972).

Lee, S. B., Go, Y. S., Bae, H. –J., Park, J. H., Cho, S. H., Cho, H. J., Lee, D. S., Park, O. K., Hwang, I. & Suh, M. C. Disruption of glycosylphosphatidylinositol-anchored lipid transfer protein gene altered cuticular lipid composition, increased plastoglobules, and enhanced susceptibility to infection by the fungal pathogen *Alternaria brassicicola*. *Plant Physiol.* **150,** 42–54 (2009).

Lee, Y. K., Kim, G. –T., Kim, I.-J., Park, J., Kwak, S.-S., Choi, G. & Chung, W.-I. *Longifolia1* and *Longifolia2*, two homologous genes, regulate longitudinal cell elongation in *Arabidopsis*. *Development* **133,** 4305-14 (2006).

Lelivelt, C. L. C. & Hoogendoorn, J. The development of juveniles of *Heterodera schachtii* in roots of resistant and susceptible genotypes of *Sinapis alba*, *Brassica napus*, *Raphanus sativus* and hybrids. *Netherlands J. Plant Pathol.* **99,** 13–22 (1993).

Liu, F., Zhang, X., Lu, C., Zeng, X., Li, Y., Fu, D. & Wu, G. Non-specific lipid transfer proteins in plants: presenting new advances and an integrated functional analysis. *J. Exp. Bot.* **66,** 5663–81 (2015).

Mahalingam, R., Wang, G. & Knap, H. T. Polygalacturonase and polygalacturonase inhibitor protein: gene isolation and transcription in *Glycine max - Heterodera glycines* interactions. *Mol. Plant-Microbe Interact.* **490,** 490–498 (1999).

Molz, E. Versuche zur Er mittlung des Einflusses äusserer Faktoren auf des GeschlechtsverhaItnis des Rtibennematoden (*Heterodera schachtii* A. Schmidt). *Landw. Jb.* **54,** 769–91 (1920).

Müller, J., Rehbock, K. & Wyss, U. Growth of *Heterodera schachtii* with remarks on amounts of food consumed. *Rev. Nematol.* **4,** 227–234 (1981).

nematode *Heterodera goettingiana*. *Mol. Plant Pathol.* **12,** 275–87 (2011).

Nguema-Ona, E., Moore, J. P., Fagerström, A. D., Fangel, J. U., Willats, W.G.T., Hugo, A. & Vivier, M. A. Overexpression of the grapevine PGIP1 in tobacco results in compositional changes in the leaf arabinoxyloglucan network in the absence of fungal

infection. *BMC Plant Biol.* **13,** 1-15 (2013).

Puthoff, D. P., Nettleton, D., Rodermel, S. R. & Baum, T. J. *Arabidopsis* gene expression changes during cyst nematode parasitism revealed by statistical analyses of microarray expression profiles. *Plant J.* **33,** 911–921 (2003).

Ramos, B., González-Melendi, P., Sánchez-Vallet, A., Sánchez-Rodríguez, C., López, G. & Molina, A. Functional genomics tools to decipher the pathogenicity mechanisms of the necrotrophic fungus *Plectosphaerella cucumerina* in *Arabidopsis thaliana*. *Mol. Plant Pathol.* **14,** 44–57 (2013).

Seinhorst, J. W. The development of individuals and populations of cyst nematodes on plants: In *Cyst Nematodes* (eds. Lamberti, F. & Taylor, C.E) 101–117 (Springer US, 1986).

Sengbusch, R. V. Beitrag zur Biologie des Rfibennematoden *Heterodera schachtii*. *Z. Pflanzenkr. Pflanzenschutz* **37,** 86–102 (1927).

Siddique, S., Radakovic, Z. S., De L. T., Carola M., Chronis, D., Novák, O., Ramireddy, E., Holbein, J., Matera, C., Hütten, M., Gutbrod, P., Anjam, M. S., Rozanska, E., Habash, S., Elashry, A., Sobczak, M., Kakimoto, T., Strnad, M., Schmülling, T., Mitchum, M. G. & Grundler, F. M. W. A parasitic nematode releases cytokinin that controls cell division and orchestrates feeding site formation in host plants. *Proc. Natl. Acad. Sci. USA* **112,** 12669–12674 (2015).

Siddique, S., Sobczak, M., Tenhaken, R., Grundler, F. M. W. & Bohlmann, H. Cell wall ingrowths in nematode induced syncytia require UGD2 and UGD3. *PLoS One* **7,** e41515 (2012).

Sobczak, M. & Golinowski, W. Cyst nematodes and syncytia: In *Genomics and Molecular Genetics of Plant-Nematode Interactions* (eds. Jones, J., Gheysen, G. & Fenoll, C.) 61–81 (Springer Netherlands, 2011).

Sobczak, M., Golinowski, W. & Grundler, F. M. W. Changes in the structure of *Arabidopsis thaliana* roots induced during development of males of the plant parasitic nematode *Heterodera schachtii*. *Eur. J. Plant Pathol.* **103,** 113–124 (1997).

Steele, E. A. Orientation and development of *Heterodera schachtii* larvae on tomato and sugarbeet roots. *J. Nematol.* **3,** 424-426 (1981).

Szakasits, D., Heinen, P., Wieczorek, K., Hofmann, J., Wagner, F., Kreil, D. P., Sykacek, P., Grundler, F. M. W. & Bohlmann, H. The transcriptome of syncytia induced by the cyst nematode *Heterodera schachtii* in *Arabidopsis* roots. *Plant J.* **57,** 771–784 (2009).

Toubart, P., Desiderio, A., Salvi, G., Cervonel, F., Daroda, L., De, G., Casaccia, C. P., Bergmann, C., Darvill, A. G. & Albersheim, P. Cloning and characterization of the gene encoding the endopolygalacturonase-inhibiting protein (PGIP) of *Phaseolus vulgaris* L. *Plant J.* **2,** 367–373 (1992).

Triantaphyllou, A.C. Oogenesis and the chromosomes of twelve bisexual species of *Heterodera* (Nematoda: Heteroderidae). *J. Nematol.* **7,** 34-40 (1975).

Turner, S. R. & Somerville, C. R. Collapsed xylem phenotype of *Arabidopsis* identifies mutants deficient in cellulose deposition in the secondary cell wall. *Plant Cell* **9,** 689–701 (1997).

Veronico, P., Melillo, M. T., Saponaro, C., Leonetti, P., Picardi, E. & Jones, J. T. A polygalacturonase-inhibiting protein with a role in pea defence against the cyst

Wieczorek, K., Golecki, B., Gerdes, L., Heinen, P., Szakasits, D., Durachko, D.

M., Cosgrove, D. J., Kreil, D. P., Puzio P. S., Bohlmann, H. & Grundler, F. M. W. Expansins are involved in the formation of nematode-induced syncytia in roots of *Arabidopsis thaliana*. *Plant J.* **48,** 98–112 (2006).

Wieczorek, K., Hofmann, J., Blöchl, A., Szakasits, D., Bohlmann, H. & Grundler, F. M. W. *Arabidopsis* endo-1,4-β-glucanases are involved in the formation of root syncytia induced by *Heterodera schachtii*. *Plant J.* **53,** 336–351 (2008).

Yokoyama, R. & Nishitani, K. Identification and characterization of *Arabidopsis thaliana* genes involved in xylem secondary cell walls. *J. Plant Res.* **119,** 189–194 (2006).

5. Anex-I

5.1. Supplementary

Figure S1: Native expression of top 100 FAS upregulated genes (analysed by Genevestigator)

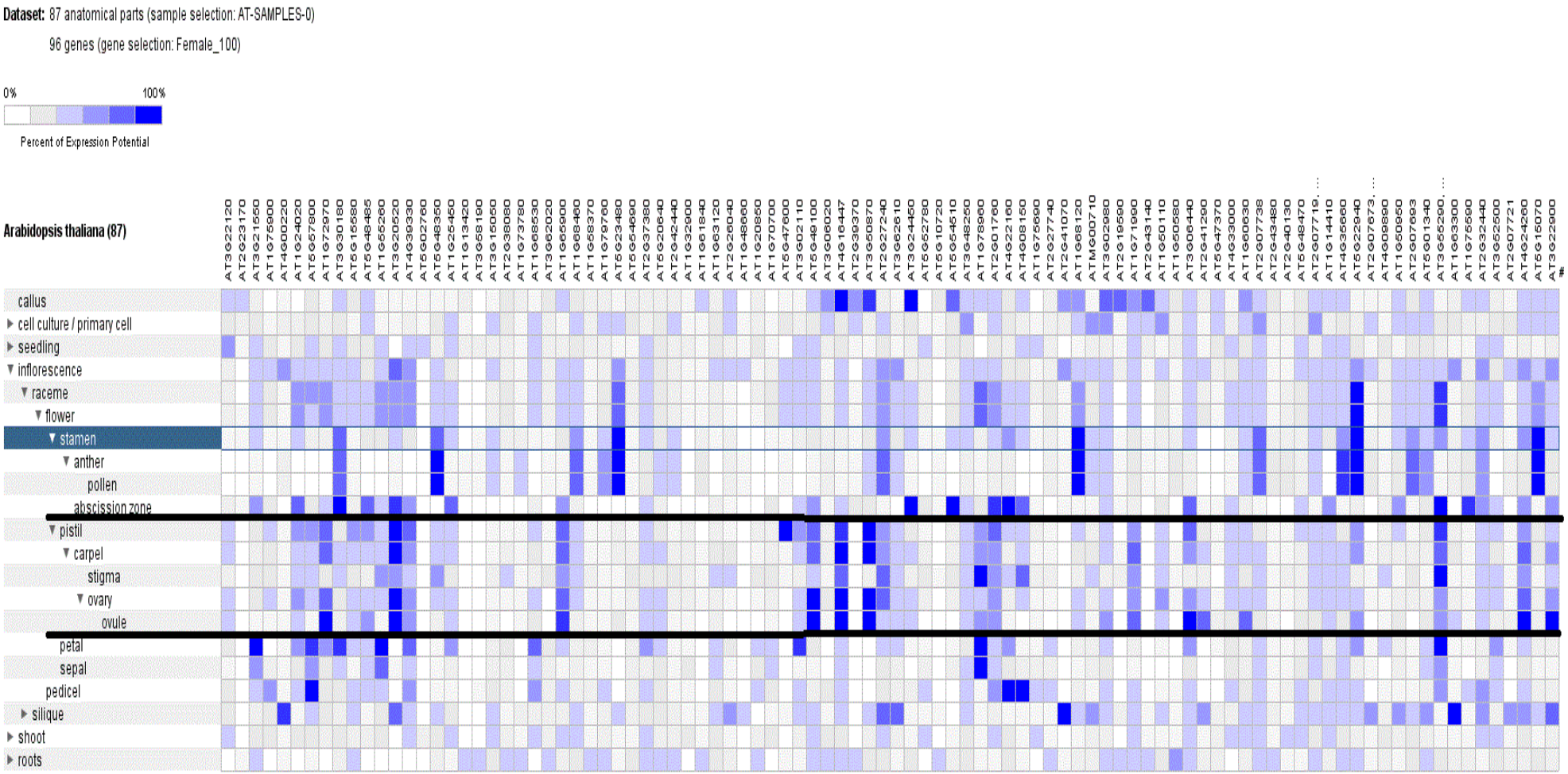

Figure S2: Native expression of top 100 MAS upregulated genes (analysed by Genevestigator)

Figure S3: Genes strongly upregulated in MAS (Genevestigator analysis for biotic stress)

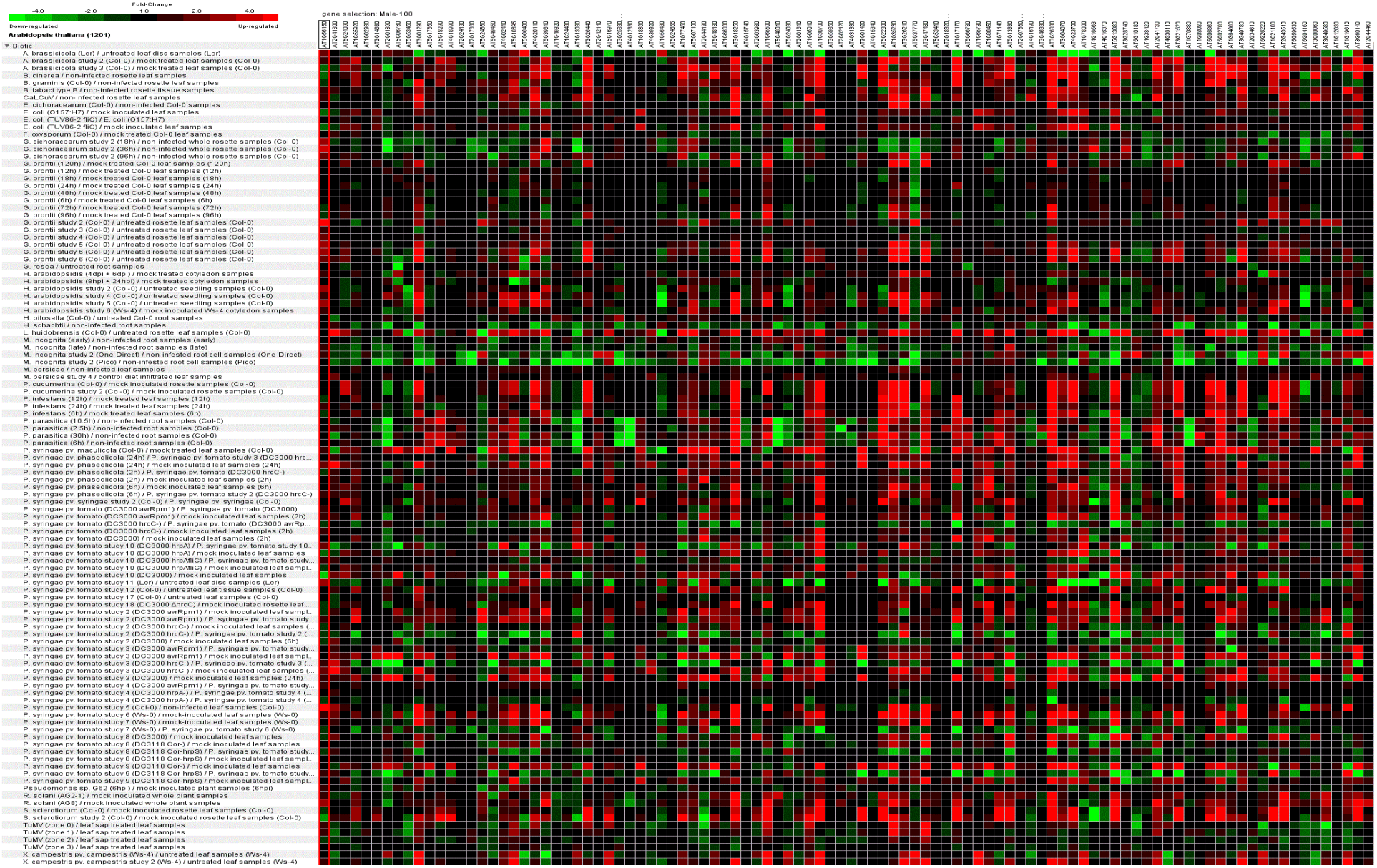

Figure S4: Genes strongly upregulated in FAS (Genevestigator analysis for biotic stress)

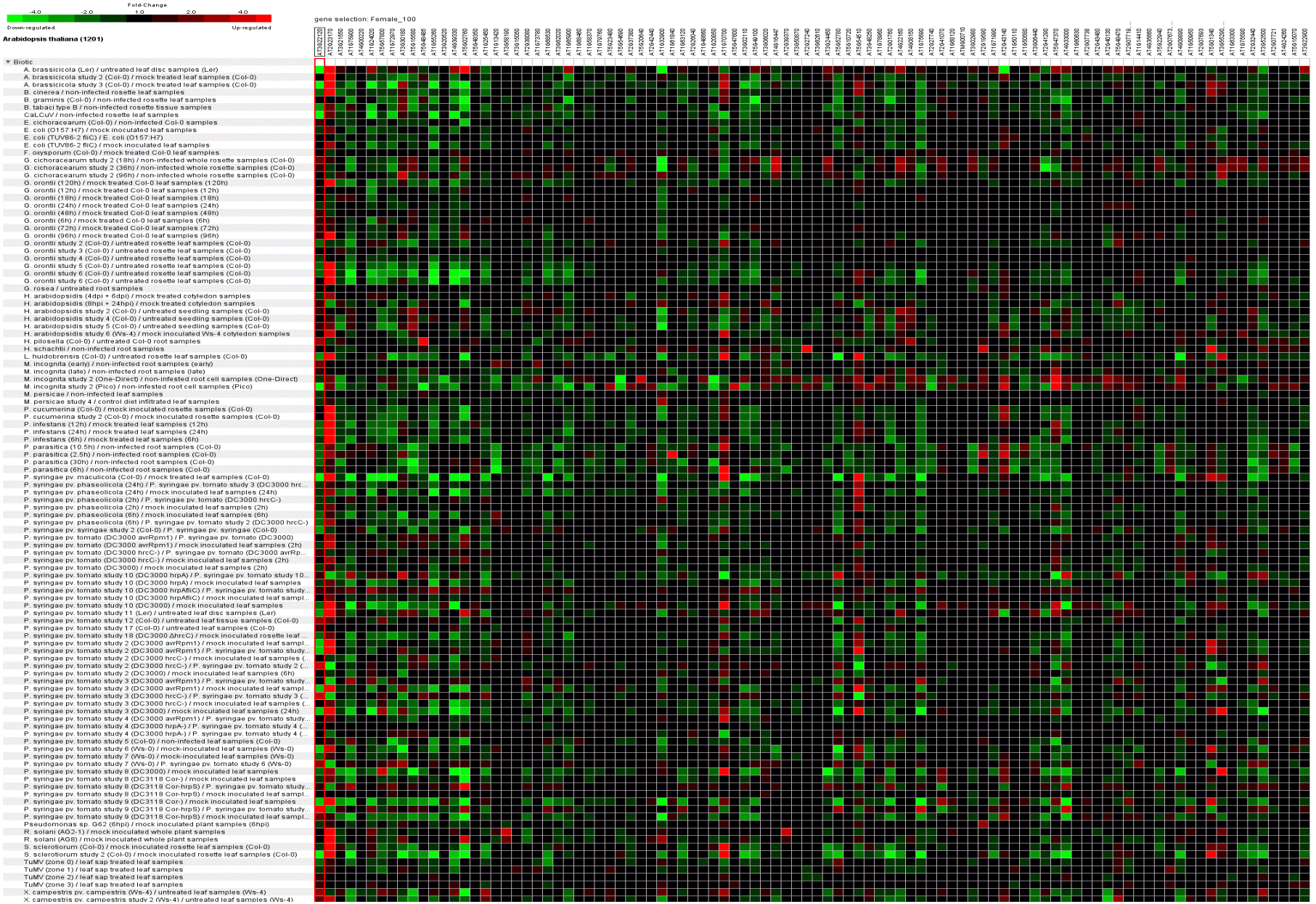

Figure S5: Genes strongly upregulated in FAS (Genevestigator analysis for nutrient stress)

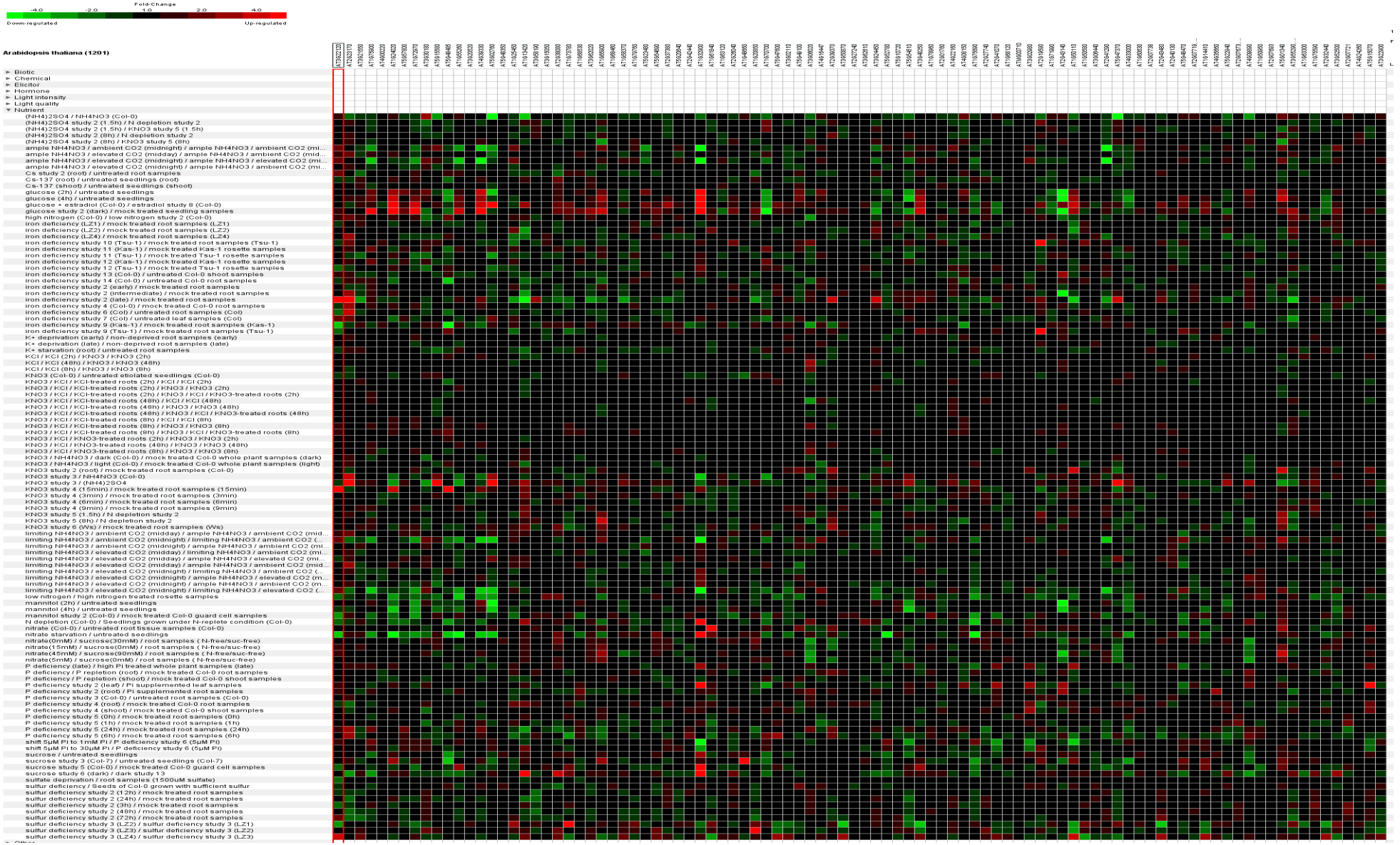

Figure S6: Genes strongly upregulated in MAS (Genevestigator analysis for nutrient stress)

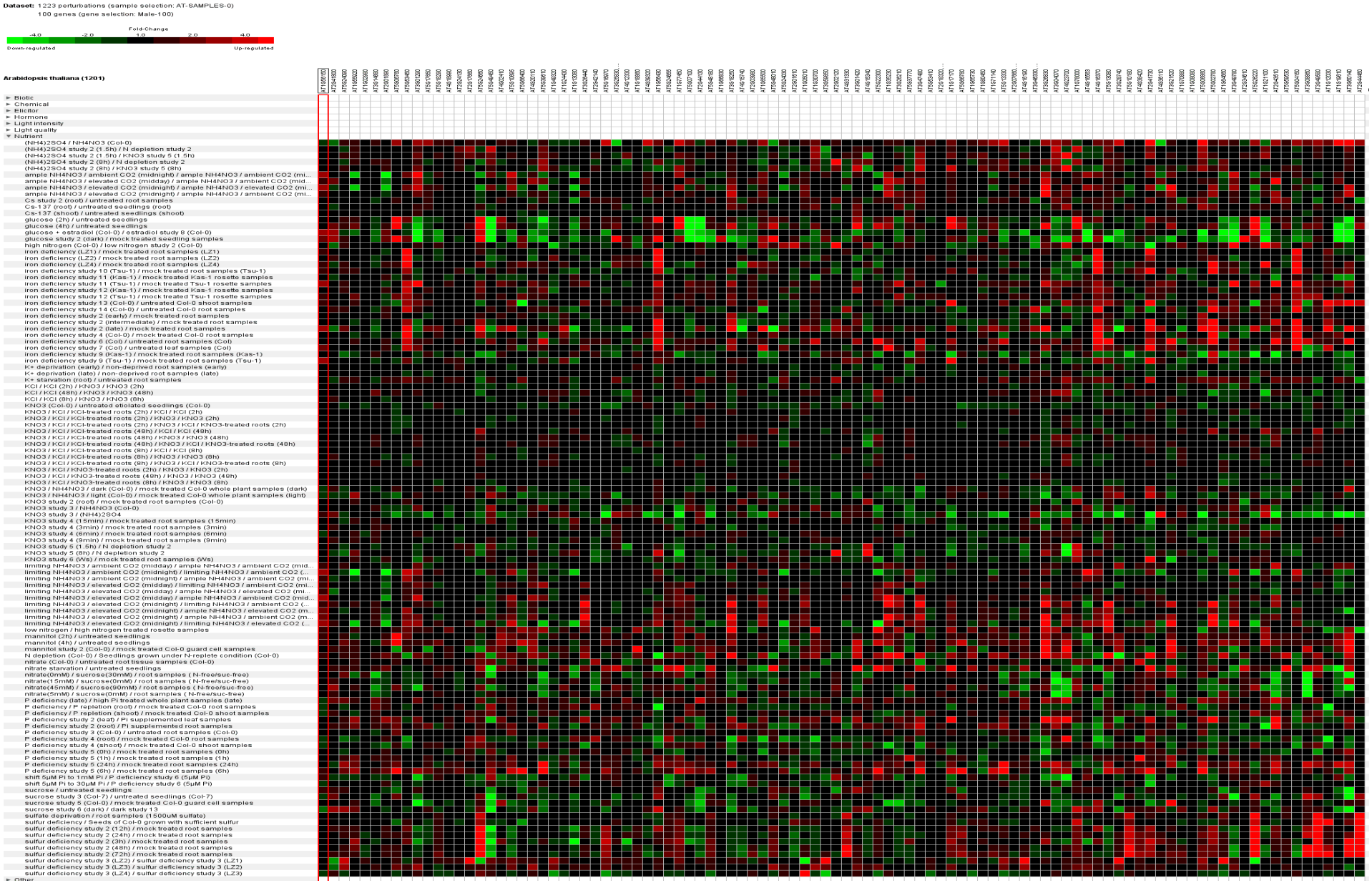

Figure S7: Expression analysis of mutant lines

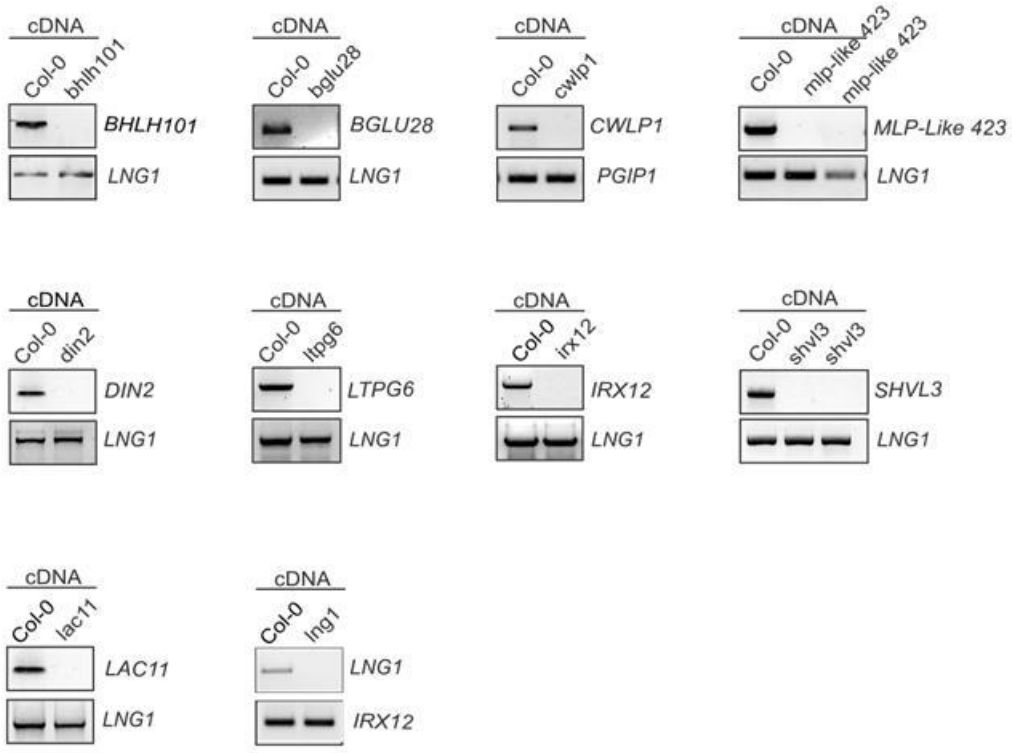

Figure S8: Cloning strategy for prmoter::gus constructs

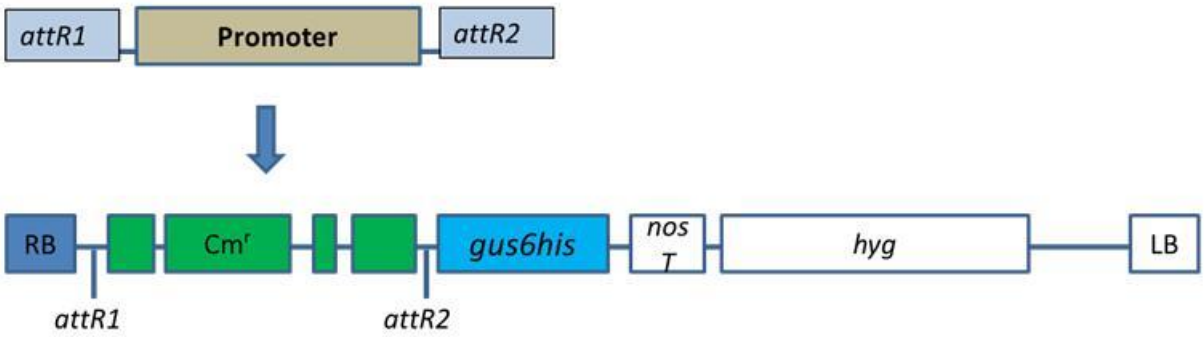

Figure S9: Destination expression vector map (ABRC Stock Center, www.arabidopsis.org)

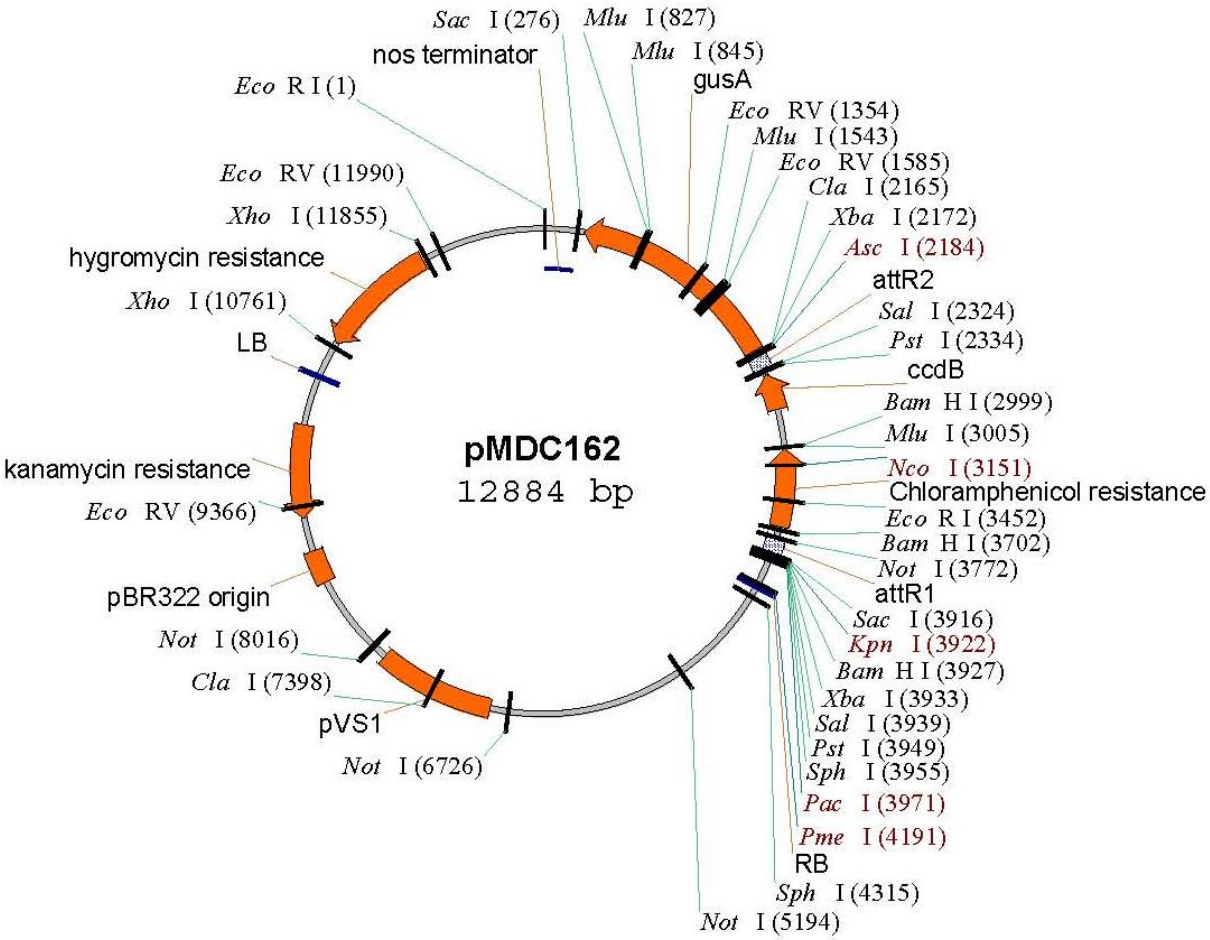

Table S1: List of 455 strongly differentially genes (Fold change FAS vs MAS >1.5; false discovery rate < 5%)

ATG locus	p-value	Log2	Fold change	Gene Symbol	Gene Title
At3g22120	0.0032	3.8	13.5	CWLP	CWLP (Cell Wall-plasma Membrane Linker Protein); lipid binding
At2g23170	0.0259	2.0	3.9	GH3.3	GH3.3; indole-3-acetic acid amido synthetase
At3g21550	0.0278	1.7	3.2	DUF679	Molecular Function not known
At1g75900	0.0494	1.6	3.0	Lipase	GDSL-like Lipase/Acylhydrolase superfamily protein
At4g00220	0.0415	1.5	2.9	JLO	JLO (Jagged Lateral Organs)
At1g24020	0.0006	1.5	2.9	MLP423	MLP423 (MLP-like protein 423)
At5g57800	0.0264	1.5	2.8	CER3	CER3 (ECERIFERUM 3); binding / catalytic/ iron ion binding / oxidoreductase
At1g72970	0.0365	1.5	2.8	HTH	HTH (Hothead); FAD binding / aldehyde-lyase/ mandelonitrile lyase
At3g30180	0.0297	1.4	2.7	BR6OX2	BR6OX2 (Brassinosteroid-6-Oxidase 2); monooxygenase/ oxygen binding
At5g15580	0.0291	1.4	2.7	LNG1	Regulates leaf morphology by promoting cell expansion in the leaf-length direction
At5g48485	0.0479	1.4	2.7	DIR1	DIR1 (Defective In Induced Resistance 1); lipid binding / lipid transporter
At1g55260	0.0411	1.4	2.7	LTPG6	Lipid Protein Transfer 6

At3g20520	0.0008	1.4	2.6	SVL3	SVL3 (SHV3-LIKE 3); glycerophosphodiester phosphodiesterase/ phosphoric diester hydrolase
At4g39330	0.0410	1.4	2.6	CAD9	CAD9 (Cinnamyl Alcohol Dehydrogenase 9); binding / catalytic/ oxidoreductase/ zinc ion binding
At5g02760	0.0220	1.4	2.6		Protein phosphatase 2C
At5g48350	0.0228	1.4	2.6		(Has 02 Loci) Polynucleotidyl transferase, ribonuclease H-like superfamily protein, 3'-5' exonuclease activity, nucleic acid binding
At1g25450	0.0134	1.3	2.4	KCS5	KCS5 (3-Ketoacyl-Coa Synthase 5); fatty acid elongase
At1g13420	0.0328	1.2	2.4	ST4B	ST4B (Sulfotransferase 4B); brassinosteroid sulfotransferase/ sulfotransferase
At3g58190	0.0416	1.2	2.4	LBD29	LBD29 (Lateral Organ Boundaries-Domain 29)
At3g15050	0.0361	1.2	2.3	IQD10	IQD10 (IQ-domain 10); calmodulin binding
At2g38080	0.0295	1.2	2.3	IRX12	IRX12 (Irregular Xylem 12); laccase
At3g30270	0.0040	1.2	2.3	AGL79	AGL79 (Agamous-Like 79); DNA binding / transcription factor
At1g73780	0.0114	1.2	2.2		Bifunctional inhibitor/lipid-transfer protein/seed storage
At1g68530	0.0209	1.2	2.2	KCS6	KCS6 (3-Ketoacyl-Coa Synthase 6); catalytic/ transferase, transferring acyl groups other than amino-acyl groups
At3g62020	0.0445	1.1	2.2	GLP10	GLP10 (Germin-Like Protein 10); manganese ion binding / nutrient reservoir
At1g65900	0.0016	1.1	2.2		Unknown protein
At1g68460	0.0197	1.1	2.1	ATIPT1	ATIPT1 (Isopentenyltransferase 1); adenylate dimethylallyltransferase
At1g58370	0.0438	1.1	2.1	RXF12	RXF12; endo-1,4-beta-xylanase/ hydrolase, hydrolyzing O-glycosyl compounds
At1g79760	0.0395	1.0	2.1	DTA4	DTA4 (Downstream Target Of Agl15-4)
At5g23480	0.0119	1.0	2.1	SWIB/MDM2 domain	DNA binding (02 loci in database)
At5g54690	0.0083	1.0	2.1	GAUT12	GAUT12 (Galacturonosyltransferase 12)
At2g37380	0.0300	1.0	2.0	MAKR	Found at 08 loci, molecular function unknown
At5g20640	0.0267	1.0	2.0	DUF567	Protein of unknown function
At2g42440	0.0333	1.0	2.0	ASL15	Asymmetric Leaves 2-Like 15
At1g32900	0.0344	1.0	2.0	GBSS1	Granule bound Starch Synthase 1
At1g61840	0.0142	1.0	2.0		Cysteine/Histidine-rich C1 domain family protein
At1g63120	0.0443	1.0	2.0	ATRBL2	ATRBL2 (*Arabidopsis thaliana* Rhomboid-like 2); serine-type endopeptidase
At2g26040	0.0325	1.0	1.9	PYL2	Pyr1-Like 2, Rcar14
At1g48660	0.0001	0.9	1.9		Auxin-responsive GH3 family protein
At1g20850	0.0484	0.9	1.9	XCP2	XCP2 (xylem cysteine peptidase 2); cysteine-type peptidase/ peptidase
At1g70700	0.0095	0.9	1.9	TIFY7	TIFY7
At5g47600	0.0230	0.9	1.9		HSP20-like chaperones superfamily protein
At3g02110	0.0045	0.9	1.9	scpl25	scpl25 (serine carboxypeptidase-like 25); serine-type carboxypeptidase
At5g49100	0.0082	0.9	1.9		Unknown protein
At3g06020	0.0031	0.9	1.9	FAF4	Fantastic Four 4
At4g16447	0.0173	0.9	1.8		Unknown protein
At2g39370	0.0470	0.9	1.8	MAKR4	Membrane-associated kinase regulator 4
At3g50870	0.0117	0.9	1.8	MNP	MNP (Monopole); transcription factor
At2g27240	0.0385	0.9	1.8		Aluminium activated malate transporter family protein
At3g62610	0.0042	0.9	1.8	ATMYB11	ATMYB11 (MYB Domain protein 11); DNA binding / transcription factor
At3g24450	0.0416	0.8	1.8		Heavy metal transport/detoxification superfamily protein
At5g52780	0.0225	0.8	1.8	DUF3464	Protein of unknown function

At5g10720	0.0159	0.8	1.8	AHK5	AHK5 (*Arabidopsis* Histidine Kinase 5); protein histidine kinase
At5g54510	0.0306	0.8	1.8	DFL1	DFL1 (Dwarf in light 1); indole-3-acetic acid amido synthetase
At3g48250	0.0039	0.8	1.8	BIR6	Buthionine sulfoximine-insensitive roots 6
At1g78960	0.0175	0.8	1.8	ATLUP2	ATLUP2; beta-amyrin synthase/ lupeol synthase
At2g01760	0.0055	0.8	1.8	ARR14	ARR14 (*Arabidopsis* response regulator 14)
At4g22160	0.0375	0.8	1.7		Unknown protein
At4g08150	0.0094	0.8	1.7	KNAT1	KNAT1 (Knotted-like from *Arabidopsis thaliana*); transcription factor
At1g75690	0.0132	0.8	1.7	LQY1	Low quantum yield of photosystem II 1
At2g27740	0.0233	0.8	1.7	DUF662	Family of unknown function
At2g41070	0.0052	0.8	1.7	EEL	EEL (Enhanced em level); DNA binding / transcription factor
At1g68120	0.0383	0.8	1.7	BPC3	BPC3 (Basic pentacysteine 3); DNA binding / transcription factor
AtMg00710	0.0400	0.8	1.7	ORF120	Polynucleotidyl transferase
At3g02980	0.0143	0.8	1.7	MCC1	Meiotic control of crossovers1
At2g19590	0.0480	0.8	1.7	ACO1	ACO1 (ACC Oxidase 1); 1-aminocyclopropane-1-carboxylate oxidase
At1g71990	0.0108	0.7	1.7	FUT13	FUT13 (Fucosyltransferase 13); fucosyltransferase/ transferase, transferring glycosyl groups
At2g43140	0.0467	0.7	1.7	BHLH129	Basic Helix loop Helix Protein
At1g50110	0.0348	0.7	1.7	BCAT6	Ranched-Chain Aminotransferase 6
At1g50580	0.0007	0.7	1.7		UDP-Glycosyltransferase superfamily protein
At3g06440	0.0300	0.7	1.7	GALT3	Encodes a Golgi-localized hydroxyproline-O-galactosyltransferase
At2g41290	0.0484	0.7	1.7	SSL2	Strictosidine Synthase-Like 2
At5g47370	0.0345	0.7	1.7	HAT2	HAT2; DNA binding / transcription factor/ transcription repressor
At4g33000	0.0470	0.7	1.7	CBL10	CBL10 (Calcineurin B-like 10); Calcium ion binding
At4g33340	0.0057	0.7	1.7	PGSIP3	transferase, transferring glycosyl groups
At1g60630	0.0015	0.7	1.6		Leucine-rich repeat protein kinase family protein
At2g07738	0.0331	0.7	1.6		Unknown protein
At2g43480	0.0155	0.7	1.6		Peroxidase superfamily protein
At2g40130	0.0001	0.7	1.6	SMXL8	Smax1-like 8
At5g48470	0.0068	0.7	1.6	PRDA1	Pep-Related Development Arrested 1
At2g07719	0.0356	0.7	1.6		Putative membrane lipoprotein
At1g14410	0.0041	0.7	1.6	WHY1	WHY1 (Whirly 1); DNA binding / telomeric DNA binding
At4g35660	0.0484	0.7	1.6	DUF241	*Arabidopsis* protein of unknown function
At5g22940	0.0367	0.7	1.6	F8H	F8H (FRA8 Homolog); catalytic
At2g07673	0.0298	0.7	1.6		Unknown protein
At4g09890	0.0095	0.7	1.6	PMP	PMP (Putative type 1 Membrane Protein)
At1g50950	0.0208	0.7	1.6		Involved in: cell redox homeostasis
At2g07693	0.0244	0.7	1.6		Copia-like retrotransposon family
At5g01340	0.0181	0.7	1.6	ATMSFC1	Mitochondrial Succinate-Fumarate Carrier 1
At3g55310	0.0355	0.7	1.6		NAD(P)-binding Rossmann-fold superfamily protein
At3g22121	0.0090	0.7	1.6		miscRNA, Potential natural antisense genes
At1g63300	0.0187	0.7	1.6		Myosin heavy chain-related protein
At1g75590	0.0465	0.7	1.6	SAUR52	Small auxin upregulated rna 52
At2g32440	0.0055	0.7	1.6	KAO2	KAO2 (Ent-kaurenoic acid hydroxylase 2); ent-Kaurenoate oxidase/ oxygen binding
At3g52500	0.0150	0.7	1.6		Eukaryotic aspartyl protease family protein

At2g07721	0.0189	0.7	1.6		Unknown protein
At4g24260	0.0104	0.7	1.6	ATGH9A3	*Arabidopsis thaliana* Glycosyl Hydrolase 9a3
At5g15070	0.0146	0.7	1.6	VIP1 2	*Arabidopsis* homolog of yeast
At3g22900	0.0395	0.7	1.6	NRPD7	NRPD7; DNA-directed RNA polymerase
At2g21650	0.0187	0.7	1.6	MEE3	MEE3 (Maternal Effect Embryo Arrest 3); DNA binding / transcription factor
At1g72360	0.0213	0.7	1.6	ERF73	Ethylene Response Factor 73
At2g40150	0.0153	0.7	1.6	TBL28	Trichome Birefringence-Like 28
At2g07703	0.0077	0.6	1.6		Copia-like retrotransposon family,
At2g32690	0.0013	0.6	1.6	GRP23	GRP23 (Glycine-rich protein 23)
At4g34760	0.0491	0.6	1.6	SAUR50	Small auxin upregulated RNA 50
At2g18230	0.0191	0.6	1.6	AtPPA2	AtPPA2 (*Arabidopsis thaliana* pyrophosphorylase 2); inorganic diphosphatase/ pyrophosphatase
At2g07714	0.0239	0.6	1.6		Transcription factor-related
At3g07000	0.0228	0.6	1.5		Cysteine/Histidine-rich C1 domain family protein
At3g16180	0.0410	0.6	1.5	NRT1.12	Nitrate transporter 1.12
At4g37240	0.0184	0.6	1.5		Unknown protein
At5g62840	0.0408	0.6	1.5		Phosphoglycerate mutase family protein
At4g10270	0.0357	0.6	1.5		Wound-responsive family protein
At1g53070	0.0339	0.6	1.5		Legume lectin family protein
At1g76450	0.0418	0.6	1.5		Photosystem II reaction center PsbP family protein
At3g43190	0.0377	0.6	1.5	SUS4	SUS4; UDP-glycosyltransferase/ sucrose synthase/ transferase, transferring glycosyl groups
At5g20040	0.0288	0.6	1.5	IPT9	ATIPT9; ATP binding / tRNA isopentenyltransferase
At3g15550	0.0205	0.6	1.5		Unknown protein
At3g18080	0.0249	0.6	1.5	BGLU44	BGLU44 (B-S Glucosidase 44); (R)-amygdalin beta-glucosidase/ 4-methylumbelliferyl-beta-D-glucopyranoside beta-glucosidase/ beta-gentiobiose beta-glucosidase
At5g47630	0.0096	0.6	1.5	mtACP3	mtACP3 (mitochondrial acyl carrier protein 3); acyl carrier/ cofactor binding
At3g14310	0.0274	0.6	1.5	ATPME3	ATPME3; pectinesterase
At2g46730	0.0479	0.6	1.5		Pseudogene, similar to 68 kDa protein
At3g05430	0.0107	0.6	1.5		Tudor/PWWP/MBT superfamily protein
At5g46910	0.0074	0.6	1.5		Transcription factor jumonji (jmj) family protein / zinc finger (C5HC2 type) family protein
At3g50220	0.0405	0.6	1.5	IRX15	Irregular Xylem 15
At2g44460	0.026	-4.3	-19.8	BGLU28	BGLU28 (Beta Glucosidase 28); catalytic/ cation binding / hydrolase, hydrolyzing O-glycosyl compounds
At3g60140	0.006	-3.2	-9.3	DIN2	DIN2 (Dark Inducible 2); catalytic/ cation binding / hydrolase, hydrolyzing O-glycosyl compounds
At1g19610	0.004	-2.1	-4.3	PDF1.4	PDF1.4
At1g12030	0.013	-2.1	-4.3	DUF506	Protein of unknown function
At3g49580	0.014	-2.1	-4.2	LSU1	LSU1 (Response To Low Sulfur 1)
At3g08860	0.026	-2.0	-4.1	PYD4	Pyrimidine 4
At5g04150	0.004	-1.9	-3.8	BHLH101	BHLH101; DNA binding / transcription factor
At5g59530	0.009	-1.8	-3.4		2-oxoglutarate (2OG) and Fe(II)-dependent oxygenase superfamily protein
At2g43510	0.013	-1.7	-3.3	ATTI1	ATTI1; serine-type endopeptidase inhibitor
At1g21100	0.016	-1.6	-3.1	IGMT1	Indole Glucosinolate O-Methyltransferase 1
At5g26220	0.033	-1.6	-3.0	ATGGCT2;1	Gamma-Glutamyl Cyclotransferase 2;1, Ggct2;1
At2g34610	0.004	-1.5	-2.9		Unknown Protein
At3g49780	0.024	-1.5	-2.8	ATPSK4	Phytosulfokine 4 Precursor); growth factor

At1g64660	0.020	-1.5	-2.8	ATMGL	*Arabidopsis thaliana* Methionine Gamma-Lyase; catalytic/ methionine gamma-lyase
At5g02780	0.011	-1.5	-2.7	GSTL1	Glutathione transferase lambda 1
At5g06860	0.002	-1.4	-2.7	PGIP1	Polygalacturonase inhibiting protein 1; protein binding
At1g08080	0.006	-1.4	-2.6	ACA7	Alpha carbonic anhydrase 7; carbonate dehydratase/ zinc ion binding
At1g70880	0.034	-1.4	-2.6		Polyketide cyclase/dehydrase and lipid transport superfamily protein
At3g21520	0.002	-1.4	-2.6	ATDMP1	*Arabidopsis thaliana* duf679 domain membrane protein 1
At4g36110	0.016	-1.3	-2.5	SAUR9	Small auxin upregulated RNA 9
At2g41730	0.031	-1.3	-2.5		Unknown protein
At4g38420	0.010	-1.3	-2.5	Sks9	sks9 (SKU5 Similar 9); copper ion binding / Oxidoreductase
At5g10180	0.010	-1.3	-2.5	SULTR2;1	AST68; sulfate transmembrane transporter
At3g28740	0.012	-1.3	-2.5	CYP81D1	CYP81D1; electron carrier/ heme binding / iron ion binding / monooxygenase/ oxygen binding
At1g27470	0.035	-1.3	-2.4		Transducin family protein / WD-40 repeat family protein
At5g13080	0.001	-1.3	-2.4	WRKY75	WRKY75; transcription factor
At4g16370	0.021	-1.2	-2.4	ATOPT3	Oligopeptide Transporter; oligopeptide transporter
At4g16563	0.001	-1.2	-2.3		Eukaryotic aspartyl protease family protein
At1g78000	0.020	-1.2	-2.3	SULTR1;2	Sulfate Transporter 1;2; Sulfate transmembrane transporter
At4g23700	0.029	-1.2	-2.3	ATCHX17	Cation/H^+ Exchanger 17; monovalent cation:proton antiporter/ sodium:hydrogen antiporter
At3g04070	0.032	-1.2	-2.3	ANAC47	*Arabidopsis* NAC domain containing protein 47; transcription factor
At3g26830	0.032	-1.2	-2.3	PAD3	PAD3 (Phytoalexin deficient 3); dihydrocamalexic acid decarboxylase/ monooxygenase/ oxygen binding
At3g45920	0.002	-1.2	-2.3	MEE39	MEE39 (maternal effect embryo arrest 39); kinase
At4g16190	0.007	-1.2	-2.3		Papain family cysteine protease
At2g06470	0.018	-1.2	-2.3		Gypsy-like retrotransposon family
At5g13330	0.009	-1.2	-2.2	Rap2.6L	Rap2.6L (Related to AP2 6L); DNA binding / transcription factor
At1g71140	0.016	-1.2	-2.2		MATE efflux family protein
At1g80450	0.008	-1.2	-2.2		VQ motif-containing protein
At1g65730	0.028	-1.2	-2.2	YSL7	YSL7 (Yellow Stripe Like 7); Oligopeptide transporter
At5g66780	0.032	-1.2	-2.2		Unknown protein
At1g17170	0.024	-1.1	-2.2	ATGSTU24	ATGSTU24 (Glutathione s-transferase TAU 24); glutathione binding / glutathione transferase
At5g53410	0.005	-1.1	-2.2		Unknown protein
At3g47480	0.049	-1.1	-2.2		Calcium-binding EF-hand family protein
At5g37770	0.025	-1.1	-2.2	TCH2	TCH2 (Touch 2); calcium ion binding
At3g26210	0.023	-1.1	-2.2	CYP71B23	CYP71B23; electron carrier/ heme binding / iron ion binding / monooxygenase/ oxygen binding
At1g35230	0.017	-1.1	-2.2	AGP5	AGP5 (Arabinogalactan-protein 5)
At5g22300	0.003	-1.1	-2.2	GAPB	GAPB (Glyceraldehyde-3-phosphate dehydrogenase b subunit)
At4g15340	0.036	-1.1	-2.2	ATPEN1	ATPEN1 (*Arabidopsis thaliana* pentacyclic triterpene synthase 1); Arabidiol synthase
At3g01420	0.019	-1.1	-2.2	DOX1	DOX1; Lipoxygenase
At4g31330	0.007	-1.1	-2.2	DUF599	Protein of unknown function
At2g02120	0.032	-1.1	-2.2	PDF2.1	PDF2.1; Peptidase inhibitor
At3g59850	0.013	-1.1	-2.1		Pectin lyase-like superfamily protein
At1g30700	0.036	-1.1	-2.1	ATBBE8	FAD-binding Berberine family protein
At1g05010	0.004	-1.1	-2.1	EFE	EFE (Ethylene-Forming Enzyme); 1-aminocyclopropane-1-carboxylate oxidase
At2g01610	0.018	-1.1	-2.1		Plant invertase/pectin methylesterase inhibitor superfamily protein

At5g24030	0.036	-1.1	-2.1	SLAH3	SLAH3 (SLAC1 Homologue 3); transporter
At5g48010	0.039	-1.1	-2.1	THAS1	THAS1 (Thalianol Synthase 1); catalytic/ thalianol synthase
At1g65500	0.029	-1.0	-2.1		Unknown Protein
At2g03980	0.006	-1.0	-2.1		GDSL-motif esterase/acyltransferase/lipase
At2g28210	0.001	-1.0	-2.1	ATACA2	ATACA2 (Alpha Carbonic Anhydrase 2); carbonate dehydratase/ zinc ion binding
At4g15740	0.001	-1.0	-2.1		Calcium-dependent lipid-binding (CaLB domain) family protein
At3g18250	0.016	-1.0	-2.1		Putative membrane lipoprotein
At1g66830	0.039	-1.0	-2.0		Leucine-rich repeat protein kinase family protein
At5g48180	0.004	-1.0	-2.0	NSP5	NSP5 (Nitrile Specifier Protein 5)
At2g44130	0.024	-1.0	-2.0	KFB39	Kelch-Domain-Containing F-Box Protein 39
At5g07100	0.029	-1.0	-2.0	WRKY26	WRKY26; transcription factor
At1g77450	0.022	-1.0	-2.0	anac032	anac032 (*Arabidopsis* NAC domain containing protein 32); transcription factor
At5g24655	0.006	-1.0	-2.0	LSU4	LSU4 (Response To Low Sulfur 4)
At1g56430	0.023	-1.0	-2.0	NAS4	NAS4 (Nicotianamine Synthase 4); nicotianamine synthase
At4g39320	0.005	-1.0	-2.0		Microtubule-Associated Protein-Related
At1g18860	0.030	-1.0	-2.0	WRKY61	WRKY61; transcription factor
At4g12330	0.009	-1.0	-2.0	CYP706A7	CYP706A7; electron carrier/ heme binding / iron ion binding / monooxygenase/ oxygen binding
At3g25830	0.028	-1.0	-2.0	ATTPS-CIN	ATTPS-CIN (terpene synthase-like sequence-1,8-cineole); (E)-beta-ocimene synthase/ myrcene synthase
At5g16970	0.026	-1.0	-2.0	AT-AER	AT-AER (alkenal reductase); 2-alkenal reductase
At2g42140	0.016	-1.0	-2.0		VQ motif-containing protein
At3g26440	0.011	-1.0	-2.0	DUF707	Protein of unknown function
At1g13080	0.018	-1.0	-2.0	CYP71B2	CYP71B2 (Cytochrome P450 71B2); electron carrier/ heme binding / iron ion binding / monooxygenase/ oxygen binding
At1g24430	0.015	-1.0	-2.0		HXXXD-type acyl-transferase family protein
At1g49320	0.007	-1.0	-2.0	ATUSPL1	Unknown Seed Protein Like 1
At5g39610	0.032	-1.0	-2.0	ATNAC6	NAC6 (NAC Domain Containing Protein 6); protein heterodimerization/ protein homodimerization/ transcription factor
At4g20110	0.025	-1.0	-2.0	VSR7	Vacuolar Sorting Receptor 7
At5g66400	0.049	-1.0	-2.0	RAB18	RAB18 (Responsive to ABA 18)
At5g10695	0.010	-1.0	-2.0		Unknown Protein
At4g02410	0.007	-1.0	-2.0	ATLPK1	Lectin-Like Protein Kinase 1
At5g49450	0.004	-1.0	-1.9	CPuORF4	CPuORF4 (Conserved peptide upstream open reading frame 4)
At5g24660	0.022	-1.0	-1.9	LSU2	LSU2 (Response To Low Sulfur 2)
At2g17660	0.029	-1.0	-1.9		RPM1-interacting protein 4 (RIN4) family protein
At2g24130	0.027	-1.0	-1.9		Leucine-rich receptor-like protein kinase family protein
At4g18990	0.028	-0.9	-1.9	XTH29	Xyloglucan Endotransglucosylase/Hydrolase 29
At5g18290	0.005	-0.9	-1.9	SIP1;2	SIP1;2; water channel
At5g17650	0.014	-0.9	-1.9		Glycine/proline-rich protein
At3g01290	0.032	-0.9	-1.9	HIR2	Hypersensitive Induced Reaction 2
At5g53450	0.044	-0.9	-1.9	ORG1	ORG1 (OBP3-responsive gene 1); ATP binding / kinase/ protein kinase
At5g06760	0.020	-0.9	-1.9	LEA4-5	Late Embryogenesis Abundant 4-5. Typically accumulates in response to low water availability conditions
At2g01890	0.046	-0.9	-1.9	PAP8	PAP8 (PURPLE ACID PHOSPHATASE 8); acid phosphatase/ protein serine/threonine phosphatase
At3g14680	0.038	-0.9	-1.9	CYP72A14	CYP72A14; electron carrier/ heme binding / iron ion binding / monooxygenase/ oxygen binding
At1g02980	0.009	-0.9	-1.9	CUL2	CUL2 (Cullin 2); ubiquitin protein ligase binding
At1g55920	0.005	-0.9	-1.9	SERAT2;1	Serine Acetyltransferase 2;1; serine O-acetyltransferase

At5g24090	0.027	-0.9	-1.9	CHIA	Chitinase A (class III) expressed exclusively under environmental stress conditions.
At2g41800	0.014	-0.9	-1.9	TEB	Long in the Mayo-Yoreme Language. Encodes a DUF642 cell wall protein that is highly induced during the M/G1 phases of the cell cycle
At1g56150	0.023	-0.9	-1.9	SAUR71	Small Auxin Upregulated 71
At1g64950	0.028	-0.9	-1.9	CYP89A5	CYP89A5; electron carrier/ heme binding / iron ion binding / monooxygenase/ oxygen binding
At5g66690	0.007	-0.9	-1.9	UGT72E2	UGT72E2; UDP-glycosyltransferase/ coniferyl-alcohol glucosyltransferase/ transferase, transferring glycosyl groups
At4g35720	0.030	-0.9	-1.9	DUF241	*Arabidopsis* protein of unknown function
At2g39980	0.021	-0.9	-1.9		HXXXD-type acyl-transferase family protein
At5g45380	0.016	-0.9	-1.9	ATDUR3	Degradation of Urea 3
At1g72900	0.003	-0.9	-1.9		Protein containing Toll-Interleukin-Resistance (TIR) domain
At5g13750	0.018	-0.9	-1.9	ZIFL1	ZIFL1 (Zinc Induced Facilitator-like 1); tetracycline:hydrogen antiporter
At1g63530	0.047	-0.9	-1.9		Best match: Hydroxyproline-rich glycoprotein family protein
At5g06870	0.013	-0.9	-1.9	PGIP2	PGIP2 (Polygalacturonase Inhibiting Protein 2); protein binding
At4g12280	0.047	-0.9	-1.9		Copper amine oxidase family protein
At5g27350	0.006	-0.9	-1.9	SFP1	SFP1; carbohydrate transmembrane transporter/ sugar:hydrogen symporter
At4g17980	0.005	-0.9	-1.9	anac071	anac071 (*Arabidopsis* NAC domain containing protein 71); transcription factor
At4g15280	0.008	-0.9	-1.9	UGT71B5	UGT71B5 (UDP-Glucosyl Transferase 71B5); UDP-glycosyltransferase/ quercetin 3-O-glucosyltransferase/ transferase, transferring glycosyl groups
At1g64590	0.010	-0.9	-1.8		NAD(P)-binding Rossmann-fold superfamily protein
At5g22860	0.033	-0.9	-1.8		Serine carboxypeptidase S28 family protein
At5g67370	0.018	-0.9	-1.8	CGLD27	Conserved In The Green Lineage and Diatoms 27
At1g59700	0.005	-0.9	-1.8	ATGSTU16	ATGSTU16 (Glutathione S-Transferase Tau 16); glutathione transferase
At3g14060	0.019	-0.9	-1.8	GAPC1	GAPC1 (Glyceraldehyde-3-Phosphate Dehydrogenase C Subunit 1); glyceraldehyde-3-phosphate dehydrogenase (phosphorylating)/ glyceraldehyde-3-phosphate dehydrogenase
At1g68150	0.047	-0.9	-1.8	WRKY9	WRKY9; transcription factor
At2g38250	0.008	-0.9	-1.8		Homeodomain-like superfamily protein
At2g41380	0.016	-0.9	-1.8		S-adenosyl-L-methionine-dependent methyltransferases superfamily protein
At5g01380	0.026	-0.9	-1.8		Homeodomain-like superfamily protein
At5g42580	0.010	-0.9	-1.8	CYP705A12	CYP705A12; electron carrier/ heme binding / iron ion binding / monooxygenase/ oxygen binding
At2g34830	0.011	-0.9	-1.8	WRKY35	WRKY35 (WRKY DNA-binding protein 35); transcription factor
At2g19320	0.016	-0.9	-1.8		Unknown protein
At4g16820	0.022	-0.9	-1.8	DALL1	Phospholipase A I Beta 2. Encodes a lipase that hydrolyzes phosphatidylcholine, glycolipids as well as triacylglycerols
At5g06840	0.018	-0.9	-1.8		bZIP transcription like protein
At1g56010	0.033	-0.9	-1.8	NAC1	NAC1; transcription factor
At2g22860	0.010	-0.9	-1.8	ATPSK2	ATPSK2 (Phytosulfokine 2 Precursor); growth factor
At5g11410	0.027	-0.8	-1.8		Protein kinase superfamily protein
At3g14280	0.017	-0.8	-1.8		Unknown protein
At3g13710	0.045	-0.8	-1.8	PRA1.F4	Prenylated Rab Acceptor 1.F4
At5g52390	0.013	-0.8	-1.8		PAR1 protein. Unknown molecular function
At4g01870	0.020	-0.8	-1.8		Related to tolB protein. Unknown molecular function
At4g03620	0.013	-0.8	-1.8		Myosin heavy chain-related

At1g30040	0.000	-0.8	-1.8	ATGA2OX2	ATGA2OX2 (Gibberellin 2-Oxidase); gibberellin 2-beta-dioxygenase
At2g24430	0.034	-0.8	-1.8	ANAC038	ANAC038 (NAC Domain Containing Protein 38); transcription factor
At4g21680	0.026	-0.8	-1.8	NPF7.2	Encodes a nitrate transporter (NRT1.8)
At1g35280	0.018	-0.8	-1.8		CACTA-like transposase family (Tnp2/En/Spm)
At2g40200	0.017	-0.8	-1.8		Basic helix-loop-helix (bHLH) DNA-binding superfamily protein
At1g65510	0.031	-0.8	-1.8		Unknown protein
At1g22990	0.001	-0.8	-1.8	HIPP22	Heavy Metal Associated Isoprenylated Plant Protein 22
At3g22370	0.020	-0.8	-1.8	AOX1A	AOX1A (ALTERNATIVE OXIDASE 1A); alternative oxidase
At3g60420	0.050	-0.8	-1.8		Phosphoglycerate mutase family protein
At1g64900	0.020	-0.8	-1.8	CYP89A2	CYP89A2 (Cytochrome P450 89A2); electron carrier/ heme binding / iron ion binding / monooxygenase/ oxygen binding
At2g18370	0.014	-0.8	-1.8		Predicted to encode a PR (pathogenesis-related) protein
At3g59730	0.000	-0.8	-1.8	LECRK-V.6	L-Type Lectin Receptor Kinase V.6
At5g63560	0.008	-0.8	-1.8	FACT	Fatty Alcohol:Caffeoyl-Coa Caffeoyl Transferase
At1g71710	0.025	-0.8	-1.8		DNAse I-like superfamily protein
At5g06570	0.001	-0.8	-1.8		Alpha/beta-Hydrolases superfamily protein
At1g62320	0.013	-0.8	-1.8	ERD	Early-responsive to dehydration stress) family protein
At4g26890	0.027	-0.8	-1.8	MAPKKK16	MAPKKK16; ATP binding / kinase/ protein kinase/ protein serine/threonine kinase/ protein tyrosine kinase
At1g69920	0.029	-0.8	-1.8	ATGSTU12	ATGSTU12 (Glutathione S-Transferase TAU 12); glutathione transferase
At2g34650	0.014	-0.8	-1.8	PID	PID (PINOID); kinase/ protein kinase/ protein serine/threonine kinase
At2g39410	0.021	-0.8	-1.8	MAGL7	Alpha/Beta-Hydrolases Superfamily Protein
At2g23760	0.016	-0.8	-1.7	BLH4	BLH4 (Bel1-Like Homeodomain 4); DNA binding / transcription factor
At3g59060	0.011	-0.8	-1.7	PIL6	PIL6 (Phytochrome Interacting Factor 3-Like 6); DNA binding / transcription factor
At4g15610	0.003	-0.8	-1.7	CASPL1D1	Casp-Like Protein 1d1
At1g70140	0.003	-0.8	-1.7	ATFH8	ATFH8 (formin 8); actin binding / actin filament binding / profilin binding
At5g52250	0.007	-0.8	-1.7	EFO1, RUP1	Early Flowering By Overexpression 1, Repressor of UV-B Photomorphogenesis
At1g76410	0.017	-0.8	-1.7	ATL8	ATL8; protein binding / zinc ion binding
At3g62730	0.006	-0.8	-1.7		Unknown Protein
At5g59540	0.037	-0.8	-1.7		2-oxoglutarate (2OG) and Fe(II)-dependent oxygenase superfamily protein
At1g55850	0.001	-0.8	-1.7	CSLE1	ATCSLE1; cellulose synthase/ transferase, transferring glycosyl groups
At4g35480	0.003	-0.8	-1.7	RHA3B	RHA3B; protein binding / zinc ion binding
At3g13640	0.016	-0.8	-1.7	ATRLI1	ATRLI1; transporter
At3g15280	0.038	-0.8	-1.7		Unknown Protein
At2g44480	0.022	-0.8	-1.7	BGLU17	Beta Glucosidase 17; catalytic/ cation binding / hydrolase, hydrolyzing O-glycosyl compounds
At3g05165	0.032	-0.8	-1.7		Major facilitator superfamily protein
At1g09380	0.041	-0.8	-1.7	UMAMIT25	Usually Multiple Acids Move in and out Transporters 25
At3g17110	0.018	-0.8	-1.7		Pseudogene, glycine-rich protein
At5g64410	0.036	-0.8	-1.7	OPT4	OPT4 (Oligopeptide Transporter 4); oligopeptide transporter
At3g58550	0.013	-0.8	-1.7		Bifunctional inhibitor/lipid-transfer protein/seed storage 2S albumin superfamily protein
At3g08040	0.009	-0.8	-1.7	FRD3	FRD3 (Ferric Reductase Defective 3); antiporter/ transporter
At5g46115	0.023	-0.8	-1.7		Unknown Protein
At2g27080	0.006	-0.8	-1.7	NHL13	NDR/HIN1-Like 13

At1g11210	0.007	-0.8	-1.7	DUF761	Protein of unknown function
At2g27390	0.000	-0.8	-1.7		Proline-Rich Family Protein
At4g22753	0.002	-0.8	-1.7	SMO1-3	SMO1-3 (Sterol 4-Alpha Methyl Oxidase 1-3); 4,4-dimethyl-9beta,19-cyclopropylsterol-4alpha-methyl oxidase/ catalytic
At3g12910	0.040	-0.8	-1.7		NAC (No Apical Meristem) domain transcriptional regulator superfamily protein
At5g04340	0.043	-0.8	-1.7	ZAT6	ZAT6 (Zinc Finger Of *Arabidopsis* thaliana 6); nucleic acid binding / transcription factor/ zinc ion binding
At3g11160	0.036	-0.8	-1.7		Unknown Protein
At1g09155	0.044	-0.8	-1.7	AtPP2-B15	AtPP2-B15 (Phloem protein 2-B15); carbohydrate binding
At5g41810	0.010	-0.7	-1.7		Unknown Protein
At4g34135	0.031	-0.7	-1.7	UGT73B2	UGT73B2 (UDP-Glucosyl Transferase 73B2); UDP-glucosyltransferase/ UDP-glycosyltransferase/ flavonol 3-O-glucosyltransferase/ quercetin 7-O-glucosyltransferase
At3g14690	0.004	-0.7	-1.7	CYP72A15	CYP72A15; electron carrier/ heme binding / iron ion binding / monooxygenase/ oxygen binding
At4g36040	0.025	-0.7	-1.7	DNAJ11	DNA J Protein C23
At5g43580	0.050	-0.7	-1.7	UPI	Unusual Serine Protease Inhibitor
At5g53110	0.016	-0.7	-1.7		RING/U-box superfamily protein
At3g18830	0.033	-0.7	-1.7	ATPLT5	Polyol Transporter 5; D-ribose transmembrane transporter/ D-xylose transmembrane transporter/ carbohydrate transmembrane transporter/ galactose transmembrane transporter/ glucose transmembrane transporter/ glycerol transmembrane transporter/ mann
At2g39110	0.025	-0.7	-1.7		Protein kinase superfamily protein
At5g37450	0.048	-0.7	-1.7		Leucine-rich repeat protein kinase family protein
At5g66170	0.019	-0.7	-1.7	STR18	Sulfur Transferase 18
At5g50200	0.022	-0.7	-1.7	WR3	WR3 (Wound-Responsive 3); nitrate transmembrane transporter
At3g24400	0.022	-0.7	-1.7	PERK2	Proline-Rich Extensin-Like Receptor Kinase 2
At1g01720	0.007	-0.7	-1.7	ATAF1	ATAF1; transcription activator/ transcription factor
At1g36370	0.037	-0.7	-1.7	SHM7	SHM7 (serine hydroxymethyltransferase 7); catalytic/ glycine hydroxymethyltransferase/ pyridoxal phosphate binding
At4g18170	0.010	-0.7	-1.6	WRKY28	WRKY28; transcription factor
At5g06330	0.003	-0.7	-1.6		Late embryogenesis abundant (LEA) hydroxyproline-rich glycoprotein family
At5g47740	0.002	-0.7	-1.6		Adenine nucleotide alpha hydrolases-like superfamily protein
At3g61150	0.042	-0.7	-1.6	HDG1	HDG1 (Homeodomain Glabrous 1); DNA binding / transcription factor
At1g06540	0.047	-0.7	-1.6		Unknown Protein
At4g13190	0.038	-0.7	-1.6		Protein kinase superfamily protein
At4g15330	0.009	-0.7	-1.6	CYP705A1	CYP705A1; electron carrier/ heme binding / iron ion binding / monooxygenase/ oxygen binding
At3g18290	0.014	-0.7	-1.6	EMB2454	EMB2454 (embryo defective 2454); protein binding / zinc ion binding
At1g80580	0.033	-0.7	-1.6		Encodes a member of the ERF (ethylene response factor) subfamily B-1 of ERF/AP2 transcription factor family.
At1g55240	0.009	-0.7	-1.6	DUF716	Family of unknown function
At1g53990	0.007	-0.7	-1.6	GLIP3	GLIP3; carboxylesterase/ lipase
At2g40170	0.018	-0.7	-1.6	GEA6	GEA6 (Late Embryogenesis Abundant 6)
At3g61930	0.010	-0.7	-1.6		Unknown Protein
At4g35120	0.003	-0.7	-1.6		Galactose oxidase/kelch repeat superfamily protein
At1g10070	0.020	-0.7	-1.6	ATBCAT-2	(*Arabidopsis thaliana* Branched-Chain Amino Acid Transaminase 2; branched-chain-amino-acid transaminase/ catalytic
At2g46680	0.008	-0.7	-1.6	ATHB-7	ATHB-7 (*Arabidopsis thaliana* Homeobox 7); transcription

					activator/ transcription factor
At2g47130	0.001	-0.7	-1.6	SDR3	Short-Chain Dehydrogenase/Reductase 2
At2g39650	0.038	-0.7	-1.6	DUF506	Protein of unknown function
At4g36880	0.032	-0.7	-1.6	CP1	CP1 (Cysteine Proteinase1); cysteine-type endopeptidase/ cysteine-type peptidase
At3g19660	0.038	-0.7	-1.6		Unknown Protein
At1g69810	0.006	-0.7	-1.6	WRKY36	WRKY36; transcription factor
At1g09310	0.023	-0.7	-1.6	DUF538	Protein of unknown function
At5g25440	0.017	-0.7	-1.6		Protein kinase superfamily protein
At1g09070	0.006	-0.7	-1.6	SRC2	SRC2 (Soybean Gene Regulated By Cold-2); protein binding
At4g16000	0.017	-0.7	-1.6		Unknown Protein
At1g14080	0.048	-0.7	-1.6	FUT6	FUT6 (Fucosyltransferase 6); fucosyltransferase/ transferase, transferring glycosyl groups
At2g32660	0.018	-0.7	-1.6	AtRLP22	AtRLP22 (Receptor Like Protein 22); kinase/ protein binding
At1g02400	0.035	-0.7	-1.6	GA2OX6	GA2OX6 (Gibberellin 2-Oxidase 6); gibberellin 2-beta-dioxygenase
At2g05580	0.033	-0.7	-1.6		Glycine-rich protein family
At1g80440	0.027	-0.7	-1.6	KFB20	Kelch Repeat F-Box 20
At2g23810	0.012	-0.7	-1.6	TET8	TET8 (Tetraspanin8)
At4g18910	0.018	-0.7	-1.6	NIP1;2	NOD26-Like Intrinsic Protein 1;2); Arsenite transmembrane transporter/ water channel
At1g06520	0.009	-0.7	-1.6	GPAT1	Glycerol-3-Phosphate Acyltransferase 1; 1-acylglycerol-3-phosphate O-acyltransferase/ acyltransferase
At5g59340	0.045	-0.7	-1.6	WOX2	WOX2 (Wuschel Related Homeobox 2); transcription factor
At2g41010	0.008	-0.7	-1.6	CAMBP25	Calmodulin (Cam)-Binding Protein Of 25 Kda; calmodulin binding
At4g15800	0.016	-0.7	-1.6	RALFL33	RALFL33 (ralf-like 33); signal transducer
At4g28290	0.041	-0.7	-1.6		Unknown Protein
At4g25200	0.002	-0.7	-1.6	HSP23.6-MITO	Mitochondrion-Localized Small Heat Shock Protein 23.6
At4g28270	0.012	-0.7	-1.6	ATRMA2	Ring Membrane-Anchor 2
At5g49700	0.022	-0.7	-1.6	AHL17	AT-Hook Motif Nuclear Localized Protein 17
At2g19110	0.047	-0.7	-1.6	HMA4	HMA4; cadmium ion transmembrane transporter/ cadmium-transporting ATPase/ zinc ion transmembrane transporter
At5g03790	0.022	-0.7	-1.6	HB51	HB51; DNA binding / sequence-specific DNA binding / transcription factor
At2g13360	0.001	-0.7	-1.6	AGT	AGT (Alanine:Glyoxylate aminotransferase); alanine-glyoxylate transaminase/ serine-glyoxylate transaminase/ serine-pyruvate transaminase
At2g28420	0.004	-0.7	-1.6	GLYI8	Glyoxylase I 8
At2g25940	0.036	-0.7	-1.6	ALPHA-VPE	ALPHA-VPE (alpha-vacuolar processing enzyme); cysteine-type endopeptidase
At3g01970	0.027	-0.7	-1.6	WRKY45	WRKY45; transcription factor
At1g74450	0.044	-0.7	-1.6		Plants overexpressing At1g74450 are stunted in height and have reduced male fertility.
At3g59740	0.009	-0.7	-1.6	LECRK-V.7	L-Type Lectin Receptor Kinase V.7
At1g76590	0.024	-0.7	-1.6		PLATZ transcription factor family protein
At1g32560	0.028	-0.7	-1.6	ATLEA4-1	Late Embryogenesis Abundant 4-1
At5g43450	0.004	-0.7	-1.6		Encodes a protein whose sequence is similar to ACC oxidase
At1g72460	0.030	-0.7	-1.6	PRK8	Leucine-rich repeat protein kinase family protein
At2g30550	0.006	-0.7	-1.6	DALL3	Dad1-Like Lipase 3
At1g80180	0.017	-0.7	-1.6		Encodes a substrate of the MAPK kinases
At1g67920	0.002	-0.7	-1.6		Unknown Protein
At2g30760	0.007	-0.7	-1.6		Unknown Protein
At4g36870	0.004	-0.7	-1.6	BLH2	BLH2 (BEL1-Like Homeodomain 2); DNA binding / transcription factor

At3g02440	0.006	-0.7	-1.6	TBL20	Trichome birefringence-like 20
At2g29480	0.002	-0.7	-1.6	ATGSTU2	ATGSTU2 (*Arabidopsis thaliana* glutathione s-transferase TAU 2); glutathione transferase
At4g36220	0.021	-0.7	-1.6	FAH1	FAH1 (Ferulic acid 5-hydroxylase 1); ferulate 5-hydroxylase/ monooxygenase
At1g68320	0.040	-0.7	-1.6	MYB62	MYB62 (myb domain protein 62); DNA binding / transcription factor
At2g04100	0.007	-0.7	-1.6		MATE efflux family protein
At4g34138	0.012	-0.7	-1.6	UGT73B1	UGT73B1 (UDP-glucosyl transferase 73B1); UDP-glycosyltransferase/ abscisic acid glucosyltransferase/ quercetin 3-O-glucosyltransferase/ quercetin 7-O-glucosyltransferase
At2g44490	0.007	-0.7	-1.6	PEN2	PEN2 (Penetration 2); hydrolase, hydrolyzing O-glycosyl compounds / thioglucosidase
At3g05400	0.022	-0.6	-1.6		Involved in: carbohydrate transmembrane transporter activity
At3g15500	0.046	-0.6	-1.6	ANAC055	ANAC055 (NAC Domain Containing Protein 55); transcription factor
At5g03490	0.038	-0.6	-1.6	UGT89A2	UDP Glycosyl Transferase 89A2
At4g20860	0.046	-0.6	-1.6	BBE22	FAD-binding Berberine family protein
At2g18340	0.048	-0.6	-1.6		Late embryogenesis abundant domain-containing protein
At5g38900	0.049	-0.6	-1.6		Thioredoxin superfamily protein
At3g27400	0.043	-0.6	-1.6	PLL18	Pectin lyase-like superfamily protein
At4g13030	0.001	-0.6	-1.6		P-loop containing nucleoside triphosphate hydrolases superfamily protein
At5g24080	0.031	-0.6	-1.6		Protein kinase superfamily protein
At3g20160	0.025	-0.6	-1.6	PPPS2	Polyprenyl Pyrophosphate Synthase 2
At2g23150	0.028	-0.6	-1.6	NRAMP3	NRAMP3 (Natural Resistance-Associated Macrophage Protein 3); inorganic anion transmembrane transporter/ manganese ion transmembrane transporter/ metal ion transmembrane transporter
At3g61120	0.005	-0.6	-1.6	AGL13	AGL13 (AGAMOUS-LIKE 13); DNA binding / transcription factor
At5g35370	0.003	-0.6	-1.6		S-locus lectin protein kinase family protein
At4g39130	0.034	-0.6	-1.6		Dehydrin family protein
At4g07720	0.044	-0.6	-1.6		Hypothetical protein (pseudogene)
At1g07500	0.041	-0.6	-1.6	SMR5	SMR5 is a member of the Siamese-Related Cyclin-Dependent Kinase Inhibitor family. It is induced by ROS/oxidative stress
At1g73870	0.045	-0.6	-1.6	BBX16, COL7	B-Box Domain Protein 16, Constans-Like 7
At3g16800	0.009	-0.6	-1.6		Protein phosphatase 2C family protein
At1g10520	0.016	-0.6	-1.6		Encodes a homolog of the mammalian DNA polymerase lambda that is involved in the repair of UV-B induced DNA damage
At1g44070	0.041	-0.6	-1.5		CACTA-like transposase family
At5g65380	0.039	-0.6	-1.5		MATE efflux family protein
At2g41640	0.037	-0.6	-1.5		Glycosyltransferase family 61 protein
At5g08240	0.000	-0.6	-1.5		Unknown Protein
At5g46180	0.004	-0.6	-1.5	DELTA-OAT	delta-OAT; ornithine-oxo-acid transaminase
At1g22890	0.003	-0.6	-1.5		Unknown Protein
At4g31520	0.028	-0.6	-1.5		SDA1 family protein
At1g79170	0.047	-0.6	-1.5		Unknown Protein
At4g05300	0.033	-0.6	-1.5		Unknown Protein
At3g04640	0.028	-0.6	-1.5		Glycine-rich protein
At1g70240	0.029	-0.6	-1.5		Previously annotated as Lipid transfer protein. Curently discontinued
At5g53830	0.003	-0.6	-1.5	MVQ3	MPK3/6-Targeted VQP 3

At3g23410	0.010	-0.6	-1.5	FAO3	Fatty Alcohol Oxidase 3
At1g63440	0.001	-0.6	-1.5	HMA5	HMA5 (Heavy Metal Atpase 5); ATPase, coupled to transmembrane movement of ions, phosphorylative mechanism
At1g18290	0.001	-0.6	-1.5		Unknown Protein
At3g09020	0.009	-0.6	-1.5		Alpha 1,4-glycosyltransferase family protein
At3g09520	0.017	-0.6	-1.5	ATEXO70H4	ATEXO70H4 (exocyst subunit EXO70 family protein H4); protein binding
At3g47640	0.015	-0.6	-1.5	PYE	Encodes Popeye (PYE), a bHLH transcription factor regulating response to iron deficiency in *Arabidopsis* roots
At1g26800	0.002	-0.6	-1.5		RING/U-box superfamily protein
At5g48410	0.026	-0.6	-1.5	GLR1.3	ATGLR1.3; intracellular ligand-gated ion channel
At3g04220	0.005	-0.6	-1.5		Disease resistance protein (TIR-NBS-LRR class) family
At2g23030	0.040	-0.6	-1.5	SNRK2.9	SNRK2.9 (Snf1-related protein kinase 2.9); ATP binding / kinase/ protein kinase/ protein serine/threonine kinase
At2g43010	0.044	-0.6	-1.5	PIF4	PIF4 (phytochrome interacting factor 4); DNA binding / protein binding / transcription factor
At4g31875	0.030	-0.6	-1.5		Unknown Protein
At3g10500	0.009	-0.6	-1.5	ANAC053	anac053 (*Arabidopsis* NAC domain containing protein 53); transcription factor
At1g63750	0.006	-0.6	-1.5		Disease resistance protein (TIR-NBS-LRR class) family
At1g74590	0.043	-0.6	-1.5	GSTU10	GSTU10 (Glutathione s-transferase tau 10); glutathione transferase
At1g13100	0.008	-0.6	-1.5	CYP71B29	CYP71B29; electron carrier/ iron ion binding / monooxygenase/ oxygen binding
At1g21140	0.037	-0.6	-1.5	ATVTL1	Vacuolar Iron Transporter-Like 1
At1g70250	0.011	-0.6	-1.5		Encodes a Protease inhibitor/seed storage/LTP family protein
At5g21130	0.041	-0.6	-1.5		Late embryogenesis abundant (LEA) hydroxyproline-rich glycoprotein family
At2g40000	0.027	-0.6	-1.5	HSPRO2	HSPRO2 (*Arabidopsis* ortholog of sugar beet hs1 pro-1 2)
At5g49520	0.046	-0.6	-1.5	WRKY48	WRKY48; transcription factor
At3g50260	0.013	-0.6	-1.5	CEJ1	CEJ1 (Cooperatively regulated by ethylene and jasmonate 1); DNA binding / transcription factor
At2g29670	0.025	-0.6	-1.5		Tetratricopeptide repeat (TPR)-like superfamily protein
At5g43860	0.011	-0.6	-1.5	CLH2	ATCLH2; Chlorophyllase
At4g15270	0.012	-0.6	-1.5		Glucosyltransferase-related
At3g55890	0.022	-0.6	-1.5		Yippee family putative zinc-binding protein
At4g13830	0.017	-0.6	-1.5	J20	J20 (DNAJ-LIKE 20); heat shock protein binding
At1g23040	0.004	-0.6	-1.5		Hydroxyproline-rich glycoprotein family protein
At2g23770	0.005	-0.6	-1.5	LYK4	Lysm-Containing Receptor-like kinase 4
At5g67020	0.044	-0.6	-1.5		Unknown protein
At3g26840	0.010	-0.6	-1.5	PES2	Phytyl Ester Synthase 2
At5g25450	0.018	-0.6	-1.5		Cytochrome bd ubiquinol oxidase
At5g62680	0.015	-0.6	-1.5	GTR2	Glucosinolate transporter-2
At5g23530	0.018	-0.6	-1.5	AtCXE18	AtCXE18 (*Arabidopsis thaliana* carboxyesterase 18); carboxylesterase
At2g41690	0.019	-0.6	-1.5	AT-HSFB3	AT-HSFB3; DNA binding / transcription factor
At3g14620	0.014	-0.6	-1.5	CYP72A8	CYP72A8; electron carrier/ heme binding / iron ion binding / monooxygenase/ oxygen binding
At3g07350	0.044	-0.6	-1.5	DUF506	Protein of unknown function
At5g48000	0.020	-0.6	-1.5	CYP708A2	CYP708A2; oxygen binding / thalianol hydroxylase

Table S2: List of GO categories preferrentially enriched for FAS genes (p-value <0.05)

Gene set name (no. Genes)	Description	NO. Genes in Overlap (k)	p-value	FDR
Polysaccharide biosynthetic process (587)	GO:0000271 polysaccharide biosynthetic process, GOslim:biological_process	15	5.01e-08	3.1e-4
Carbohydrate biosynthetic process (1069)	GO:0016051 carbohydrate biosynthetic process, GOslim:biological_process	18	9.4e-07	1.39e-3
Polysaccharide metabolic process (707)	GO:0005976 polysaccharide metabolic process, GOslim:biological_process	15	5.13e-07	1.39e-3
Cell wall macromolecule biosynthetic process (185)	GO:0044038 cell wall macromolecule biosynthetic process, GOslim:biological_process	8	1.94e-06	1.39e-3
Xylan metabolic process (186)	GO:0045491 xylan metabolic process, GOslim:biological_process	8	2.02e-06	1.39e-3
Cell wall polysaccharide biosynthetic process (185)	GO:0070592 cell wall polysaccharide biosynthetic process, GOslim:biological_process	8	1.94e-06	1.39e-3
Cellular component macromolecule biosynthetic process (185)	GO:0070589 cellular component macromolecule biosynthetic process, GOslim:biological_process	8	1.94e-06	1.39e-3
Glucuronoxylan metabolic process (182)	GO:0010413 glucuronoxylan metabolic process, GOslim:biological_process	8	1.73e-06	1.39e-3
Xylan biosynthetic process (183)	GO:0045492 xylan biosynthetic process, GOslim:biological_process	8	1.8e-06	1.39e-3
Hemicellulose metabolic process (198)	GO:0010410 hemicellulose metabolic process, GOslim:biological_process	8	3.16e-06	1.95e-3
Cellular cell wall macromolecule metabolic process (201)	GO:0010382 cellular cell wall macromolecule metabolic process, GOslim:biological_process	8	3.51e-06	1.98e-3
Cell wall polysaccharide metabolic process (229)	GO:0010383 cell wall polysaccharide metabolic process, GOslim:biological_process	8	8.84e-06	4.55e-3
Cell wall macromolecule metabolic process (317)	GO:0044036 cell wall macromolecule metabolic process, GOslim:biological_process	9	1.21e-05	5.74e-3
Cell wall organization or biogenesis (958)	GO:0071554 cell wall organization or biogenesis, GOslim:biological_process	15	1.9e-05	7.34e-3
Cellular polysaccharide biosynthetic process (520)	GO:0033692 cellular polysaccharide biosynthetic process, GOslim:biological_process	11	1.9e-05	7.34e-3
Cell wall biogenesis (333)	GO:0042546 cell wall biogenesis, GOslim:biological_process	9	1.76e-05	7.34e-3
Carbohydrate metabolic process (2239)	GO:0005975 carbohydrate metabolic process, GOslim:biological_process	24	3.02e-05	0.011
Cellular cell wall organization or biogenesis (364)	GO:0070882 cellular cell wall organization or biogenesis, GOslim:biological_process	9	3.48e-05	0.0119
Cellular carbohydrate biosynthetic process (938)	GO:0034637 cellular carbohydrate biosynthetic process, GOslim:biological_process	14	6.09e-05	0.0197
Cellular polysaccharide metabolic process (596)	GO:0044264 cellular polysaccharide metabolic process, GOslim:biological_process	11	6.37e-05	0.0197
Cuticle development (48)	GO:0042335 cuticle development,	4	7.45e-05	0.0219

	GOslim:biological_process			
Very long chain fatty acid metabolic process (55)	GO:0000038 very long-chain fatty acid metabolic process, GOslim:biological_process	4	1.22e-4	0.0344

Table S3: List of GO categories preferrentially enriched for MAS genes (p-value <0.05)

Gene set name(no. Genes)	Description	NO. Genes in Overlap (k)	p-value	FDR
Response to chemical stimulus (3953)	GO:0042221 response to chemical stimulus, GOslim:biological_process	120	2.68e-24	2.09e-20
Response to stimulus (6222)	GO:0050896 response to stimulus, GOslim:biological_process	152	2.44e-22	9.55e-19
Toxin catabolic process (211)	GO:0009407 toxin catabolic process, GOslim:biological_process	24	4.49e-16	7.79e-13
Response to organic cyclic compound (148)	GO:0014070 response to organic cyclic compound, GOslim:biological_process	21	5.98e-16	7.79e-13
Toxin metabolic process (211)	GO:0009404 toxin metabolic process, GOslim:biological_process	24	4.49e-16	7.79e-13
Response to cyclopentenone (148)	GO:0010583 response to cyclopentenone, GOslim:biological_process	21	5.98e-16	7.79e-13
Response to nitrate (197)	GO:0010167 response to nitrate, GOslim:biological_process	23	1.12e-15	1.25e-12
Response to organic substance (2739)	GO:0010033 response to organic substance, GOslim:biological_process	81	3.66e-15	3.57e-12
Inorganic anion transport(266)	GO:0015698 inorganic anion transport, GOslim:biological_process	24	5.04e-14	4.37e-11
Nitrate transport (207)	GO:0015706 nitrate transport, GOslim:biological_process	21	2.48e-13	1.94e-10
Anion transport (350)	GO:0006820 anion transport, GOslim:biological_process	26	2.93e-13	2.08e-10
Response to stress (4037)	GO:0006950 response to stress, GOslim:biological_process	95	6.08e-12	3.96e-09
Response to inorganic substance (1075)	GO:0010035 response to inorganic substance, GOslim:biological_process	42	1.34e-11	8.06e-09
Response to external stimulus (1047)	GO:0009605 response to external stimulus, GOslim:biological_process	41	2.25e-11	1.25e-08
Secondary metabolic process (1241)	GO:0019748 secondary metabolic process, GOslim:biological_process	44	8.65e-11	4.5e-08
Cellular response to nutrient levels (314)	GO:0031669 cellular response to nutrient levels, GOslim:biological_process	21	3.64e-10	1.78e-07
Cellular response to extracellular stimulus (352)	GO:0031668 cellular response to extracellular stimulus, GOslim:biological_process	22	4.58e-10	2.09e-07
Cellular response to external stimulus (353)	GO:0071496 cellular response to external stimulus, GOslim:biological_process	22	4.82e-10	2.09e-07
Cellular response to stimulus (2302)	GO:0051716 cellular response to stimulus, GOslim:biological_process	62	5.21e-10	2.14e-07
Response to nutrient levels (331)	GO:0031667 response to nutrient	21	8.92e-10	3.48e-07

	levels, GOslim:biological_process			
Cellular response to starvation(300)	GO:0009267 cellular response to starvation, GOslim:biological_process	20	1.02e-09	3.77e-07
Response to extracellular stimulus (370)	GO:0009991 response to extracellular stimulus, GOslim:biological_process	22	1.1e-09	3.91e-07
Response to starvation (308)	GO:0042594 response to starvation, GOslim:biological_process	20	1.56e-09	5.28e-07
Cellular response to stress (1431)	GO:0033554 cellular response to stress, GOslim:biological_process	45	2.04e-09	6.63e-07
Amino acid transport (266)	GO:0006865 amino acid transport, GOslim:biological_process	18	5.67e-09	1.64e-06
Ion homeostasis(2 34)	GO:0050801 ion homeostasis, GOslim:biological_process	17	5.63e-09	1.64e-06
Ion transport(1016)	GO:0006811 ion transport, GOslim:biological_process	36	5.27e-09	1.64e-06
Amine transport (272)	GO:0015837 amine transport, GOslim:biological_process	18	7.86e-09	2.19e-06
Transport (3558)	GO:0006810 transport, GOslim:biological_process	79	9.18e-09	2.47e-06
Response to chitin (421)	GO:0010200 response to chitin, GOslim:biological_process	22	1.03e-08	2.69e-06
Signaling (2317)	GO:0023052 signaling, GOslim:biological_process	59	1.11e-08	2.79e-06
Carboxylic acid transport (283)	GO:0046942 carboxylic acid transport, GOslim:biological_process	18	1.4e-08	3.42e-06
Localization (3799)	GO:0051179 localization, GOslim:biological_process	82	1.53e-08	3.63e-06
Organic acid transport (289)	GO:0015849 organic acid transport, GOslim:biological_process	18	1.9e-08	4.36e-06
Establishment of localization (3633)	GO:0051234 establishment of localization, GOslim:biological_process	79	2.25e-08	5.03e-06
Cell communication (705)	GO:0007154 cell communication, GOslim:biological_process	28	3.03e-08	6.58e-06
Response to carbohydrate stimulus (811)	GO:0009743 response to carbohydrate stimulus, GOslim:biological_process	30	4.36e-08	9.19e-06
Chemical homeostasis (275)	GO:0048878 chemical homeostasis, GOslim:biological_process	17	5.24e-08	1.08e-05
Cation homeostasis (215)	GO:0055080 cation homeostasis, GOslim:biological_process	15	7.39e-08	1.48e-05
Defense response (1644)	GO:0006952 defense response, GOslim:biological_process	45	1.11e-07	2.17e-05
Innate immune response (926)	GO:0045087 innate immune response, GOslim:biological_process	31	2.17e-07	4.14e-05
Cellular response to iron ion starvation (116)	GO:0010106 cellular response to iron ion starvation, GOslim:biological_process	11	2.47e-07	4.6e-05
Transition metal ion transport (243)	GO:0000041 transition metal ion transport, GOslim:biological_process	15	3.27e-07	5.94e-05
Oxidoreductase activity, acting on paired donors, with incorporation or reduction of molecular oxygen (461)	GO:0016705 oxidoreductase activity, acting on paired donors, with incorporation or reduction of molecular oxygen, GOslim:molecular_function	22	4.79e-08	1.02e-4

Immune system process (980)	GO:0002376 immune system process, GOslim:biological_process	31	7.03e-07	1.22e-4
Immune response (980)	GO:0006955 immune response, GOslim:biological_process	31	7.03e-07	1.22e-4
Response to water stimulus (421)	GO:0009415 response to water stimulus, GOslim:biological_process	19	8.91e-07	1.51e-4
Response to zinc ion (60)	GO:0010043 response to zinc ion, GOslim:biological_process	8	1.07e-06	1.78e-4
Regulation of response to stimulus (662)	GO:0048583 regulation of response to stimulus, GOslim:biological_process	24	1.44e-06	2.34e-4
Cellular response to chemical stimulus (1403)	GO:0070887 cellular response to chemical stimulus, GOslim:biological_process	38	1.52e-06	2.42e-4
Metal ion transport (573)	GO:0030001 metal ion transport, GOslim:biological_process	22	1.63e-06	2.55e-4
Regulation of defense response (529)	GO:0031347 regulation of defense response, GOslim:biological_process	21	1.71e-06	2.61e-4
Cellular ion homeostasis (181)	GO:0006873 cellular ion homeostasis, GOslim:biological_process	12	2.48e-06	3.72e-4
Regulation of response to stress (544)	GO:0080134 regulation of response to stress, GOslim:biological_process	21	2.6e-06	3.78e-4
Cellular chemical homeostasis (182)	GO:0055082 cellular chemical homeostasis, GOslim:biological_process	12	2.62e-06	3.78e-4
Response to water deprivation (413)	GO:0009414 response to water deprivation, GOslim:biological_process	18	2.76e-06	3.93e-4
Cellular response to organic substance (1221)	GO:0071310 cellular response to organic substance, GOslim:biological_process	34	3.15e-06	4.39e-4
Response to abiotic stimulus (2615)	GO:0009628 response to abiotic stimulus, GOslim:biological_process	56	6.2e-06	8.46e-4
Negative regulation of defense response (273)	GO:0031348 negative regulation of defense response, GOslim:biological_process	14	6.28e-06	8.46e-4
Plant type hypersensitive response (401)	GO:0009626 plant-type hypersensitive response, GOslim:biological_process	17	7.41e-06	9.81e-4
Host programmed cell death induced by symbiont (402)	GO:0034050 host programmed cell death induced by symbiont, GOslim:biological_process	17	7.64e-06	9.95e-4
Regulation of cell death (405)	GO:0010941 regulation of cell death, GOslim:biological_process	17	8.39e-06	1.07e-3
Cellular cation homeostasis (172)	GO:0030003 cellular cation homeostasis, GOslim:biological_process	11	8.98e-06	1.12e-3
Cell death (498)	GO:0008219 cell death, GOslim:biological_process	19	9.18e-06	1.12e-3
Death (498)	GO:0016265 death, GOslim:biological_process	19	9.18e-06	1.12e-3
Oxygen binding (234)	GO:0019825 oxygen binding, GOslim:molecular_function	14	1.15e-06	1.22e-3
Regulation of plant type hypersensitive response (371)	GO:0010363 regulation of plant-type hypersensitive response, GOslim:biological_process	16	1.12e-05	1.35e-3

Aging (145)	GO:0007568 aging, GOslim:biological_process	10	1.24e-05	1.47e-3
Cation transport (810)	GO:0006812 cation transport, GOslim:biological_process	25	1.3e-05	1.52e-3
Regulation of cellular response to stress (379)	GO:0080135 regulation of cellular response to stress, GOslim:biological_process	16	1.44e-05	1.66e-3
Response to bacterium (572)	GO:0009617 response to bacterium, GOslim:biological_process	20	1.81e-05	2.05e-3
Negative regulation of response to stimulus (346)	GO:0048585 negative regulation of response to stimulus, GOslim:biological_process	15	1.99e-05	2.22e-3
Protein targeting to membrane (392)	GO:0006612 protein targeting to membrane, GOslim:biological_process	16	2.14e-05	2.36e-3
Defense response, incompatible interaction (535)	GO:0009814 defense response, incompatible interaction, GOslim:biological_process	19	2.39e-05	2.59e-3
Regulation of programmed cell death (397)	GO:0043067 regulation of programmed cell death, GOslim:biological_process	16	2.48e-05	2.66e-3
Systemic acquired resistance (444)	GO:0009627 systemic acquired resistance, GOslim:biological_process	17	2.6e-05	2.74e-3
Programmed cell death (450)	GO:0012501 programmed cell death, GOslim:biological_process	17	3.06e-05	3.18e-3
Response to biotic stimulus (1675)	GO:0009607 response to biotic stimulus, GOslim:biological_process	39	3.32e-05	3.41e-3
Sequence specific dna binding transcription factor activity (1680)	GO:0003700 sequence-specific DNA binding transcription factor activity, GOslim:molecular_function	41	6.99e-06	3.82e-3
Sequence specific dna binding (400)	GO:0043565 sequence-specific DNA binding, GOslim:molecular_function	17	7.18e-06	3.82e-3
Regulation of innate immune response (415)	GO:0045088 regulation of innate immune response, GOslim:biological_process	16	4.14e-05	4.2e-3
Regulation of immune system process (419)	GO:0002682 regulation of immune system process, GOslim:biological_process	16	4.62e-05	4.57e-3
Regulation of immune response (419)	GO:0050776 regulation of immune response, GOslim:biological_process	16	4.62e-05	4.57e-3
Tricyclic triterpenoid metabolic process (4)	GO:0010683 tricyclic triterpenoid metabolic process, GOslim:biological_process	3	4.98e-05	4.86e-3
Response to salicylic acid stimulus (470)	GO:0009751 response to salicylic acid stimulus, GOslim:biological_process	17	5.15e-05	4.96e-3
Heme binding (373)	GO:0020037 heme binding, GOslim:molecular_function	16	1.2e-05	5.09e-3
Cellular cell wall disassembly (15)	GO:0060871 cellular cell wall disassembly, GOslim:biological_process	4	5.63e-05	5.23e-3
Cell wall disassembly (15)	GO:0044277 cell wall disassembly, GOslim:biological_process	4	5.63e-05	5.23e-3
Cell wall modification involved in abscission (15)	GO:0009830 cell wall modification involved in abscission, GOslim:biological_process	4	5.63e-05	5.23e-3

Electron carrier activity (522)	GO:0009055 electron carrier activity, GOslim:molecular_function	19	1.73e-05	5.24e-3
Transcription regulator activity (1738)	GO:0030528 transcription regulator activity, GOslim:molecular_function	41	1.53e-05	5.24e-3
Response to other organism (1411)	GO:0051707 response to other organism, GOslim:biological_process	34	5.72e-05	5.26e-3
Homeostatic process (481)	GO:0042592 homeostatic process, GOslim:biological_process	17	6.76e-05	6.14e-3
Cellular cell wall organization (16)	GO:0007047 cellular cell wall organization, GOslim:biological_process	4	6.97e-05	6.26e-3
Multi organism process (1804)	GO:0051704 multi-organism process, GOslim:biological_process	40	7.45e-05	6.61e-3
Tetrapyrrole binding (406)	GO:0046906 tetrapyrrole binding, GOslim:molecular_function	16	3.22e-05	7.61e-3
Iron ion binding (499)	GO:0005506 iron ion binding, GOslim:molecular_function	18	3.21e-05	7.61e-3
Cellular response to endogenous stimulus (804)	GO:0071495 cellular response to endogenous stimulus, GOslim:biological_process	23	8.87e-05	7.69e-3
Cellular response to salicylic acid stimulus (351)	GO:0071446 cellular response to salicylic acid stimulus, GOslim:biological_process	14	8.82e-05	7.69e-3
Cellular process (14300)	GO:0009987 cellular process, GOslim:biological_process	199	1.23e-4	0.0105
Response to mechanical stimulus (63)	GO:0009612 response to mechanical stimulus, GOslim:biological_process	6	1.38e-4	0.0117
Secondary active transmembrane transporter activity (295)	GO:0015291 secondary active transmembrane transporter activity, GOslim:molecular_function	13	6.03e-05	0.0128
Iron ion transport (126)	GO:0006826 iron ion transport, GOslim:biological_process	8	1.58e-4	0.0133
Response to karrikin (128)	GO:0080167 response to karrikin, GOslim:biological_process	8	1.75e-4	0.0145
Negative regulation of programmed cell death (170)	GO:0043069 negative regulation of programmed cell death, GOslim:biological_process	9	2.28e-4	0.0188
Systemic acquired resistance, salicylic acid mediated signaling pathway (251)	GO:0009862 systemic acquired resistance, salicylic acid mediated signaling pathway, GOslim:biological_process	11	2.31e-4	0.0188
Negative regulation of cell death (174)	GO:0060548 negative regulation of cell death, GOslim:biological_process	9	2.69e-4	0.0216
Response to endogenous stimulus (1604)	GO:0009719 response to endogenous stimulus, GOslim:biological_process	35	2.88e-4	0.023
Salicylic acid mediated signaling pathway (349)	GO:0009863 salicylic acid mediated signaling pathway, GOslim:biological_process	13	2.96e-4	0.0234
Response to metal ion (603)	GO:0010038 response to metal ion, GOslim:biological_process	18	3.16e-4	0.0247
Transferase activity (2997)	GO:0016740 transferase activity, GOslim:molecular_function	57	1.35e-4	0.0262
Inorganic anion transmembrane transporter activity (67)	GO:0015103 inorganic anion transmembrane transporter activity, GOslim:molecular_function	6	1.88e-4	0.0334
Cellular lipid metabolic process (1394)	GO:0044255 cellular lipid metabolic process, GOslim:biological_process	31	4.75e-4	0.0367

Cellular ketone metabolic process (2121)	GO:0042180 cellular ketone metabolic process, GOslim:biological_process	42	5.19e-4	0.0397
Oligopeptide transport (116)	GO:0006857 oligopeptide transport, GOslim:biological_process	7	5.41e-4	0.0399
Metabolic process (13568)	GO:0008152 metabolic process, GOslim:biological_process	187	5.34e-4	0.0399
Cellular homeostasis (324)	GO:0019725 cellular homeostasis, GOslim:biological_process	12	5.27e-4	0.0399
Peptide transport (116)	GO:0015833 peptide transport, GOslim:biological_process	7	5.41e-4	0.0399
Heat acclimation (84)	GO:0010286 heat acclimation, GOslim:biological_process	6	5.86e-4	0.0428
Respiratory burst involved in defense response (121)	GO:0002679 respiratory burst involved in defense response, GOslim:biological_process	7	6.86e-4	0.0492
Respiratory burst (121)	GO:0045730 respiratory burst, GOslim:biological_process	7	6.86e-4	0.0492

Table S4: T-DNA mutant lines of *Arabidopsis*

Locus	T-DNA insertion	Fold change (FAS vs MAS)	p-value	Comments	Gene/protein name
AT2G44460	SALK_067086	-19.5	0.02	No change	BGLU28; B-glucosidase 28
AT3G60140	GK-423F04	-9.2	0.005	No change	BGLU30, DIN2; B-glucosidase 30
AT5G04150	GK-123D06	-3.8	0.0003	No change	BHLH 101; Basic helix-loop-helix transcription factor
AT3G22120	GK-382D01	13.6	0.003	No change	CWLP; Cell wall plasma membrane linker protein
AT1G24020	GK-433F05	2.9	0.0005	No change	MLP423; MLP-like protein 423
AT3G20520	SALK_152374	2.6	0.0007	No change	SHVL3; Glycerophosphodiester phosphodiesterase (GDPD) like 5
AT5G03260	SALK_063746	2.8	0.05	No change	LAC11; Laccase 11
AT5G15580	GK-870B09	2.7	0.02	More male and less females	LNG1; Longifolia1
AT2G38080	GK-720G02	2.7	0.02	More males and less females	IRX12; Irregular xylem 12
AT1G55260	SALK_152374	2.65	0.04	Less females	LTPG; Glycosylphosphatidylinositol-anchored lipid protein transfer 6

Table S5: List of primers for analysis of T-DNA mutant lines

Locus	T-DNA insertion	Primers	Gene/protein name
Primers for genotyping of mutant lines			
AT2G44460	SALK_067086	F: AACCTCATGGTTGTCGGAGA R: CCGGCAAGTTTCTTCATCAT	BGLU28; B-glucosidase 28
AT3G20520	SALK_152374	F: GGATGGTGTTGGAATCTGCT R: TCGCTTGCAGCTCTCTGATA	SHVL3; Glycerophosphodiester phosphodiesterase (GDPD) like 5
AT5G03260	SALK_063746	F: ATTTCAATGTGACCGGACAAC R: TAAGTCTTGTCCCCGTTGATG	LAC11, Laccase 11
AT1G55260	SALK_152374	F: GTATGCGATCTCCAAAAATCG R: GGAGTTAATGCTTGATTGCTTG	LTPG6; Glycosylphosphatidylinositol-anchored lipid protein transfer 6
List of primers used for expression analysis in mutant lines			
AT2G44460	SALK_067086	F: AACCTCATGGTTGTCGGAGA R: CCGGCAAGTTTCTTCATCAT	BGLU28; B-glucosidase 28
AT3G60140	GK-423F04	F:GTGACTAATCACAGTGGTCACAT R: AAAATGAAGATGGGTTCTCTATGC	BGLU30, DIN2: B-glucosidase 30
AT5G04150	GK-123D06	F: TACCATTGATGAGTTCCTCCAGTC R: TAGATGATTCCAAGAGCCATAACA	BHLH10; Basic helix-loop-helix transcription factor
AT3G22120	GK-382D01	F: CCTAAACCACCGGCAGTAAA R: AAAACCGGACAACATTCTGC	CWLP; Cell wall plasma membrane linker protein
AT1G24020	GK-433F05	F: AAACAAATGGGGTTGAGTGG R: TCTACCACAAGGTTCGATTTTT	MLP423; MLP-like protein 423
AT3G20520	SALK_152374	F: GGATGGTGTTGGAATCTGCT R: TCGCTTGCAGCTCTCTGATA	SHVL3; Glycerophosphodiester phosphodiesterase (GDPD) like 5
AT5G03260	SALK_063746	F: ATTTCAATGTGACCGGACAAC R: TAAGTCTTGTCCCCGTTGATG	LAC11; Laccase 11
AT5G15580	GK-870B09	F: CTTTCAGCTTCACTACTCTCCGTC R: GTTCTTCTTTGTCCTCCTGTCTCT	LNG1; Longifolia1
AT2G38080	GK-720G02	F: GGTTCGCCACTACAAGTTTAACG R: TTTCAGTATCCGATTTCCACCAT	IRX12; Irregular xylem 12
AT1G55260	SALK_152374	F: ATGATCCCATCATCCAACCAATACG R: CTCAACACCCAACCAACTCTTC	LTPG6; Glycosylphosphatidylinositol-anchored lipid protein transfer 6

Table S6: List of primers used in cloning

Locus	Primer sequences
AT3G22120	F: GGGGACAAGTTTGTACAAAAAAGCAGGCTGCGGAAATGATTGTGGGGGTAG R:GGGGACCACTTTGTACAAGAAAGCTGGGTCTCTGAAAGGAGTGAGTAAGTAGATAC
AT2G44460	F: GGGGACAAGTTTGTACAAAAAAGCAGGCTGCTCCAAAGACTTATGCACGGT R: GGGGACCACTTTGTACAAG AAAGCTGGGTCTGTTGGTCTACGTGGAAAGGT
F: TGCCAATTGAGGAAAGTGTG (For sequencing to confirm cloning of AT3G22120 promoter in destination vector)	
F: TCCGTAAAAGGGAACGTCAG (For sequencing to confirm cloning of At2g44460 promoter in destination vector)	
R: TCTGCCAGTTCAGTTCGTTG (Sequencing primer from gus reporter gene for in frame confirmation)	

Table S7: List of primers for qRT-PCR

Locus	Primers
AT2G44460	F: CGCGTTACGTTGCTCATATTC R: TGTGATTTGTTACTCGCCATTG
AT2G23170	F: CTCATGCCTGTGATGAATCTCTA R: GGAGTCTTCGATTCCGTCTTC
AT3G22120	F: CGCCTATTCCAGAGACTTGC R: CCTCCTAAAACCGGACAACA
AT5G06860	F: CCATTCCAAGTTCTCTCTCTACG R: GACTCTGGTATGGAACCTGTAAG
AT5G06870	F: AACAAGCTTCAAGGCGATGC R: AACCTTGGAGAGATCGAACTGG
AT1G55260	F: TCGATTCTGCATCTACCTCGT R: CTTCACTGGTTCGGCTTTTC
At5g15580	F: GCAACGTAAGCTTGGCCTCT R: CAGCGACCTCATTCCCAAGT
AT1G19610	F: GGGTTTTGTGGCAACACTCG R: AAACATGCGAAACCCGGGAA

6. Acknowledgements

I would like to express my sincere gratitude to my advisor, Prof. Dr. Florian M. W. Grundler, who always extended a hand to help me. His immense support, motivation, and guidance in Ph.D. research and discussions while I drafted my thesis contributed greatly to my success. He also helped in personal matters during my stay in Germay. His support is price less.

I would also like to thank Dr. Shahid Siddique for his supervision during my experiments, stimulating discussions and helping with writing. He always critically looked, examined my work and helped keep me on track over the course of Ph.D. studies. Thanks for all his timely support and encouragement.

I would also like to extend my gratitude to Prof. Dr. Tina Kyndt, Prof. Dr. Frank Hochholdinger and Prof. Dr. Matthias Wüst for serving as committee members and for taking interest in my work. I would like to thank Prof. Dr. Frank Hochholdinger for also providing me access to laser capture microdissection.

I am very thankful to the DAAD for providing me with financial support for my Ph.D. studies. DAAD meetings and activities were instrumental in helping me to understand the local culture. I am also grateful to the Institute of Molecular Biology and Biotechnology, Bahauddin Zakariya University, Multan for granting me a leave from job to carry on my Ph.D. studies.

I profoundly acknowledge the contribution of all the authors in current studies.

I am very pleased to say thanks to a big group of my MPM colleagues. They were very supportive and made my time very memorable. I would like to particularly acknowledge to Zoran Radokovic, Christiane Matera, Marion Hütten, Syed Jehangir Shah, Arslan Anwer, Habibeh Jabbari, Marie Reuther, María Clara Hurtado Pérez, Jannani Yadev, Stefan Neumann and Thomas Gerhardt for their help during experiments. I also want to say thanks to Dr. Muhammad Ilyas for his support during images formatting.

My special thanks to my family. I am very grateful to my beloved wife, “Nageena Shahzad”, and my beloved son, “Hassan Shahzad”, for all their sacrifices made on my behalf. I would especially like to thank my wife for being so supportive. Without their support, it would have been very difficult to successfully accomplish my current study. Words cannot express my feelings and gratitude for the selfless support of my parents, brothers, and sisters throughout my journey. I am very thankful to my father-in-law and mother-in-law, for their sincere prayers, which always accompanied me. This is a time when I very much miss two precious souls from my family, my father (late) and my brother-in-law (late). Their memories will always remain close to my heart.

Muhammad Shahzad Anjam